Modelling the Neural Representation of Interaural Level Differences for Linked and Unlinked Bilateral Hearing Aids

MODELLING THE NEURAL REPRESENTATION OF INTERAURAL LEVEL DIFFERENCES FOR LINKED AND UNLINKED BILATERAL HEARING AIDS

BY

STEPHANIE T. CHEUNG, B.Eng.

A THESIS

SUBMITTED TO THE DEPARTMENT OF ELECTRICAL & COMPUTER ENGINEERING

AND THE SCHOOL OF GRADUATE STUDIES

OF MCMASTER UNIVERSITY

IN PARTIAL FULFILMENT OF THE REQUIREMENTS

FOR THE DEGREE OF

MASTER OF APPLIED SCIENCE

Master of Applied Science (2014) McMaster University

(Electrical & Computer Engineering) Hamilton, Ontario, Canada

TITLE:	Modelling the Neural Representation of Interaural Level Differences for Linked and Unlinked Bilateral Hearing Aids
AUTHOR:	Stephanie T. Cheung B.Eng., (Electrical & Biomedical Engineering) McMaster University, Hamilton, Canada
SUPERVISOR:	Dr. Ian C. Bruce
NUMBER OF PAGES:	xiii, 124

In loving memory of my PoPo, Wong Kit Fong (1930-2014)

Abstract

Sound localization is a vital aspect of hearing for safe navigation of everyday environments. It is also an important factor in speech intelligibility. This ability is facilitated by the interaural level difference (ILD) cue, which arises from binaural hearing: a sound will be more intense at the nearer ear than the farther. In a hearing-impaired listener, this binaural cue may not be available for use and localization may be diminished. While conventional, bilateral, wide dynamic range compression (WDRC) hearing aids distort the interaural level difference by independently altering sound intensities in each ear, wirelessly-linked devices have been suggested to benefit this task by matching amplification in order to preserve ILD. However, this technology has been shown to have varying degrees of success in aiding speech intelligibility and sound localization. As hearing impairment has wide-ranging adverse impacts to physical and mental health, social activity, and cognition, the task of localization improvement must be urgently addressed. Toward this end, neural modelling techniques are used to determine neural representations of ILD cues for linked and unlinked bilateral WDRC hearing aids. Findings suggest that wirelessly-linked WDRC is preferable over unlinked hearing aids or unaided, hearing-impaired listening, although parameters for optimal benefit are dependent on sound level, frequency content, and preceding sounds.

Acknowledgements

My unreserved thanks go to my supervisor, Dr. Ian Bruce, for his guidance and insight. His enthusiasm and commitment are inspiring, and I have benefitted immensely from his mentorship.

I am extremely grateful to Dr. Hubert de Bruin and Dr. Sue Becker for taking time out of their busy schedules to serve on my committee. Their feedback and suggestions have been invaluable to me and have strengthened my understanding and curiosity.

I also thank Michael Wirtzfeld, Jason Boulet, and Hugo Wang for their advice and support, especially when wrangling with code. Michael generously allowed me to adapt his neurogram code, which streamlined my own work considerably.

Many thanks also to Cheryl Gies for her tireless patience and guidance through my time in the Master of Applied Science program.

Last, my profound gratitude to my wonderful family and friends for reasons I need not explain. Particular thanks to Janine Ho, Judy Tran, and Julia Duchesne for their patience, encouragement, and edits. They are better friends than I deserve.

This work is generously supported by NSERC Discovery Grant 261736.

Notation and Abbreviations

AN Auditory nerve

ANSI American National Standards Institute

AUDIS Auditory Display catalogue of head-related transfer functions

AVCN Anteroventral cochlear nucleus

CAMEQ Cambridge loudness equalization hearing aid fit

CF Characteristic frequency

FFT Fast Fourier transform

GBC Globular bushy cells

HL Hearing loss

HRTF Head-related transfer function

IC Inferior colliculus

ILD Interaural level difference

ITD Interaural time difference

JND Just noticeable difference

LNTB Lateral nucleus of the trapezoid body

LSO Lateral superior olive

MNTB Medial nucleus of the trapezoid body

MSO Medial superior olive

REIG Real ear insertion gain

REUG Real ear unaided gain

SBC Spherical bushy cells

Slow Slow condition attack (100 ms) and release (400 ms) times

SNR Signal-to-noise ratio

SPL Sound pressure level

TIMIT Texas Instruments and Massachusetts Institute of Technology speech corpus

Very Fast Very Fast condition attack (1 ms) and release (10 ms) times

WDRC Wide dynamic range compression

WS Wiggins and Seeber (2013) condition attack (5 ms) and release (60 ms) times

Contents

List of Figures

Chapter 1

Introduction and Problem Statement

1.1 Motivaton

Sound localization is an advantageous aspect of the auditory system, arising from the binaural benefit of sound information provided to both ears. The importance of sound localization is evident in everyday situations, from navigating a noisy dinner party to identifying the origin of a car horn.

With diminished audibility, sound localization ability is hampered in hearing-impaired individuals; unheard binaural cues confer no benefit (Schum and Hansen, 2007). While hearing-impaired listeners often report struggles with understanding speech in noise (Dillon, 2001; Ibrahim *et al.*, 2012), reduced localization ability is not

frequently expressed unprompted (Dillon, 2001). However, Kapteyn (1977) suggests that sound localization is one of the important indicators of satisfactory hearing. Indeed, poor localization is a factor in poor speech understanding itself (Dillon, 2001; Kreisman *et al.*, 2010; Keidser *et al.*, 2006).

The challenges faced by those with hearing impairments are not constrained to hearing difficulties themselves. Hearing loss has been associated with poorer health and diminished cognitive and physical ability, with detrimental impact to physical and mental health (Bainbridge and Wallhagen, 2014). In Canada, 87% of individuals reporting hearing difficulties also reported challenges with mobility, agility, and pain (Statistics Canada, 2010). Perhaps most alarmingly, poor sound localization is associated with feelings of isolation and anxiety (Dillon, 2001). Hearing loss may also provoke frustration, tiredness, and depression in family members and spouses of impaired individuals (Bainbridge and Wallhagen, 2014). Though hearing aids vary widely in technology, a systematic review has shown such interventions to benefit social, psychological, and emotional health (Bainbridge and Wallhagen, 2014). When one considers the decreased quality of life associated with hearing impairment and the possible benefits of optimal prescription, the incentive to improve sound localization is clear.

This is a pressing task: sensorineural hearing loss affects a large percentage of the population and is particularly common in older individuals. In Canada, 23.4% of the population (4.1 million) is projected to be above the age of 65 by 2036 (Canadian Hearing Society, 2013). At present, nearly a quarter of Canadians self-reports hearing loss of some degree (Canadian Hearing Society, 2013). In the United States, the prevalence of individuals over 50 years of age with at least mild hearing loss doubles

every decade, and 80% of individuals over the age of 85 experience hearing loss of at least a mild nature (Bainbridge and Wallhagen, 2014). Between 2005 and 2007, over 2.8 million cases of sensorineural hearing loss were diagnosed in outpatients aged 65 or older (Bainbridge and Ramachandran, 2014).

Assistive technologies for this population continue to develop. Hearing aids have come a long way since the 1960s, when uniform amplification of all input sound levels was the dominant technology. Now, advanced algorithms are able to address the need to amplify quieter sounds to a larger degree than louder sounds for the maintenance of both audibility and comfort. To this end, wide dynamic range compression (WDRC) devices compress a large range of input sound levels to a smaller range, based upon the listener's hearing profile, or audiogram. Hearing aid interventions do not yet adequately restore hearing without neglecting or introducing other complications. While unilateral hearing aid usage denies the robust binaural benefit available to a normal-hearing listener, bilaterally-worn devices also reduce important binaural cues through independent volume adjustments at each ear.

Recent advances in small, wireless technologies have enabled the development of linked WDRC hearing aid systems, which aim to better approximate binaural hearing by synchronizing information across bilaterally-worn devices. Specifically, these synchronized amplification systems seek to maintain the interaural level difference (ILD) binaural cue integral to sound localization of higher frequencies, which conventional bilateral hearing aids reduce (Edwards, 2007). Even so, these devices are reported

to have various degrees of success in aiding speech intelligibility and localization. It is not well understood whether any benefit arising from such technologies is owed to restored binaural listening, or rather improved signal-to-noise ratio (SNR) at the ear closer to the originating sound (Wiggins and Seeber, 2013).

The current state of inadequately-restored hearing is reflected in the under-use of hearing aids. Nearly 60% of hearing-impaired individuals aged 70 or older do not use this intervention (Bainbridge and Ramachandran, 2014). Of those who do own hearing aids, many do not use them (Bainbridge and Wallhagen, 2014). Satisfaction with these devices remains low; a 2005 study found only 59% of wearers to be content with their hearing aids, with poor speech understanding being a primary complaint (Kreisman *et al.*, 2010). Bainbridge and Wallhagen (2014) also cite possible stigmas, financial burdens, and misperceptions of one's own hearing ability to be factors in underuse.

Modelling approaches have long contributed to the development of hearing aid algorithms and prescription fits (Edwards, 2007). Neural modelling can elucidate how spatial position is processed in the auditory system (Wang and Colburn, 2012). The research described herein concerns modelling the neural response to sounds originating from different azimuths, both in impaired and unimpaired hearing. Specifically, we investigate the ILD processing in the lateral superior olive (LSO) of the brainstem. In the case of the impaired model, different hearing aid interventions are assessed.

This work has implications for the continuing evaluation of device prescription and accuracy. While some psychophysical studies have been conducted into the clinical and real-world performance of linked WDRC hearing aids, modelling work of this nature has not been done before. Moreover, this research contributes to the development of hearing devices which will optimize one's ability to localize sounds, a critical endeavour for a large population.

1.2 Research Objectives

The primary aim of this work is to examine the underlying neuronal mechanisms from which reports of sound localization performance arise. Specifically, lateral superior olive processing of interaural level difference cues is modelled. These LSO models may give some indication as to whether linked WDRC technologies are performing as anticipated, whether the methodologies are flawed, or whether hearing aid prescriptions themselves are inadequate to take advantage of the devices' capabilities. Moreover, these findings may suggest future directions for fittings and methods to aid safe, comfortable listening.

Specifically, the objectives are: **(1) To examine patterns of neural response to sounds for a listener with sensorineural hearing impairment in several conditions: with bilateral, unlinked WDRC hearing aids; with linked WDRC hearing aids; and unaided.** It is hypothesized that the wirelessly-synchronized devices will enable better performance than unlinked WDRC. **(2) To elucidate the perceived horizontal position of sounds in the hearing-impaired listener, as abstracted from the neural model.** It is hypothesized that the

hearing-impaired listener will perceive smaller azimuths than the actual azimuths of sound origin. **(3) To uncover deficiencies of current systems, where they appear to exist, and to suggest solutions and future directions for improved localization.**

1.3 Thesis Organization

The research presented herein is organized as follows:

Chapter 2 presents an overview of concepts explored over the course of this research, with descriptions of relevant technologies and neural systems.

Chapter 3 explores the problem of improving localization in the hearing-impaired population and the history of solutions to that end.

Chapter 4 describes the models used in this work.

Chapter 5 outlines the stimuli used, the methods of neural response simulation, and analyses.

Chapter 6 presents results from this modelling research.

Chapter 7 discusses these findings with emphasis on similarities, deviances, and other indications given previous research on wireless hearing aids.

Chapter 8 details implications of the findings described and future directions, reiterating the contributions of this work.

Chapter 2

Background

This section presents the concepts integral to this research. A literature review specific to the challenges in impaired binaural hearing follows in Chapter 3.

2.1 Binaural Cues for Localization of Sounds

Binaural hearing facilitates localization through interaural differences which are established when a sound is received in each ear. Two of these interaural cues convey key information about a sound source.

Sounds arrive sooner at the closer ear than the farther, establishing an interaural time difference (ITD), a function of the sound source azimuth. Following convention and taking a position directly in front of the listener to be the 0° azimuth, a sound at −60° would be closer to the left ear, reaching it prior to the right ear. A basic ITD model gives an ITD of 0 μs at 0° and ITDs of 650 μs at −90° and +90° in humans (Akeroyd, 2006). This model is accurate in practice with slight variations due to sound type and individual head geometry (Akeroyd, 2006). In low frequencies

of 500 to 1000 Hz, the just noticeable difference (JND) of ITDs in pure tones can be as small as 10 μs (Akeroyd, 2006). In higher-frequency tones, however, ITD cues are less salient, though there is some suggestion that ITDs are perceptible in the envelopes of higher-frequency sounds (Akeroyd, 2006).

The interaural level difference (ILD) is a product of the acoustic head shadow, as shown in Figure 2.1. Sounds are attenuated at the farther, shadowed ear relative to the closer, unshadowed ear; the difference that arises is called the interaural level difference (ILD). Sound localization is approximately proportional to ILD up to 10 dB, with 15-20 dB indicating the edge of the head (Akeroyd, 2006). The JND of ILDs can be as small as 0.5 dB and is demonstrably independent of frequency between 200 Hz to 10 kHz, except at 1 kHz, at which ILD discrimination is poorer (Akeroyd, 2006). Hearing aid range often does not exceed 8 kHz, worsening localization by excluding speech energy above this frequency (Kreisman *et al.*, 2010).

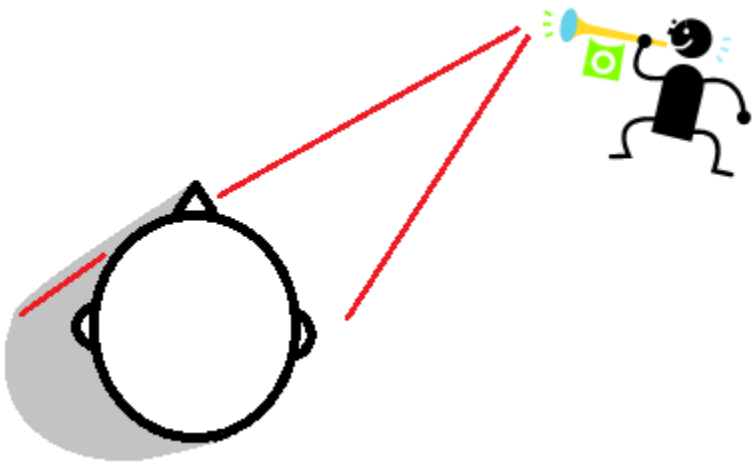

Figure 2.1: *The head shadow effect.*

The duplex theory of sound localization suggests that ITD cues are most perceptually salient at low-frequency sounds (below 1500 Hz), while ILD cues are predominant at high-frequency sounds (Akeroyd, 2006). At higher frequencies, short wavelengths make the ITD cue ambiguous (Dillon, 2001). When both interaural cues are present without confounding noise, ITD cues are predominantly used for localization; in noise, either cue may be used (Akeroyd, 2006). In humans, localization ability appears to be optimal at frequencies near 800 Hz, with a resolution of 10 μs or 1° (Dillon, 2001). At the 1500 Hz boundary between low- and high-frequency regions, localization is poorest, with a resolution of approximately 3° (Dillon, 2001).

Sensorineural hearing impairment presents challenges to listening by diminishing dynamic range, the difference between the limits of audibility and discomfort (Dillon, 2001). With such decreased range, binaural cues for localization may be less salient, such that no benefit can be derived. At low frequencies, horizontal sound localization diminishes gradually with worsening impairment (Dillon, 2001). The greatest deficits to localization seem to arise when hearing loss exceeds 50 dB hearing loss (Dillon, 2001). It should be noted that impairment is usually less at low frequencies, in which sounds carry most intensity; as a result, ITD cues may still be available to those individuals for whom ILD cues are no longer audible (Dillon, 2001).

Vertical localization and front/back discriminations are owed to monaural spectral cues from reflections in the pinna and are beyond the scope of the present work (Dillon, 2001; Keidser *et al.*, 2006).

2.2 The Human Auditory System

Sound pressure waves first encounter the auditory system at the pinna and concha of the outer ear, before travelling through the auditory meatus towards the tympanic membrane, which transfers energy through the bones of the middle ear (Pickles, 2008). This pressure information is transmitted to the fluid-filled cochlea, where the movement of cochlear membranes causes deflection of the hair cells (Pickles, 2008). The result is depolarization of the hair cells, which converts the original signal into an electrical one that is conveyed by the auditory nerve to the brainstem (Borisyuk, 2005).

The anteroventral cochlear nucleus (AVCN) contains spherical and globular bushy cells which differ in their inputs and projections (Young and Oertel, 2003). Spherical bushy cells receive inputs from a few AN fibers while globular bushy cells receive inputs from 4 to 40 (Pickles, 2008). For sound localization, spherical bushy cells provide excitatory inputs to the superior olive and globular bushy cells, the inhibitory inputs (Young and Oertel, 2003). At all levels of the auditory system, characteristic frequency (CF) is tonotopically mapped such that specific cells respond to specific frequencies (Borisyuk, 2005). From here, the previously-mentioned interaural cues are processed in their respective pathways in the superior olive. Bushy cell projections are shown in Figure 2.2.

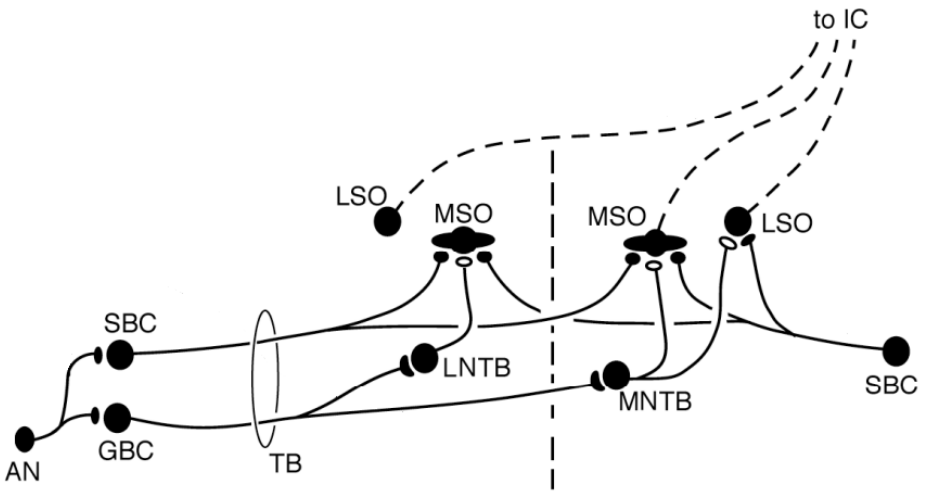

Figure 2.2: *Spherical and globular bushy cell (SBC and GBC) projections, modified from Young and Oertel (2003). The dashed centre line indicates the midline of the brainstem, and some symmetrical connections are not shown. Open-circle and filled-circle synapses indicate inhibitory and excitatory inputs, respectively.*

2.2.1 Interaural Time Difference Processing

ITD cues are processed in the medial superior olive (MSO) of the brainstem (Day and Semple, 2011). The MSO receives bilateral excitatory inputs from spherical bushy cells of the AVCN as well as inhibitory inputs from globular bushy cells, via the lateral and medial nuclei of the trapezoid body (MNTB and LNTB) (Young and Oertel, 2003). These projections are illustrated in Figure 2.2. ITD processing is performed in the MSO by coincidence detector neurons with a delay line mechanism that gives nonzero excitation at the best ITD (Day and Semple, 2011). This model suggests that MSO neurons respond most strongly (i.e. with highest spike rate) at a characteristic internal delay reflective of the ITD (Day and Semple, 2011). The MSO, too, is tonotopically mapped such that converging inputs are compared for delays within similar frequencies (Day and Semple, 2011).

2.2.2 Interaural Level Difference Processing

ILD cues are processed in the lateral superior olive (LSO) of the brainstem (Figure 2.3), which receives excitatory inputs from spherical bushy cells of the ipsilateral AVCN (Young and Oertel, 2003). Inhibitory inputs are received from contralateral globular bushy cells via the MNTB (Young and Oertel, 2003). These projections are shown in Figure 2.2. LSO cells are tonotopically mapped and are excited by greater intensity in the ipsilateral ear (Tsai *et al.*, 2010). The pattern of LSO excitation is sigmoidal in shape, where higher spike rates indicate greater level difference between the ipsilateral and contralateral ear (Tsai *et al.*, 2010). There is some suggestion that the sigmoidal tuning function shifts with respect to overall levels of sound presentation, although other studies find ILD thresholds to be invariant to stimulus level (Tsai *et al.*, 2010). LSO responses are next received by the neurons of the inferior colliculus (IC) (Tsai *et al.*, 2010). A simple difference model of IC function subtracts the contralateral LSO response from that of the ipsilateral LSO, resulting in another sigmoidally-shaped tuning curve (Tsai *et al.*, 2010). LSO tuning curves from a Tsai *et al.* (2010) study are shown in Figure 2.4.

In the research described herein, two LSO models are used: a sigmoidal phenomenological model and a Hodgkin–Huxley-type biophysical model. AVCN inputs are generated using an existing model of the auditory periphery (Zilany *et al.*, 2009, 2013, 2014). A simple IC difference model is also used. Model details are further addressed in Chapter 4.

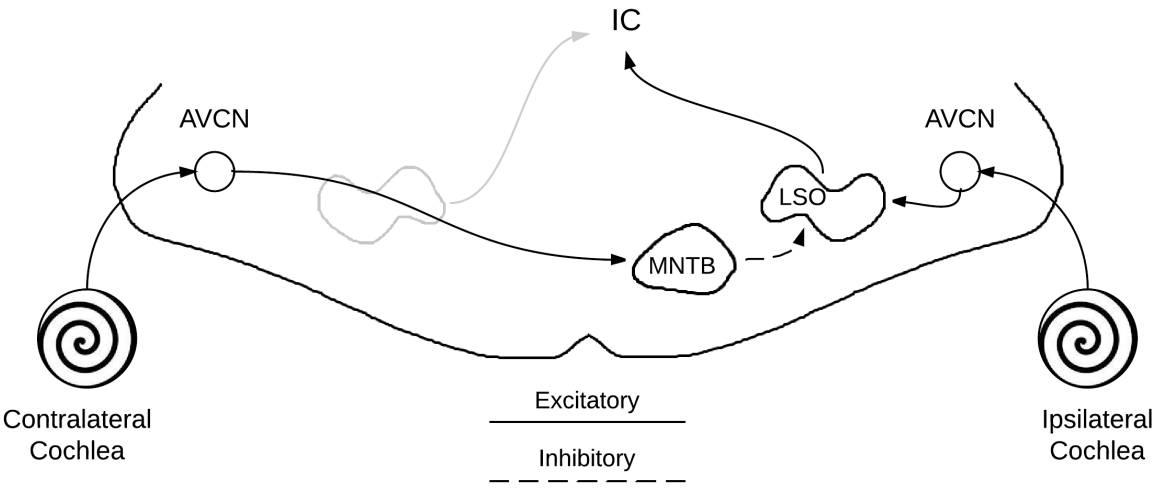

Figure 2.3: *The ILD neural pathway. Some symmetrical connections are not shown.*

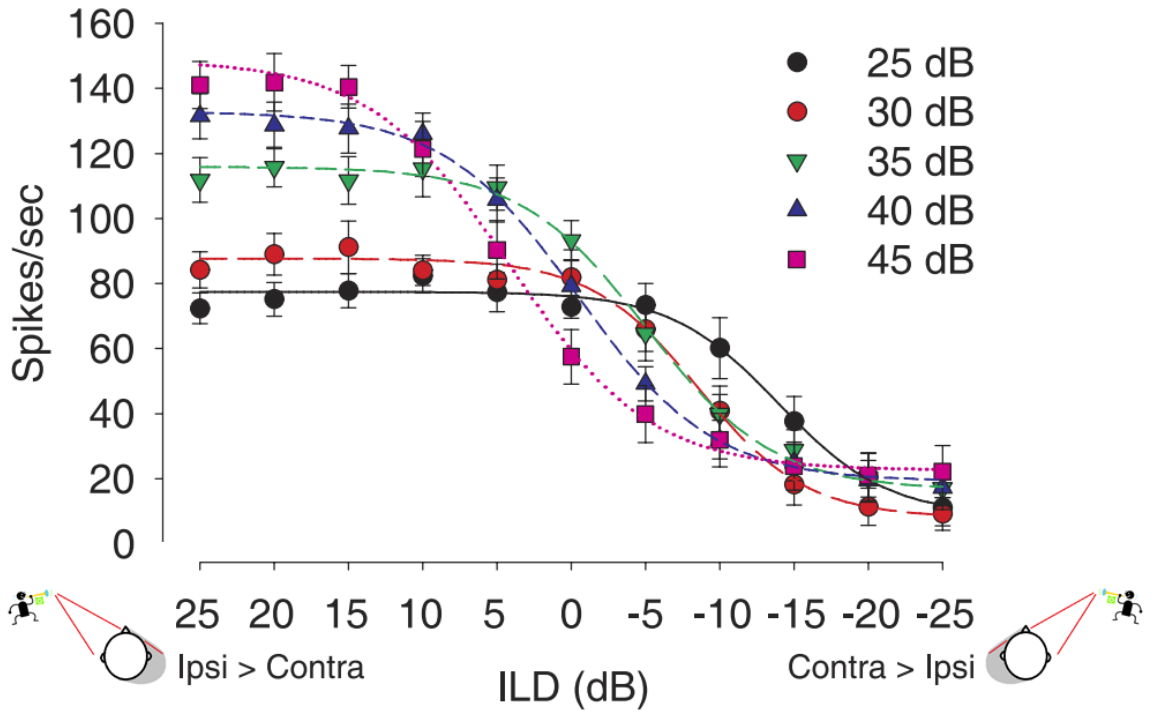

Figure 2.4: *Left LSO tuning functions from Tsai* et al. *(2010). Note the sigmoidal shape and level dependence.*

2.3 Wide Dynamic Range Compression Hearing Aids

The goal of an effective hearing aid is to restore sounds to an audible, comfortable level for the listener. Because of the reduction of dynamic range in a hearing-impaired individual, the dynamic range of sounds must be compressed. This is achieved by reducing gain as sound level increases as opposed to linear amplification of inputs of all intensities, the previously most common method. Figure 2.5 shows examples of linear amplification and WDRC compression input/output curves. Compression ratios denote the degree of gain reduction beginning at the compression threshold, the level at which WDRC begins to act. Compression and gain are not achieved immediately. Rather, attack and release times define the time constants required for the desired level to be reached (Dillon, 2001). These parameters may be chosen specifically to accomplish different hearing goals. For example, very fast attack and release times will decrease inter-syllabic differences while long time constants will reduce overall variations in signal level (Dillon, 2001). Likewise, compression ratios are chosen to suit the listener's audiogram and hearing goals (Dillon, 2001). Wide dynamic range compression (WDRC) hearing aids are now the predominant hearing aid intervention, with compression ratios ranging from 1.5:1 to 4:1 (Musa-Shufani *et al.*, 2006).

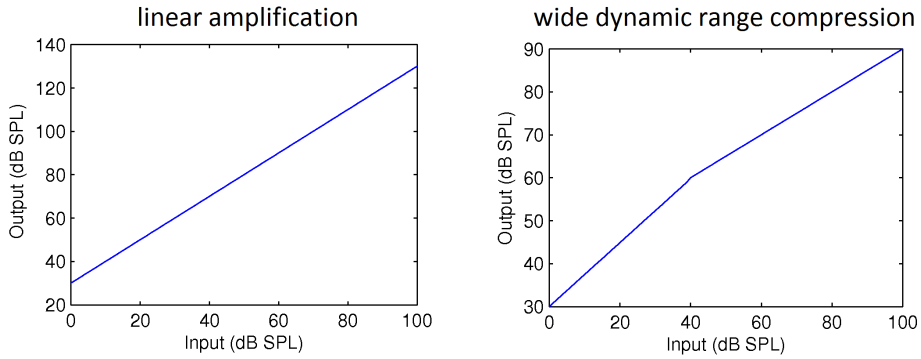

Figure 2.5: *An example of linear amplification and WDRC compression input/output curves. The linear amplification system applies the same gain to all input levels, while the compressor applies linear gain up to the compression threshold (40 dB SPL), then compresses output levels for higher input intensities.*

WDRC hearing aids may use one of two methods to detect input levels exceeding compression threshold. The input signal level can be determined from filter bank envelope detectors in the time domain, after which the appropriate gain may be calculated and applied (Kates, 2005). Alternately, overlap-and-add techniques can be used to isolate a small time frame of the incoming signal, convert it to the frequency domain, and detect threshold-crossings before amplification is applied (Kates, 2005). Both systems have advantages and disadvantages in computational time, resources, and error.

WDRC does not appear to impact lateralization consistently through altering ITD cues (Musa-Shufani *et al.*, 2006). However, ILD cues are skewed if independently-operating bilateral hearing aids apply different gains in each ear in order to bring each of those signals to an appropriate level (Ibrahim *et al.*, 2012).

2.3.1 Wirelessly-Linked Hearing Aids

The development of small, wireless technologies offers some possibilities to the improvement of localization in hearing-impaired individuals (Edwards, 2007). These devices are worn bilaterally and synchronize gain in the left and right ears so that ILD cues are preserved at all times. To both hearing aids, linked amplification applies the lowest required gain needed by either of the two (Wiggins and Seeber, 2013). In effect, the ear farthest from the sound source would receive less amplification than typical of an unlinked, bilateral WDRC solution.

Chapter 3

Literature Review

This section presents a brief review of the problem of localization in sensorineural hearing loss, with focus on recent psychophysical studies of aided localization performance. This is not an exhaustive review, but serves to provide rationale for a study of this nature.

3.1 The Problem of Localization: Difficulties for the Hearing-Impaired

Provided a stimulus with sufficient loudness, an unaided, sensorineurally hearing-impaired individual with loss below 50 dB HL can make left/right discriminations based on the available interaural cues (Keidser *et al.*, 2006). Other hearing-impaired listeners, including those with impaired function at higher frequencies and those with conductive or mixed impairments, experience greater difficulty (Keidser *et al.*, 2006).

The degree to which a hearing-impaired individual localizes sounds remains in question and appears variable with hearing loss (Simon, 2005). As diminished speech intelligibility and poor sound localization are linked, this aspect of impaired hearing must be urgently addressed.

3.2 Analog Hearing Aids

Bilateral hearing aids have been available since the 1960s, with no clear consensus on benefit over unilateral devices (Simon, 2005). During the 1970s and 1980s, impaired sound localization was already considered one of the most serious detriments; subsequently, bilaterally-fit hearing aids were expected to have the greatest advantage to sound localization in the absence of true binaural hearing (Simon, 2005). Despite this, usage of bilateral aids remained low, due in part to unclear clinical benefit (Simon, 2005). Older hearing aids could skew interaural difference cues; tubing and filters could create delays in the signals, and amplification at higher frequencies could be inadequate (Keidser *et al.*, 2006). In a study on the effect of different digital signal processing technologies on localization, Keidser *et al.* (2006) cited various reports, prior to 1993, that bilaterally-aided users performed even worse than their unaided peers. Consequently, another contributing factor to poor acceptance may have been a 1975 ruling by the Federal Trade Commission, barring marketing of bilateral hearing aids on the false basis that these aids would be demonstrably more advantageous than unilateral devices (Simon, 2005).

3.3 The Age of Digital Signal Processing: WDRC and Advanced Algorithms

With the arrival of digital signal processing technologies in 1996, new techniques to target spatial hearing became possible (Edwards, 2007). These complex algorithms, not previously available in analog systems, include noise reduction and environment detection (Edwards, 2007). Digital signal processing was a component in 93% of hearing aids sold in the US in 2005 (Edwards, 2007) and is now widely used. Despite this, satisfaction with hearing aids remains low: a 2005 study found only 59% of hearing aid users to be content with their device, with most complaints stemming from poor speech understanding in noise (Kreisman *et al.*, 2010). Cox *et al.* (2011) had 94 veterans try unilateral and bilateral digital devices for three weeks each before wearing whichever they preferred for a subsequent 9 weeks. In a survey, 46% of participants (43) preferred unilateral devices, with self-perception of greater hearing difficulty associated with preference for bilateral fits (Cox *et al.*, 2011). Other self-reports of localization ability, however, indicate bilateral advantages over unilateral interventions (Noble, 2006; Boymans *et al.*, 2009). Mueller *et al.* (2012) reason that while a second hearing aid may provide preferable amplification, the distorted interaural cues may be responsible for a detrimental effect to localization.

Clinical performance of WDRC itself also remained somewhat inconclusive (Edwards, 2007). In 2006, Keidser *et al.* (2006) found that WDRC and noise reduction techniques, compared to linear amplification, degraded ILD cues but had no impact on localization. Rather, directional microphones were observed to have the greatest impact. Also in 2006, Van den Bogaert *et al.* (2006) found bilateral WDRC to produce

worse localization scores than unaided listening, with noise reduction contributing additionally adverse effects. Kates (2010) demonstrated that success is largely variable with hearing loss, signal level, and noise level, concluding that an ideal aid should have compression parameters adjusted for the individual and be adaptable for different hearing environments. With attention to ILD cues specifically, Musa-Shufani *et al.* (2006) found just noticeable differences (JND) to increase with greater compression. Longer attack times were also found to decrease JND, with a greater impact resulting in conjunction with higher compression (Musa-Shufani *et al.*, 2006).

3.4 Wireless Technologies

Recently, wirelessly-linked hearing aids have been suggested to improve both speech intelligibility and localization by synchronizing amplification to preserve ILD cues (Kreisman *et al.*, 2010). In a review of future directions in hearing aid design, Edwards (2007) named wireless technology "the most likely candidate" for "the next revolutionary innovation", noting the importance of linked WDRC algorithms on sound localization. The first wirelessly-linked hearing aid was the Acuris e2e wireless, produced by Siemens in 2004 (Herbig *et al.*, 2014; Powers and Burton, 2005). Schum and Hansen (2007) found that the Oticon Epoq RITE, already available to consumers, restored ILD to a greater degree when wireless connectivity was enabled: for a 75-dB SPL white noise input with a natural 8 dB ILD, the linked aids provided 6.5 dB ILD where the unlinked supplied only 2.5 dB ILD. Similar findings were observed in the present research and will be further described in Chapter 6.

It should be noted that wirelessly-linked hearing aids need not operate independently from other complex signal processing schemes, nor is a wireless connection between devices to be used solely for synchronized volume control. Sockalingam *et al.* (2009) regard linked amplification to be the most basic form of binaural wireless technology, surpassed by synchronized noise reduction and directionality algorithms. The most advanced technology combines these previous schemes with gain optimization techniques for "spatial fidelity and resolution", such as the binaural algorithms of the Oticon Dual XW (Sockalingam *et al.*, 2009).

In the literature, "wireless" hearing aid technology may also refer to direct-to-hearing-aid transmissions of media signals such as television audio. The present research detailed in this thesis deals solely with wireless linking for matched amplification, and the terms "wireless" or "linked" WDRC refer to this alone. An exploration of the literature on wireless WDRC reveals that the few reports of performance, clinical or otherwise, remain mixed. A review of these works follows.

3.5 Psychophysical Studies with Wirelessly-Linked Hearing Aids

While published studies on binaural performance of wirelessly-synchronized hearing aids are few, the following provide insight into the current state of this technology. A table summarizing methodology can be found in Appendix B. Studies are presented in order of publication.

Smith *et al.* (2008) studied "real-world" preferences for wiressly-linked, unlinked bilateral, and unilateral hearing aids in 30 participants with symmetric sensorineural hearing loss. Scores on the Speech, Spatial, and Qualities questionnaire (SSQ) indicated benefits for linked versus unlinked bilateral aids under the speech and spatial categories. This difference was only significant in responses to the question, *"You are sitting around a table or at a meeting with several people. You can't see everyone. Can you tell where any person is as soon as they start speaking?"*. Preference for bilateral fits over unilateral fits was unanimous with 65% of participants preferring linked bilateral aids over the unlinked. This report showed promise for the continuing use and development of bilateral, linked hearing aids, although it indicated that localization, a primary aim of synchronized bilateral devices, remained unsatisfactory.

Sockalingam *et al.* (2009) demonstrated promising results in localization and naturalness of sound using wireless hearing aids. 30 participants with mild to moderate sensorineural hearing loss were tasked with localizing a target bird chirp amid 55-dB SPL speech-shaped noise. The target sound originated from speakers spaced 15° apart, from −150° to +150°. The noise was presented from the −150° and +150° speakers simultaneously. Using Oticon Dual XW hearing aids, participants identified the speaker from which they perceived the target chirp to emanate. These devices contain advanced gain optimization techniques for "spatial fidelity and resolution", as well as volume synchronization and noise control (Sockalingam *et al.*, 2009). Significantly fewer localization errors were made when the wireless binaural synchronization was turned on, with an average wireless benefit of 14%. Naturalness of sound was also examined via questionnaire in three simulated hearing environments: a café, a park, and a noisy street. Naturalness was reported to be significantly better for the

café scenario with the wireless synchronization enabled rather than disabled but no significant benefit was found for the street or park (Sockalingam *et al.*, 2009). While indicative of possible binaural benefits of wireless hearing aids as a whole, the study design provides limited insight into the benefits of amplification synchronization itself.

Kreisman *et al.* (2010) investigated wirelessly-linked WDRC using different hearing aids from Sockalingam *et al.* (2009): the Oticon Epoq XW RITEs (with wireless link enabled) and the Oticon Syncro V2 BTEs (with no wireless link). This crossover study had 36 hearing-impaired participants fit with either of these two devices, then switch to the other after a minimum 2-week period of acclimatization and subsequent assessment. Under review were two measures of hearing speech-in-noise: QuickSIN and the Hearing in Noise Test (HINT). In the QuickSIN phase, participants repeated 6 sentences spoken by a female talker. Speech was presented at 0° with 4-talker babble noise originating from other spatial positions. In the HINT test, speech receptive thresholds were found using an adaptive procedure and 20 HINT sentences spoken by a male speaker. In this test, target speech was also presented at 0° and noise from other spatially-separated azimuths. Kreisman *et al.* (2010) found significantly better results with wirelessly-synchronized hearing aids, on both measures in every noise condition. While localization itself was not under review in this study, these results indicate some wireless benefit to speech thresholds in noise, which may be indirectly owed to improved localization. In everyday environments, speech and noise are often spatially separated (Drennan *et al.*, 2005), as is the case here.

Schwartz and Shinn-Cunningham (2013) evaluated spatial thresholds for 39 normal-hearing participants using a simulated hearing aid. As in the present study, this link was established by applying to both ears the minimum of the gains required in either. Also as in the present work, head-related transfer functions (HRTFs) were used to simulate binaural cues. Participants repeated digits spoken by the 0° target while symmetrically-masking, spatially-separated speech also spoken by the same talker, was played on either side. An adaptive procedure found the spatial separation required for 67% accuracy. Thresholds were found to be below 30°, ranging from as small as 10°. With fast attack and release time, independent WDRC produced worse results than linked WDRC or linear amplification. There was no trend in performance using slow compression. This is not surprising, as target gain may not be reached when the compressor takes longer to act.

Interesting results have also been reported by Ibrahim *et al.* (2012) in an investigation of both speech intelligibility and sound localization in 8 normal-hearing and 12 moderate-to-severely hearing-impaired listeners. As with Kreisman *et al.* (2010), Oticon Epoq XW hearing aids were used, as well as Siemens Motion 700 aids. While both hearing aids synchronize volume control, the Oticon device also includes a proprietary "Spatial Sound" algorithm designed for binaural WDRC. This is the same device used by Schum and Hansen (2007). Both devices were assessed in the wireless on and wireless off conditions. Adaptive directionality, noise reduction, and feedback management were disabled. Similarly to Kreisman *et al.* (2010), the HINT test was used to assess speech-in-noise listening. In this case, target speech originated from 0°, while masking speech arrived either from +90°, −90°, or both, using an adaptive

procedure to find the 50% threshold. Sound localization was evaluated with two stimuli: a car horn in traffic, and a high-frequency narrow-band noise centred at 3150 Hz. For the car horn in traffic stimulus, traffic noise was played at ±90°. Both stimuli were roved in level from one presentation to another, and randomized from one of 16 evenly-spaced speakers at a time. In this task, participants turned their heads toward the perceived source of the target sound. In the HINT test, normal-hearing listeners outperformed hearing-impaired listeners significantly in all conditions and under all angles of noise presentation. The Siemens aid produced better threshold scores than the Oticon aid when noise was introduced from symmetric azimuths. Overall, Ibrahim *et al.* (2012) concluded no benefit from wireless technology on speech-in-noise scores. On the localization task, normal-hearing participants produced better scores unaided than aided. In the hearing-impaired, the synchronized-device conditions significantly aided front/back discriminations of the broadband stimulus. However, there was no effect of synchronized WDRC on left/right localization of either stimulus.

A recurring explanation for bilateral hearing aid performance is the availability of ITD cues at lower frequencies, despite potentially disturbed ILD cues above 1500 Hz (Ibrahim *et al.*, 2012; Wiggins and Seeber, 2013). Wiggins and Seeber (2013) addressed this specifically in the most recent of the reviewed literature.

The Wiggins and Seeber (2013) speech intelligibility study was conducted with 10 normal-hearing participants, using simulated two-channel WDRC. Impaired, aided speech intelligibility scores were also predicted using a hearing-impaired model and corresponding prescription. As with Schwartz and Shinn-Cunningham (2013) and the current work detailed in this thesis, linked WDRC applied the minimum gain required in the two ears and HRTFs were used to simulate interaural differences. Listeners

heard and repeated sentences of speech, and the number of correct keywords were recorded. To address the question of ITD cue availability and saliency, listeners heard the stimuli in three sets of conditions: two bandwidths (100 to 2000 Hz channel only or with the addition of a 2000 to 5000 Hz channel); two listening modes (binaural and monaural); and three compression conditions (uncompressed, unlinked WDRC, and linked WDRC). Linked WDRC performance was found to be similar to that in the uncompressed case, while linked WDRC provided the same benefit in both listening modes. That is, any benefits in performance were owed to improved SNR at the better ear rather than true preservation of ILD cues. This is not unsimilar to the findings of Ibrahim *et al.* (2012), who noted better localization performance for normal-hearing listeners in the unaided case. In both this study and Ibrahim *et al.* (2012), listeners were not allowed an acclimatization period. Although the necessary period to acclimatize remains in question (Simon, 2005), this may have had an impact on results in both cases. Wiggins and Seeber (2013) project a 10% speech intelligibility benefit of linked WDRC for a hearing-impaired listener with the stated audiogram (Table 5.1 and 5.2). This hearing-impaired audiogram is used for the present research. The AUDIS HRTFs, used by Wiggins and Seeber (2013), are also used.

3.6 Summary

The present work investigates neural representations of ILD cues due to hearing impairment and aided hearing, which is as of yet unexplored. Edwards (2007) points to modelling studies of this nature as providing valuable insight into both hearing function and algorithms for hearing devices. The benefit of wireless technology has been

demonstrated, but the extent to which ILD cues are restored for binaural use remains in question. The current research can suggest whether (a) ILDs are preserved and available and (b) whether they are salient in neural representations. Further, these computational methods may bypass some of the difficulties inherent in comparing psychophysical studies, reducing the perception of ILDs to a neural model. While individual preferences for bilateral devices undoubtedly vary with factors unrelated to hearing performance, this research may indicate whether wirelessly-linked WDRC, as a suggested improvement over unlinked WDRC, truly has any benefits of note at the most basic neural response.

Chapter 4

Models

In this section, the models developed are described in detail. All models were programmed to run in MATLAB versions 7.14.0.739 and 7.1.0.1. A flowchart of modelling steps (Fig 5.1) is included in Chapter 5.

4.1 Hearing Aid Model

A model of a WDRC hearing aid was implemented in MATLAB with adjustable parameters including attack and release time, compression threshold, and compression ratio. This model uses overlap-and-add digital signal processing techniques to segment the input signal; analyze the frequency content using the in-built fast fourier transfer (FFT) function `fft()`; calculate desired gain and compression; and apply the appropriate amplification in the frequency domain. The overlap-and-add concept is illustrated in Figures 4.1 and 4.2, and allows separate time windows to be filtered consecutively. This method is frequently used in hearing aids to apply compression in the frequency domain, operating window by window (Kates, 2005). An L-length

segment of the sound stimulus, convolved with a finite-length impulse response filter of length P, results in a processed segment of length $L + P - 1$. These new, filtered sections now overlap by $P - 1$ points and must be summed for the final output. The filter length P must be less than L to avoid erroneous overlapping. In this hearing aid model, $P = 1/5\ L$.

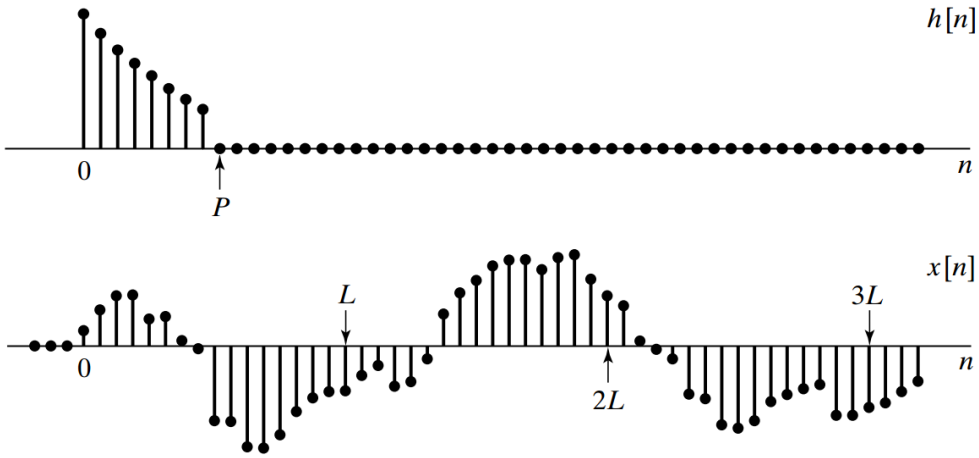

Figure 4.1: *Example overlap-and-add filter (h) and input (x). In this example,* $P = 1/2\ L$. *Figure modified from Oppenheim* et al. *(1999).*

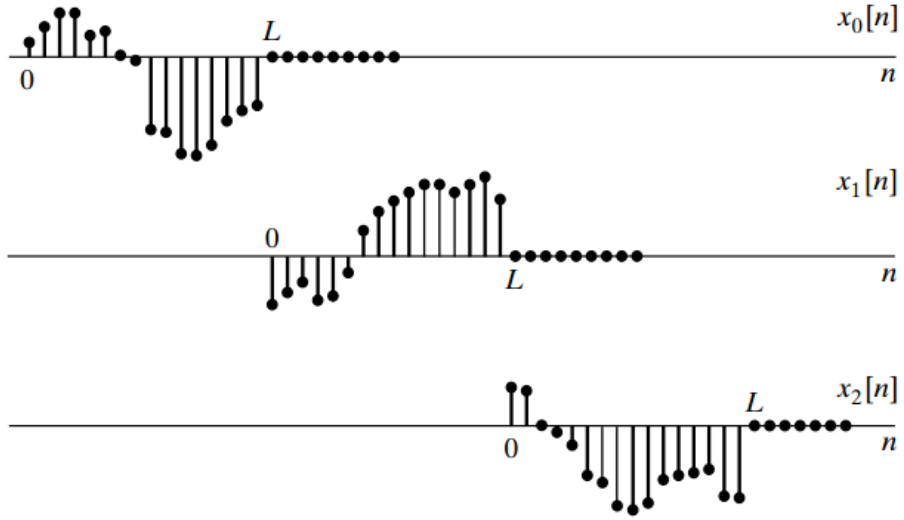

(a)

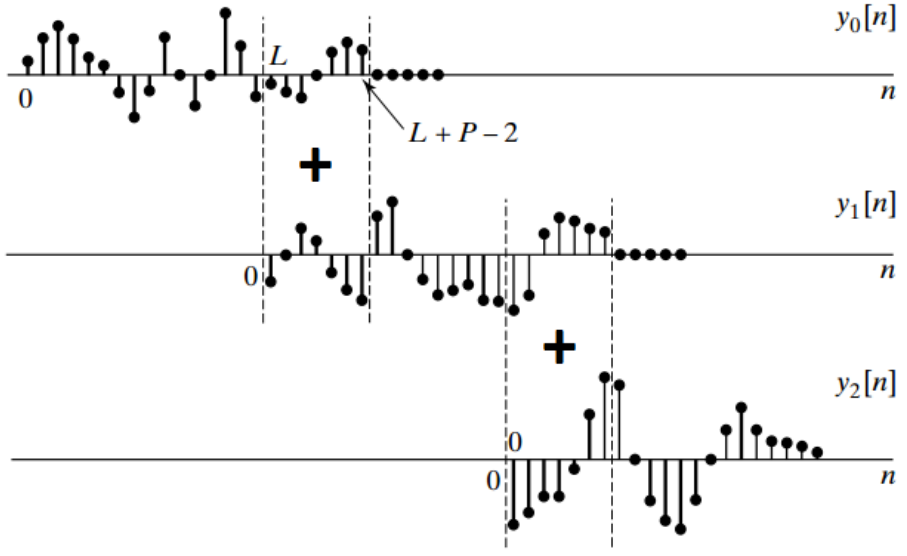

(b)

Figure 4.2: *The overlap-and-add concept. (a): Input segments of length L. (b): Filtered segments y prior to summation. Note the $P-1$ overlap. In this example, $P = 1/2\ L$. Figure modified from Oppenheim* et al. *(1999).*

The WDRC model determines the appropriate real-ear insertion gain (REIG) to apply, the amplification provided by the hearing aid itself. The AUDIS HRTFs, which are used to simulate binaural cues, are measured at 2 mm from the ear drum and thus include the real-ear unaided gain (REUG) resulting from resonances in the ear canal (Blauert, 1997).

The code models a unilateral hearing aid, operating on one signal at a time. A separate script enables synchronization between two instances with no time delay; that is, immediate communication between devices is assumed. With synchronization enabled, the script applies identical gain to both "left" and "right" hearing aid models, based on the lowest required gain of the two. This model is generalizable to some other WDRC systems, although algorithms will differ from the manufacturer's. More complex digital signal processing features such as noise reduction and environment detection are not programmed and are beyond the scope of the present research. When compression ratio is set to 1:1, the code may be used to simulate linear amplification, though it was not used for this purpose in the present work. Attack and release times are fixed as defined (i.e. not adaptive), but may be set by the user. Different sets of attack and release times are used here (see Chapter 5). The algorithm operates as shown in Figure 4.3.

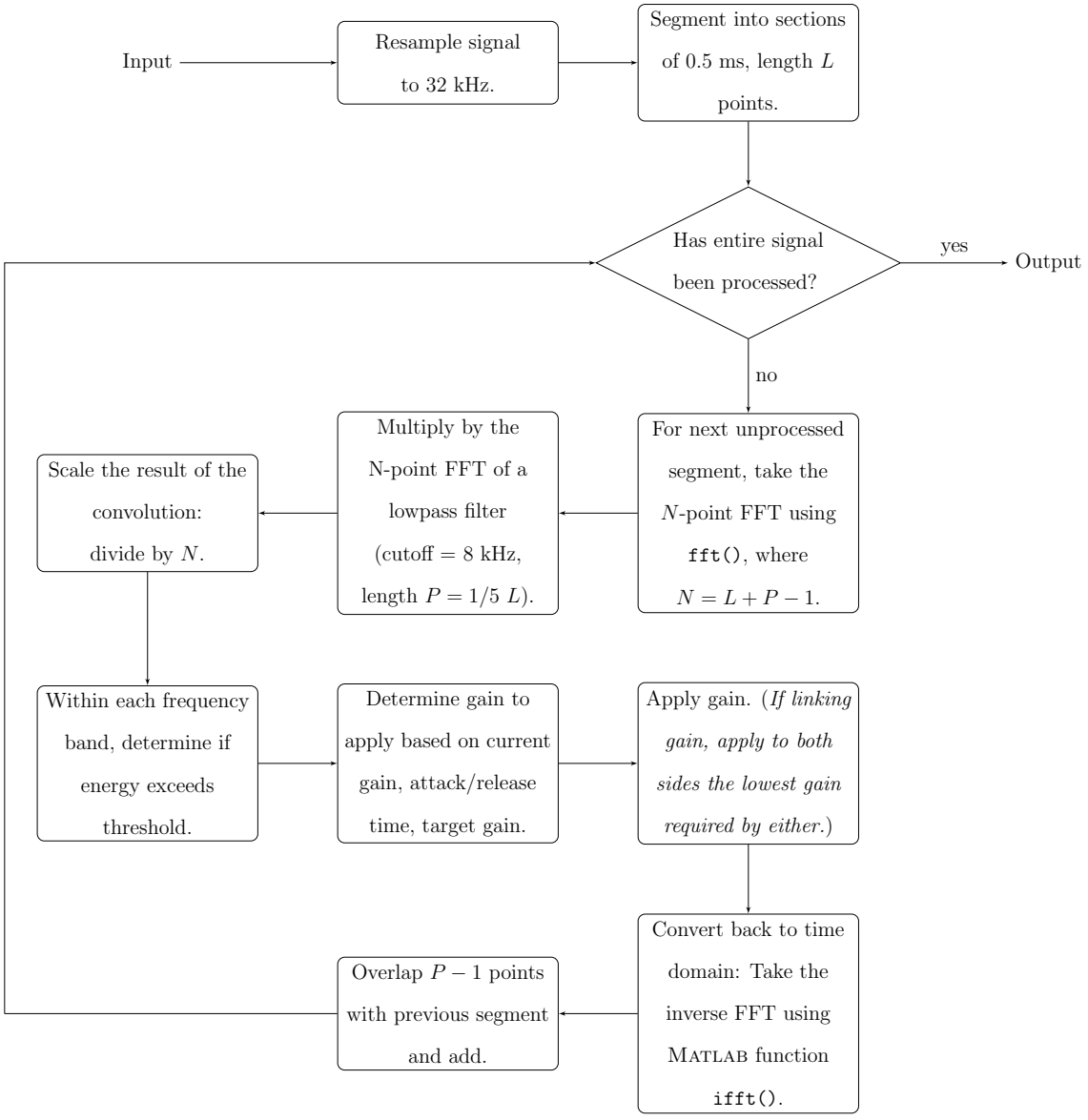

Figure 4.3: *WDRC algorithm.*

4.2 Auditory Periphery Model

An existing model of the auditory nerve was used to simulate AN spike trains (Zilany *et al.*, 2009, 2013, 2014). Spike trains were derived from the outputs of neurons at several CFs, using a modified script by Michael Wirtzfeld. This model is capable of representing normal-hearing and hearing-impaired AN responses corresponding to user-defined audiograms. A previous version of the Zilany *et al.* (2009) model has been used to generate inputs to an LSO model in a study of similar nature (Wang *et al.*, 2014).

The accompanying script was used to generate inner- and outer-hair cell control parameters consistent with the hearing profiles under review. 20 repetitions of the AN spike trains were used for each of the excitatory and inhibitory responses, which were then passed to the LSO models (see Fig 5.1).

Signals passed to this model are sampled at 100 kHz. In the case of outputs from the WDRC model, signals are resampled from 32 kHz to 100 kHz using the MATLAB function `resample()`.

4.3 Lateral Superior Olive Models

Two models of the LSO were developed: a sigmoidal phenomenological model and a Hodgkin–Huxley-type biophysical model. As in Wang *et al.* (2014), both LSO models take direct inputs from the ipsilateral and contralateral AN models, as the AVCN bushy cells and MNTB can be modelled as simple relays.

4.3.1 Sigmoidal Phenomenological Model

The sigmoidal phenomenological model is based upon the observed sigmoidal tuning function of the LSO (Tsai *et al.*, 2010). This function is of the form:

$$y = a + \frac{b}{1 + \exp\frac{c-x}{d}} \tag{4.1}$$

where y is LSO spike rate and x is the difference between contralateral and ipsilateral AN inputs in the form of spike trains from the AN model outputs. Parameters a, b, c, and d are chosen to give spike rate in the order of those described by Tsai *et al.* (2010), using normal-hearing spike train inputs and stimuli of the same level and length as in that study. The values are given in Table 4.1. Within this text, this model will be called the "phenomenological model".

Table 4.1: Parameters of the sigmoidal phenomenological LSO model.

Parameter	Value
a	10
b	140
c	1
d	25

4.3.2 Hodgkin–Huxley-type Biophysical Model

The Hodgkin–Huxley-type biophysical model is more detailed, accounting for ion channel behaviour in the LSO cells. The approach employed here is guided by the work of Wang *et al.* (2014) and Wang and Colburn (2012) and is based upon the ventral cochlear nucleus models of Rothman and Manis (2003). Membrane potential V follows the first-order differential equation:

$$C_m \frac{\mathrm{d}V}{\mathrm{d}t} = I_A + I_{\mathrm{LT}} + I_{\mathrm{HT}} + I_{\mathrm{Na}} + I_h + I_{\mathrm{lk}} + I_{\mathrm{Exc}} + I_{\mathrm{Inh}} \tag{4.2}$$

I_A is a fast-activating K^+ current; I_{LT} is a fast-activating, slow-inactivating, low-threshold K^+ current; I_{HT} is a high-threshold K^+ current; I_{Na} is a Na^+ current; I_h is a hyperpolarization-activated cation current; and I_{lk} is the leakage current (Rothman and Manis, 2003). I_{Exc} and I_{Inh} are the excitatory and inhibitory synaptic currents, derived from the ipsilateral and contralateral AN inputs, respectively. The currents I are listed in Table 4.2, and are in turn functions of conductance parameters. Additional current equations and parameter values are modified from Wang *et al.* (2014) and Wang and Colburn (2012), and given in Appendix C. This model will be referred to within this text as the "biophysical model".

Table 4.2: Currents of the Hodgkin–Huxley-type biophysical LSO model, developed by Rothman and Manis (2003)

Notation	Current Type
I_A	fast-inactivating K^+ current
I_{LT}	low-threshold K^+ current
I_{HT}	high-threshold K^+ current
I_{Na}	Na^+ current
I_h	hyperpolarization-activated cation current
I_{lk}	leakage current
I_{Exc}	excitatory synaptic current (i.e. ipsilateral AN input)
I_{Inh}	inhibitory synaptic current (i.e. contralateral AN input)

To implement this computational model, the MATLAB stiff ODE solver `ode15` was used with maximum step size set to 10 µs.

4.4 Inferior Colliculus Model

The inferior colliculus spike rate response was modelled as a simple difference between LSO contralateral and ipsilateral spike rates outputs, as guided by (Tsai *et al.*, 2010). The IC response examined was taken to be simply:

$$\mathrm{IC} = \mathrm{LSO}_{\mathrm{left}} - \mathrm{LSO}_{\mathrm{right}} \tag{4.3}$$

with negative spike rates implying greater excitation in the right LSO than the left. IC neural representations determined using phenomenological LSO model results may be referred to as "IC phenomenological representations", and those calculated from Hodgkin–Huxley-type LSO model results may be referred to as "IC biophysical representations". Note that the IC model, in all cases, is in itself simply a difference model.

Chapter 5

Methods

This research consisted of two phases: the modelling and analysis of neural representations of localization, and the backwards azimuth decoding of these discharge rate data.

5.1 Phase 1: Modelling Neural Representations

In the first phase of this research, neural responses were modelled using the algorithms described in Chapter 4. Figure 5.1 outlines the steps undertaken to generate neural responses; dashed lines indicate the order of models used in the hearing-impaired simulations, and solid lines the order of models for the normal-hearing. Phenomenological LSO models and stimulus generation were conducted in MATLAB version 7.14.0.739 in a Windows environment. For time efficiency, the AN model and Hodgkin–Huxley-type biophysical LSO model were simulated on the Department of Electrical and Computer Engineering's Sun Grid Engine, which runs MATLAB version 7.1.0.183 in Linux.

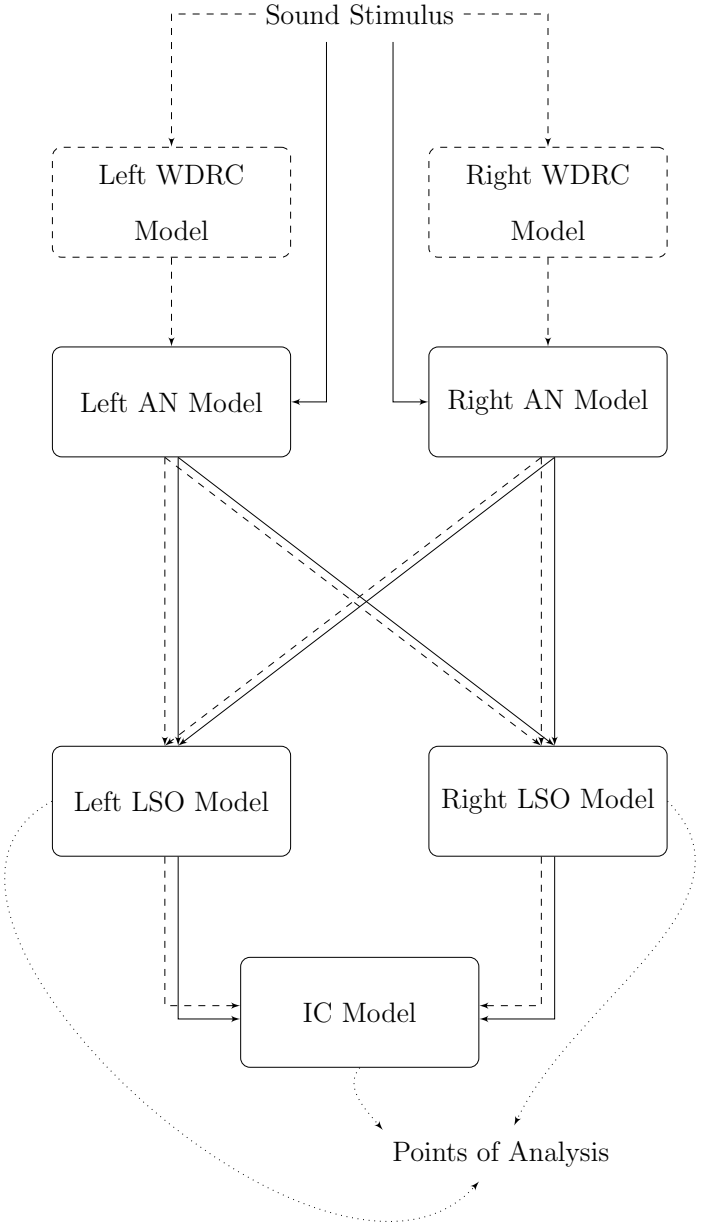

Figure 5.1: *Flowchart of modelling methods. Dashed lines indicate steps for the aided conditions, and solid lines those for the unaided condition. Left and right AN models synchronize gain when linked.*

5.1.1 Stimuli

Modelled neural responses were collected on two different types of stimuli: a 2-s, 4000-Hz sinusoid, sampled at 100 kHz; and a recording of speech from the TIMIT corpus (Garofolo *et al.*, 1993). The sinusoidal stimulus was chosen to enable direct comparisons between normal-hearing and hearing-impaired responses at a pure tone, and to establish the sufficiency of WDRC gain for this simple sound input. The TIMIT phrase chosen is from the training set (TRAIN_ DR2_ FAEM0) and features a female talker with a Northern (American) dialect, speaking:

"She had your dark suit in greasy wash water all year."

The TIMIT sentence contains phones from 7 classes: fricatives, affricatives, stops, semivowels/glides, nasals, vowels, and stop closures. Also included is a short epenthetic silence. The start and end times of these phones are listed in Table A.1 of Appendix A.

The TIMIT stimuli were resampled from 16 kHz to 100 kHz while the sinusoidal stimuli were generated at 100 kHz. Where aided conditions were simulated, these inputs are resampled to 32 kHz for processing by the WDRC model, with those outputs then resampled to 100 kHz. The sinusoid stimulus was presented at six different sound levels: 35, 45, 55, 65, 75, and 85 dB SPL, with a 5-ms on and off ramp. The TIMIT speech was presented as obtained from the database, with no modifications to sound level or length, and resampled from 32 kHz to 100 kHz. Thus, seven stimulus signals were used in total, each at 25 azimuths around the head, as shown in Figure 5.2.

To simulate interaural level differences, signals were convolved with head-related transfer functions (HRTFs) from the AUDIS database (Blauert *et al.*, 1998). Inputs were scaled so that left and right sound levels would have the presentation intensity (i.e. 35, 45, 55, 65, 75, 85 dB SPL) at 0°.

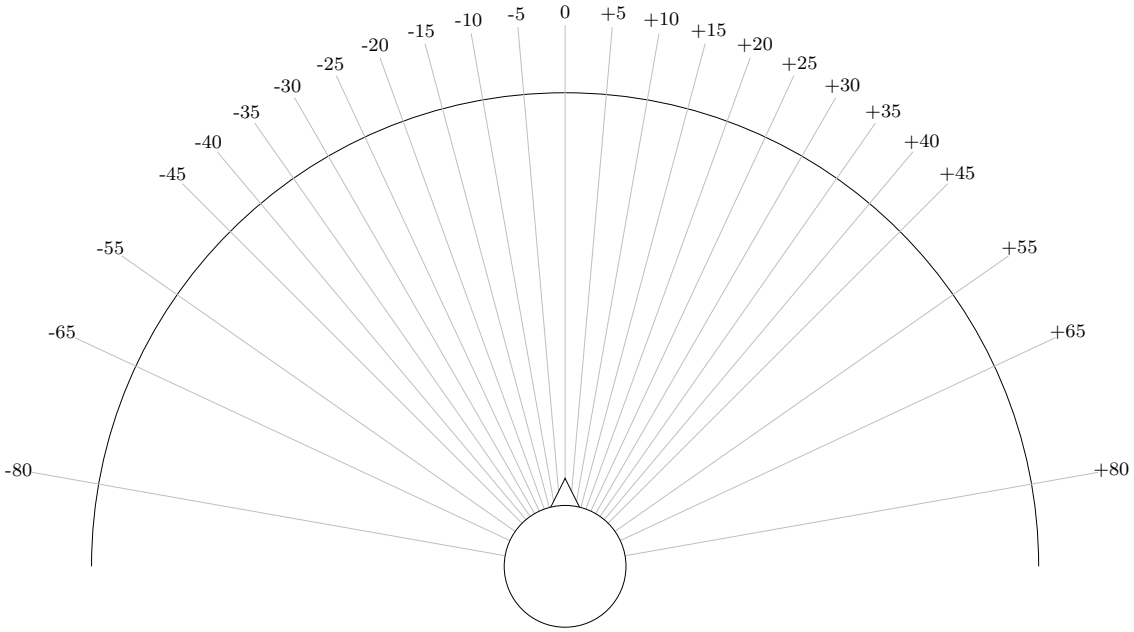

Figure 5.2: *Azimuths of stimulus presentation.*

5.1.2 Test Conditions

Two audiograms of hearing ability were used: one for an ideal normal-hearing listener experiencing no hair cell damage whatsoever, and one for a hearing-impaired listener with symmetrical loss, from (Wiggins and Seeber, 2013). The latter audiogram is the standard N_3 audiogram from Bisgaard *et al.* (2010) and represents moderate sensorineural hearing impairment. This audiogram reflects the most typical degree of loss of the 28244 ears measured for the standardization (Bisgaard *et al.*, 2010).

The hearing-impaired audiogram was originally used by Wiggins and Seeber (2013) to predict speech intelligibility scores for a hearing-impaired listener, using linked and unlinked WDRC hearing aids with CAMEQ fit. Thus, this particular audiogram (Table 5.1) and prescription (Table 5.2) were apt for the current study purposes. The compression thresholds set by this fitting are shown in Figure 5.3.

Table 5.1: N_3 audiogram, from Wiggins and Seeber (2013) and Bisgaard *et al.* (2010).

Audiogram										
Frequency (Hz)	250	375	500	750	1000	1500	2000	3000	4000	6000
dB HL	35	35	35	35	40	45	50	55	60	65

Table 5.2: CAMEQ hearing aid prescription, as set by Wiggins and Seeber (2013).

Channel	Lower Edge Frequency	Upper Edge Frequency	Compression Threshold	Compression Ratio	IG50	IG80
1	125	250	46	1.53	10.2	0.0
2	250	750	47	1.11	10.3	7.4
3	750	1250	40	1.99	20.8	5.9
4	1250	1750	30	1.89	20.5	6.4
5	1750	2250	27	1.98	22.9	8.0
6	2250	2750	28	2.01	21.7	6.6
7	2750	3250	27	1.99	20.7	5.8
8	3250	3750	24	1.99	21.4	6.5
9	3750	4250	20	2.01	22.2	7.1
10	4250	4750	22	2.22	21.6	5.1
11	4750	5250	21	2.51	20.8	2.8
12	5250	5750	22	2.80	20.2	1.0

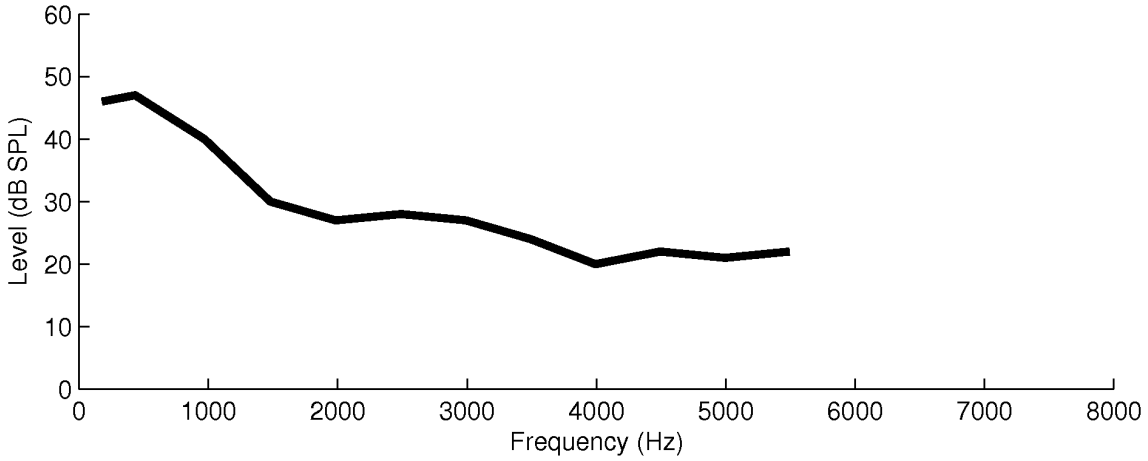

Figure 5.3: *Compression thresholds in the Wiggins and Seeber (2013) CAMEQ fit.*

For the normal-hearing model, all seven stimuli were applied without WDRC. For the hearing-impaired model, three hearing aid conditions were tested: no WDRC, unlinked WDRC, and linked WDRC for the seven stimuli. For sinusoidal inputs in the unlinked and linked WDRC conditions, Wiggins and Seeber (2013) compression parameters were employed. For TIMIT speech in the unlinked and linked WDRC cases, a further three compression time conditions were conducted: fast attack and release times as used by Wiggins and Seeber (2013) ("WS", 5-ms attack and 60-ms release); very fast attack and release times ("Very Fast", 1-ms attack and 10-ms release); and slow attack and release times ("Slow", 100-ms attack and 400-ms release). These attack and release times follow the ANSI S3.22 standard (ANSI, 2003). Very Fast and Slow conditions were chosen to be consistent with parameters for decreasing inter-syllabic differences and reducing long-term level variances, respectively (Dillon, 2001). The WS attack and release times provide fast-acting compression consistent with decreasing inter-syllabic differences, so the choice of Very Fast parameters allows for an interesting comparison of efficacy within hearing goals (Wiggins and Seeber,

2011). An investigation using a similar range of attack and release times has been conducted before. In a study of various WDRC parameters on the JND for 71% correct lateralization, Musa-Shufani *et al.* (2006) used 500 ms release time and used attack times of 2 ms, 20 ms, and 200 ms to represent very fast, fast, and slow schemes, respectively. In practice, the longer the attack time, the greater the interaction between ILDs of different sound sources; however, for very long attack times greater than a second, ILD cues stabilize (Schwartz and Shinn-Cunningham, 2013).

For the sinusoidal stimulus, the tests performed total 3600 (6 stimulus levels x 4 hearing aid conditions x 25 azimuths), where the 4 hearing conditions are:

1. Normal-hearing
2. Hearing-impaired, no WDRC
3. Hearing-impaired, unlinked WS WDRC
4. Hearing-impaired, linked WS WDRC.

For the TIMIT stimulus, the tests performed total 200 (1 speech sentence x 8 hearing and compression time conditions x 25 azimuths), where the 8 hearing conditions are:

1. Normal-hearing
2. Hearing-impaired, no WDRC
3. Hearing-impaired, unlinked WS WDRC
4. Hearing-impaired, linked WS WDRC
5. Hearing-impaired, unlinked Very Fast WDRC

6. Hearing-impaired, linked Very Fast WDRC

7. Hearing-impaired, unlinked Slow WDRC

8. Hearing-impaired, linked Slow WDRC.

Table 5.3: Test conditions. P denotes use of the physiological LSO model and B of the biophysical LSO model.

Stimulus		Normal-Hearing	Hearing-Impaired						
			No WDRC	Unlinked WDRC			Linked WDRC		
				WS	Very Fast	Slow	WS	Very Fast	Slow
Sinusoid	35 dB SPL	P/B	P	P			P		
	45 dB SPL	P	P	P			P		
	55 dB SPL	P	P	P			P		
	65 dB SPL	P/B	P	P			P		
	75 dB SPL	P	P	P			P		
	85 dB SPL	P/B	P	P			P		
TIMIT Speech		P	P	P	P	P	P	P	P

For all test conditions in Table 5.3, results were generated using the phenomenological LSO model. In the interest of time and computational efficiency, the biophysical LSO model was used with puretone stimuli at 35, 65, and 85 dB SPL in the normal-hearing condition only, in order to verify the robustness of both models.

5.1.3 Data Analysis

Each stimulus presentation resulted in a neural response of spike rates across 128 CFs, forming a 1-by-128 matrix of data. The 25 azimuth presentations per stimulus introduced a second dimension, giving 25-by-128 matrices for each stimulus for a given hearing condition. Neural responses were then interpolated between $-80°$ and $80°$ in intervals of $1°$ for a total of 161 azimuths. Colour maps of these 161-by-128 discharge rate matrices were examined for trends in stimulus level, azimuth, and hearing condition.

In addition, the mean difference in neural spike rate was calculated between each hearing-impaired response (three compression conditions for the sinusoidal stimulus, seven for the TIMIT sentence) and the normal-hearing response for the same stimulus and azimuth. This measure was obtained by subtracting each hearing-impaired matrix of 1-by-128 spike rates from the corresponding normal-hearing matrix of 1-by-128 spike rates, taking the mean across the 128 CF rate differences. The mean difference quantifies the benefit of the hearing-impaired conditions. It can be interpreted as the degree of similarity between a hearing-impaired response and the normal-hearing response expected for correct localization of that stimulus.

These analyses were performed for all phenomenological model LSO data. Mean difference was also used to compare phenomenological and biophysical IC responses to the 35, 65, and 85-dB SPL sinusoids.

5.2 Phase 2: Neural Decoders

Two neural decoders were programmed in MATLAB and trained to predict the perceived stimulus from a neural response. Decoders were only trained and tested on neural representations from the same model type (i.e. phenomenological model or biophysical model), but were used for both IC and LSO neural representations.

5.2.1 Simple Least Squares Decoder

A simple predictor was created by solving the least-squares problem that maps the normal-hearing, 65-dB SPL IC response (ic) to azimuths (azim) of that stimulus, using phenomenological model data. N and A are the maximum CF and azimuth counts, respectively. x is the mapping function.

$$\text{azim} = \text{IC} \cdot \text{x} \tag{5.1}$$

$$\text{IC} = \begin{pmatrix} \text{ic}_{1,1} & \text{ic}_{1,2} & \dots & \text{ic}_{1,\text{N}} \\ \text{ic}_{2,1} & \text{ic}_{2,2} & \dots & \text{ic}_{2,\text{N}} \\ \vdots & \vdots & \ddots & \vdots \\ \text{ic}_{A,1} & \text{ic}_{A,2} & \dots & \text{ic}_{A,\text{N}} \end{pmatrix} \tag{5.2}$$

5.2.2 Neural Population Pattern Decoder

A more advanced predictor was also used, guided by the methods of Day and Delgutte (2013) and Jazayeri and Movshon (2006). This predictor is a log likelihood function, formed by weighting individual neuron tuning functions by their spike rate. The tuning function $f_i(\theta)$ is the mean spike rate as a function of azimuth for an IC neuron i, representing the excitation for a particular CF. The term n_i is the spike rate of the corresponding IC neuron i in the IC response to be decoded.

$$\log L(\theta) = \sum_{i=1}^{N} n_i f_i(\theta) - \sum_{i=1}^{N} f_i(\theta) \tag{5.3}$$

This log likelihood model can be used for detection, identification, and discrimination tasks, and has been used for decoding of auditory and visual neural reponses (Day and Delgutte, 2013; Jazayeri and Movshon, 2006).

Chapter 6

Results

For all stimuli, right and left LSO phenomenological model responses are exact mirror images of one other, as can be seen in the normal-hearing response to a 65-dB SPL, 4000-Hz puretone in Figure 6.5. All discharge rates are given in spikes/s. Reduced responses at CFs between 2 to 3 kHz are an effect of the notched filtering of frequencies in this range by the human middle-ear model. An in-depth discussion of possible implications and conclusions follows this chapter.

6.1 ILD Cues for Puretone Stimuli

Natural ILD cues (filled dots) are independent of presentation level (clearly seen in Figure 6.1), and linked WDRC (open circles) fully preserves ILD, despite overall changes in sound level. Unlinked WDRC diminishes ILD cues, as seen in Figure 6.2. For all sound presentation levels but the 35 dB SPL input, inputs to the left and right hearing aids always triggered compression. With the 35 dB SPL input, sounds at some azimuths were above the compression threshold in one ear but below compression

threshold (and in the linear amplification region) in the other. As a result, unlinked ILD cues were the same for sound presentation levels of 45, 55, 65, 75, and 85 dB SPL, but larger for the 35 dB SPL puretone at larger azimuths. An example of this effect is illustrated in 6.3, where gain is linearly 30 dB below the compression threshold of 40 dB SPL. Above this threshold, the compression ratio is 2:1. An ILD of 20 dB SPL, above compression threshold, results in an output ILD of 10 dB SPL (shown in green and red). However, if an ILD of 20 dB SPL is established by one input above threshold and one below, the output ILD is greater than 10 dB SPL (shown in blue). The pattern of ILD increase with azimuth holds for linked compression as it does with no compression at all. ILD is largest at 65° before decreasing at 80°, due to the amplification effects of the pinna.

Figure 6.4 shows left and right sound levels for each of the six puretone stimulus presentation levels. Blue denotes levels of the left signal and red denotes levels right signal. As presentation level increases, the amount of gain applied to the natural signal (dots) is reduced, due to dynamic range compression. With linked compression (open circles), the louder of the left or right signals is amplified by the same gain as it would be in the unlinked compression condition (asterisks). Because the hearing aids are synchronized, this gain is also applied to the quieter of the left or right signals in the linked condition to maintain ILD.

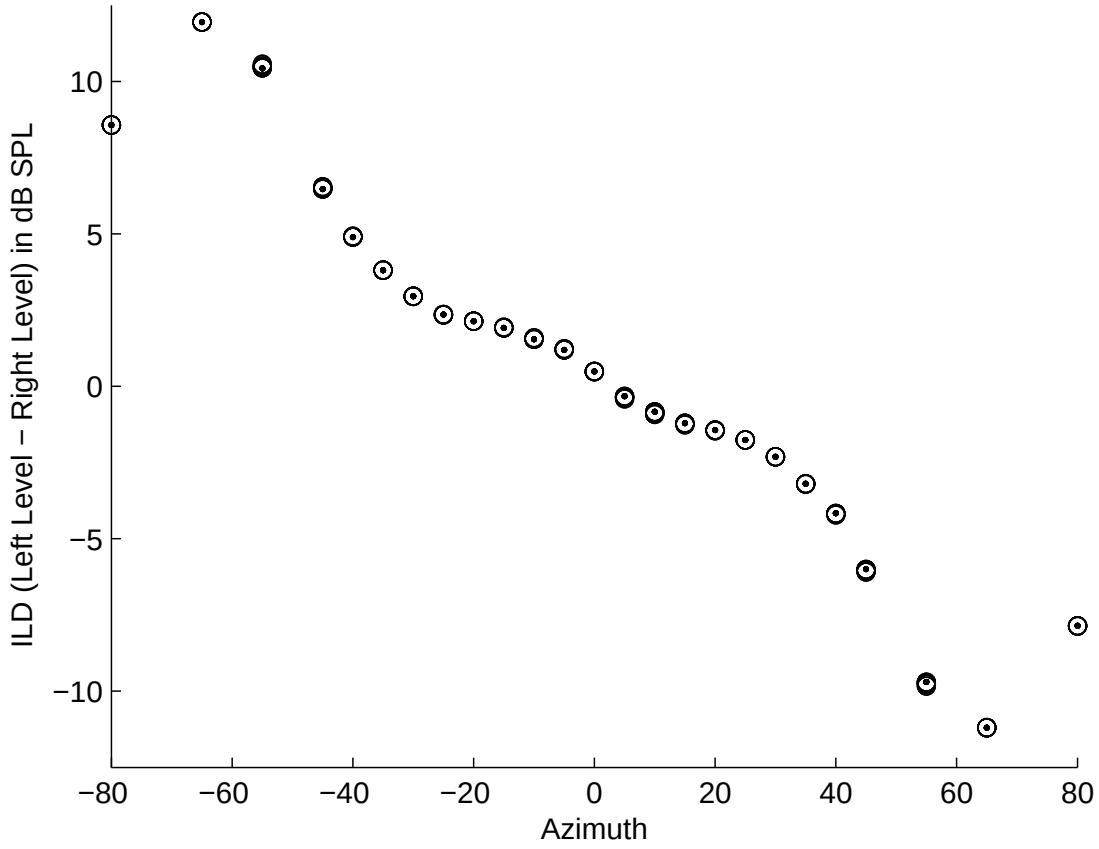

Figure 6.1: *Natural ILD cues (dots) do not change with presentation level, but vary with azimuth, becoming larger with increasing azimuth up to 65°. ILD then decreases at 80°. Linked WDRC (open circles) fully preserves ILD cues.*

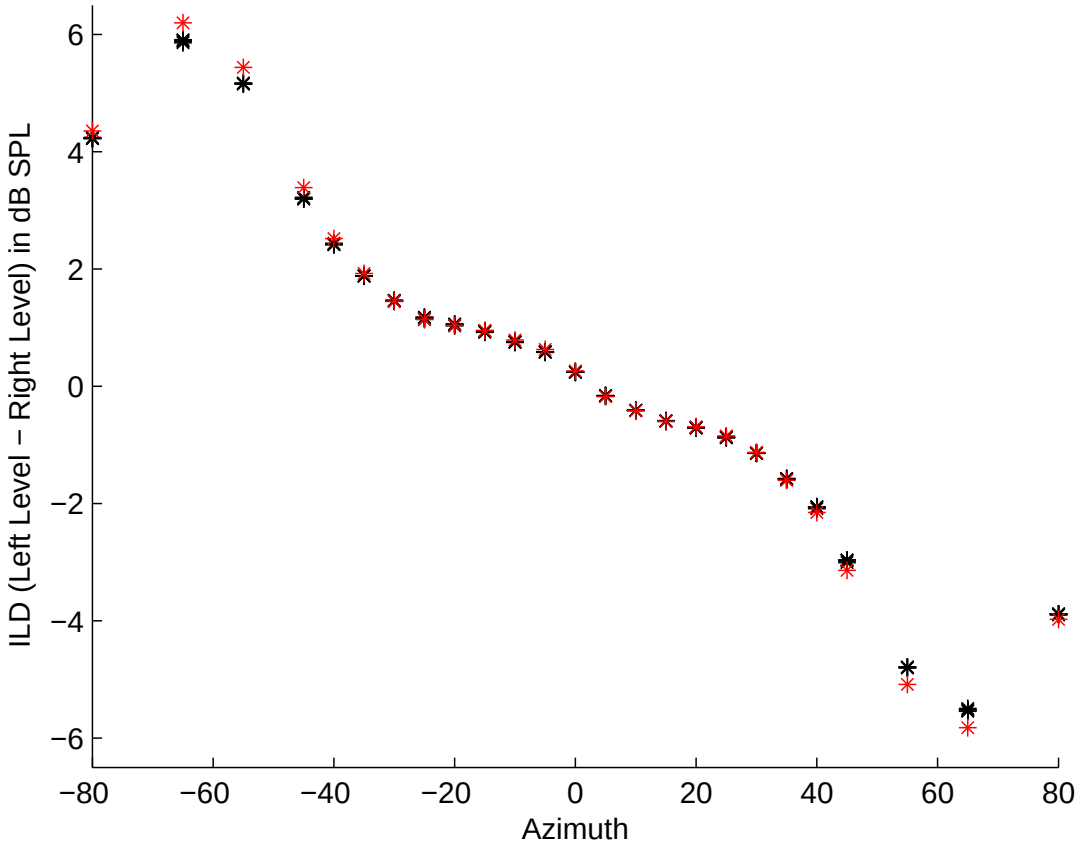

Figure 6.2: *Unlinked WDRC diminishes ILD cues. As in the natural and linked WDRC cases, ILD varies with azimuth, becoming larger with increasing azimuth up to 65°. ILD then decreases at 80°. Red: 35 dB SPL; Black: all other presentation levels.*

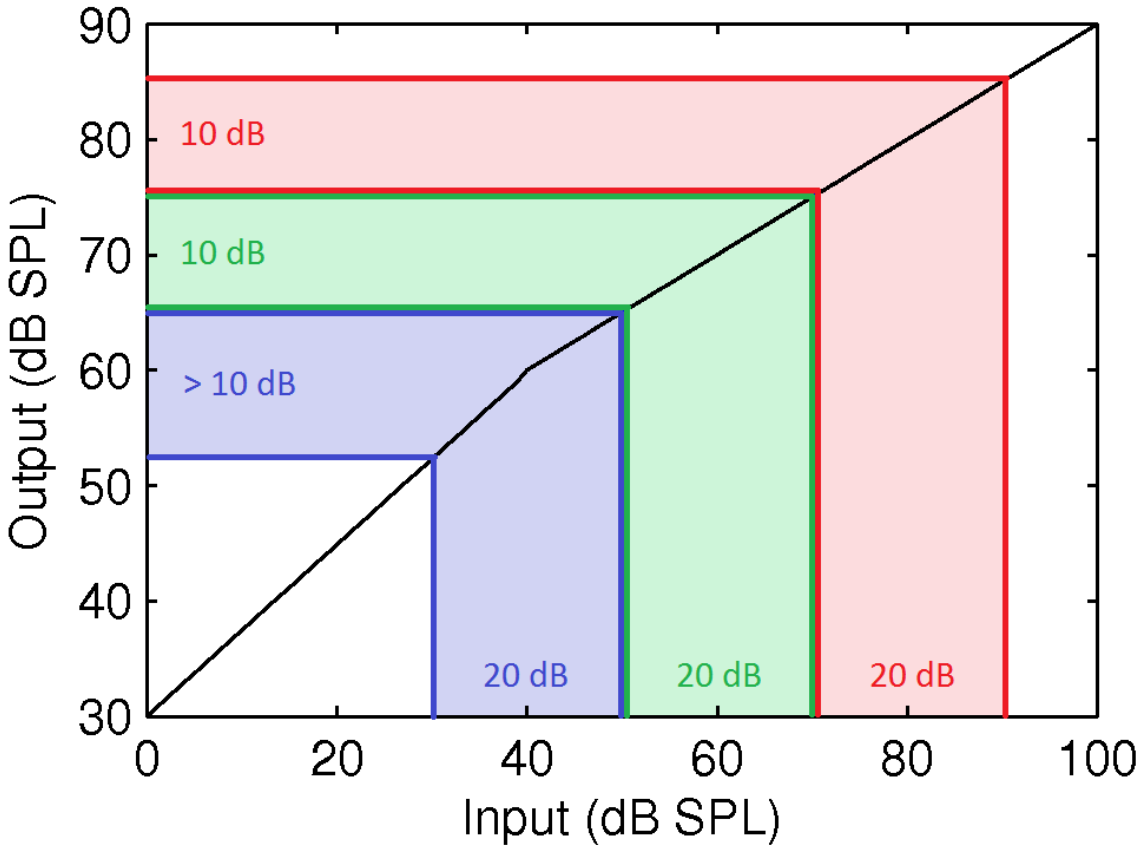

Figure 6.3: *For the same input ILD, output ILDs will be the same if both left and right inputs are above threshold (green, red) but greater if one input is above threshold and one below (blue). Compression threshold = 40 dB SPL, compression ratio = 2:1, Linear gain = 30 dB SPL.*

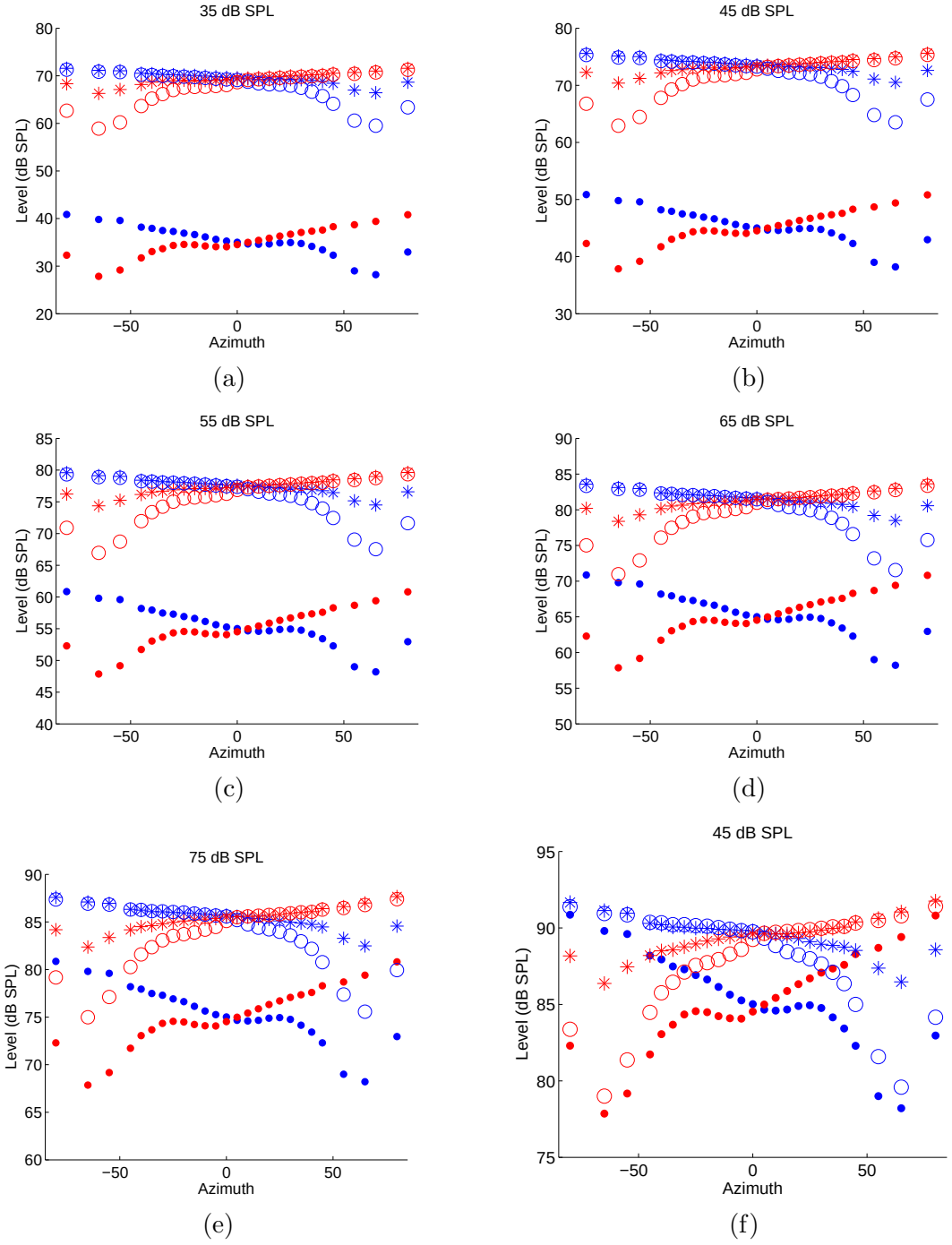

Figure 6.4: *Puretone stimulus levels before and after WDRC. Blue denotes levels of input to the left AN model and red to the right. Dots, asterisks, and open circles denote no compression, unlinked compression, and compression conditions respectively. (a): 35 dB SPL; (b): 45 dB SPL; (c): 55 dB SPL; (d): 65 dB SPL; (e): 75 dB SPL; (f): 85 dB SPL.*

6.2 Puretone Neural Representations: Phenomenological Model

Unless otherwise indicated, all phenomenological LSO and IC colour maps for puretone stimuli shown are taken from the time period 1 s to 1.5 s, in order to avoid on-ramp, off-ramp, and attack/release-time effects. This isolates the neural representation of the final, compressed level only.

Discharge rates away from the CF vary with azimuth, becoming maximal near 65° due to amplification by the pinna. This result is consistent at all presentation levels. In the normal-hearing representations, the relationship between excitation and sound level is particularly obvious. Figure 6.5 shows left and right phenomenological LSO model responses to a 65 dB SPL puretone for the normal-hearing listener model. At the tone frequency, left and right AN responses are saturated at all azimuths of presentation (see AN spike rates in Figure 6.6). The LSO, taking the excitatory inputs from one and inhibitory from the other, settles to a moderate spike rate response. For CFs away from the puretone frequency, AN excitation not saturated so that differences in left and right input levels, due to azimuth, produce higher AN spike rate on the ipsilateral side and lower AN spike rate on the contralateral side. In the LSO response (Figure 6.5), these unsaturated excitatory and inhibitory inputs result in flanking regions of excitation that spread away from the puretone frequency.

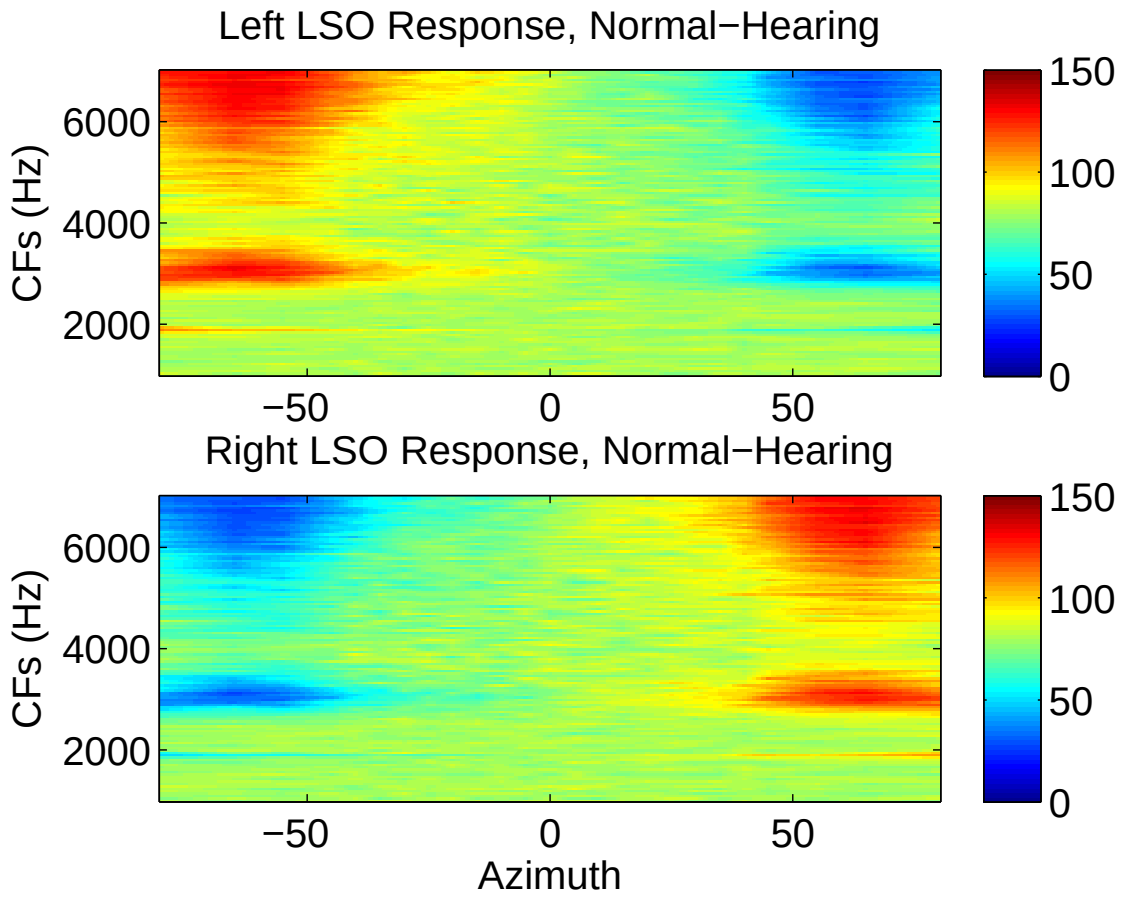

Figure 6.5: *Left and right phenomenological LSO model responses are mirror images of one another. Discharge rate is in spikes/s. Stimulus: 4000-Hz sinusoid, 65 dB SPL. Response is taken from 1 s to 1.5 s to isolate the neural representation of the final, compressed level. Note the moderate response due to AN saturation at CF = 4000 Hz.*

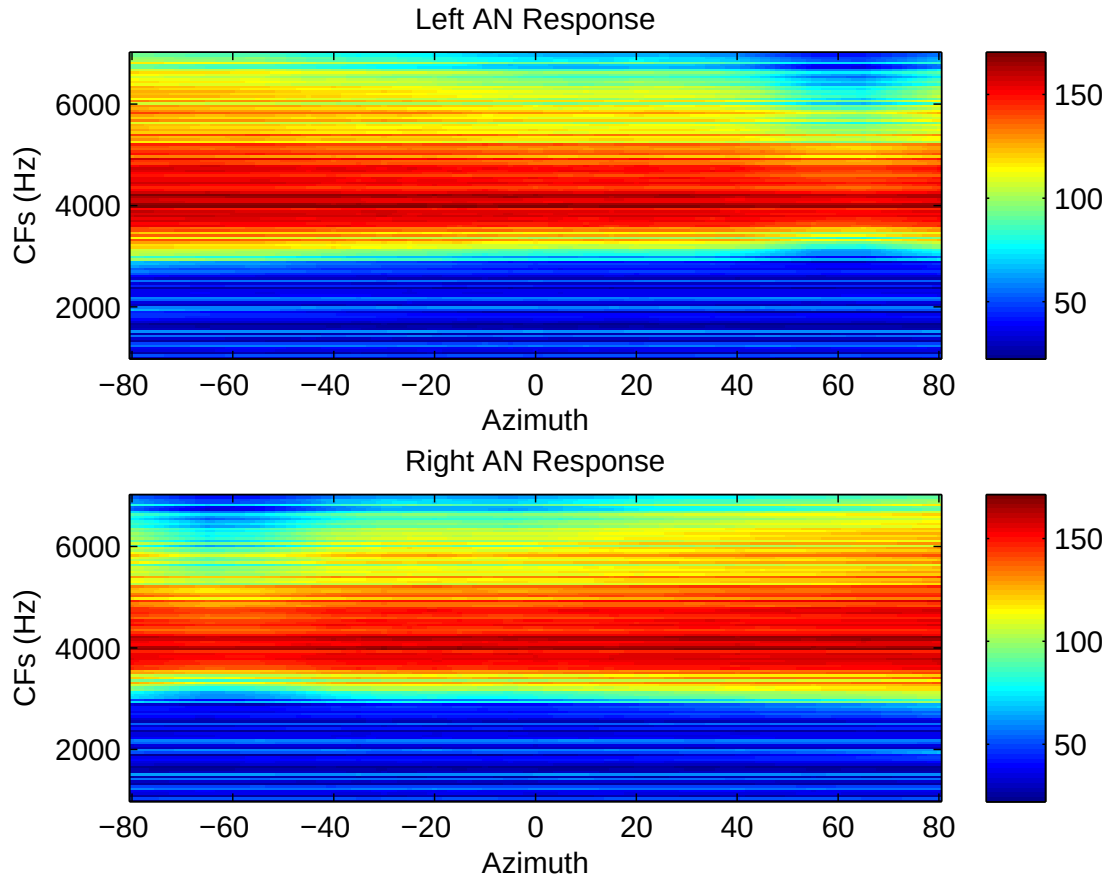

Figure 6.6: *Normal-hearing AN spike rates (spikes/s) for a 65 dB SPL puretone. Note the moderate response due to AN saturation of left and right AN responses at CF = 4000 Hz for all azimuths.*

Discharge rates for the normal-hearing model are higher than those for any of the hearing-impaired hearing conditions (unaided, unlinked, and linked), though there are still regions of excitation away from the tone frequency. An example of this can be seen in the phenomenological LSO responses to a 65 dB sinusoid in Figure 6.7. Figure 6.8 shows AN spike rates for the hearing-impaired, linked model, presented with the same stimulus. There is no saturation at the tone frequency, and this is reflected in the LSO responses of Figure 6.7 (d).

With higher presentation levels, areas of higher and lower excitation spread outward from the saturated region near the tone frequency of 4000 Hz. As sound level increases, the region of saturation expands across nearby CFs. The flanking regions of higher and lower spike rate also spread away from the tone CF. Colour maps for all other puretone presentation levels than 65 dB SPL are given in Appendix D, and the effect can also be seen in the IC data of Figure 6.11.

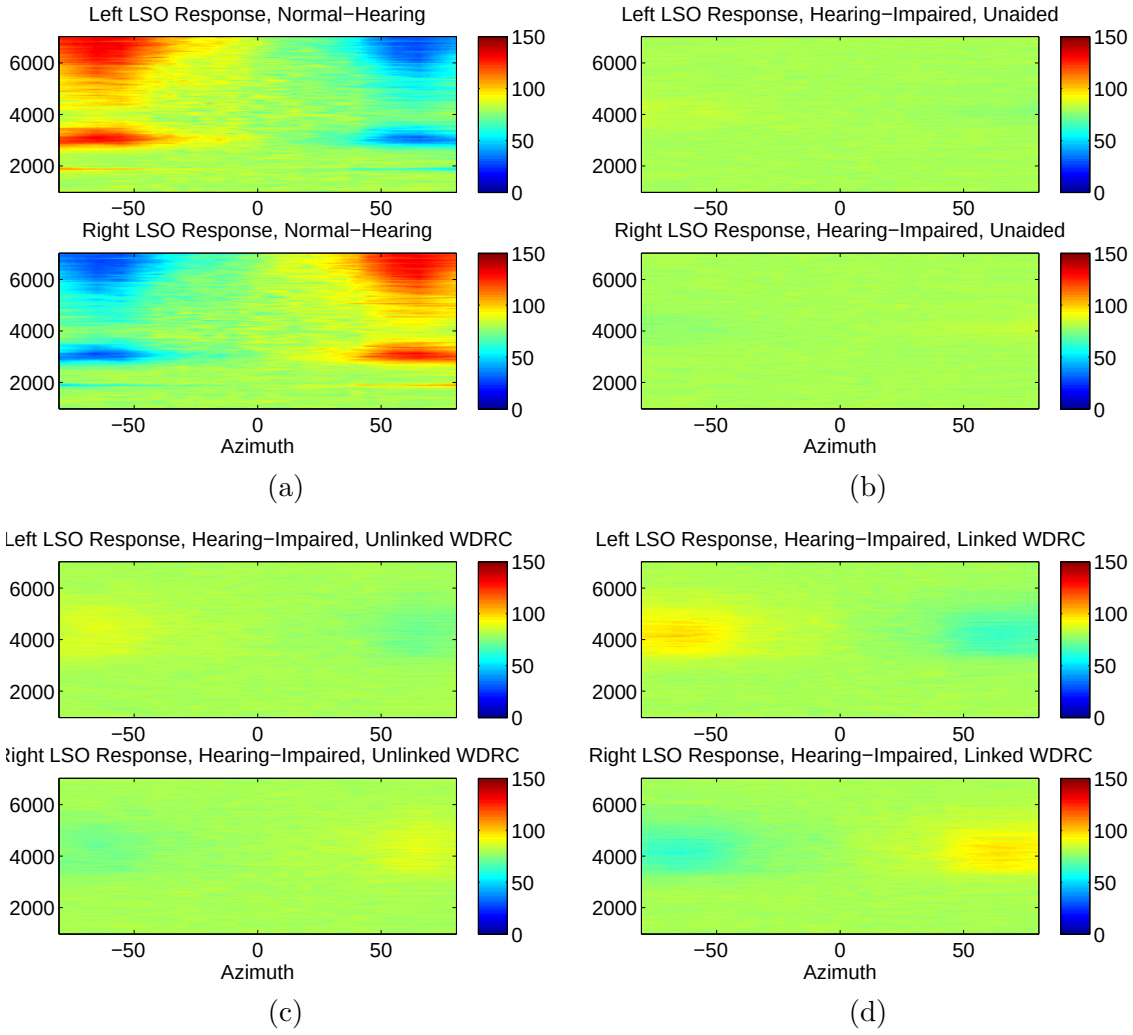

Figure 6.7: *Normal-hearing discharge rates exceed those in all hearing-impaired conditions. Stimulus: 4000-Hz sinusoid, 65 dB SPL. 4000-Hz saturation is absent in the hearing-impaired neural representations. (a): normal-hearing; (b): hearing-impaired, unaided; (c): hearing-impaired, unlinked WDRC; (d): hearing-impaired, linked WDRC.*

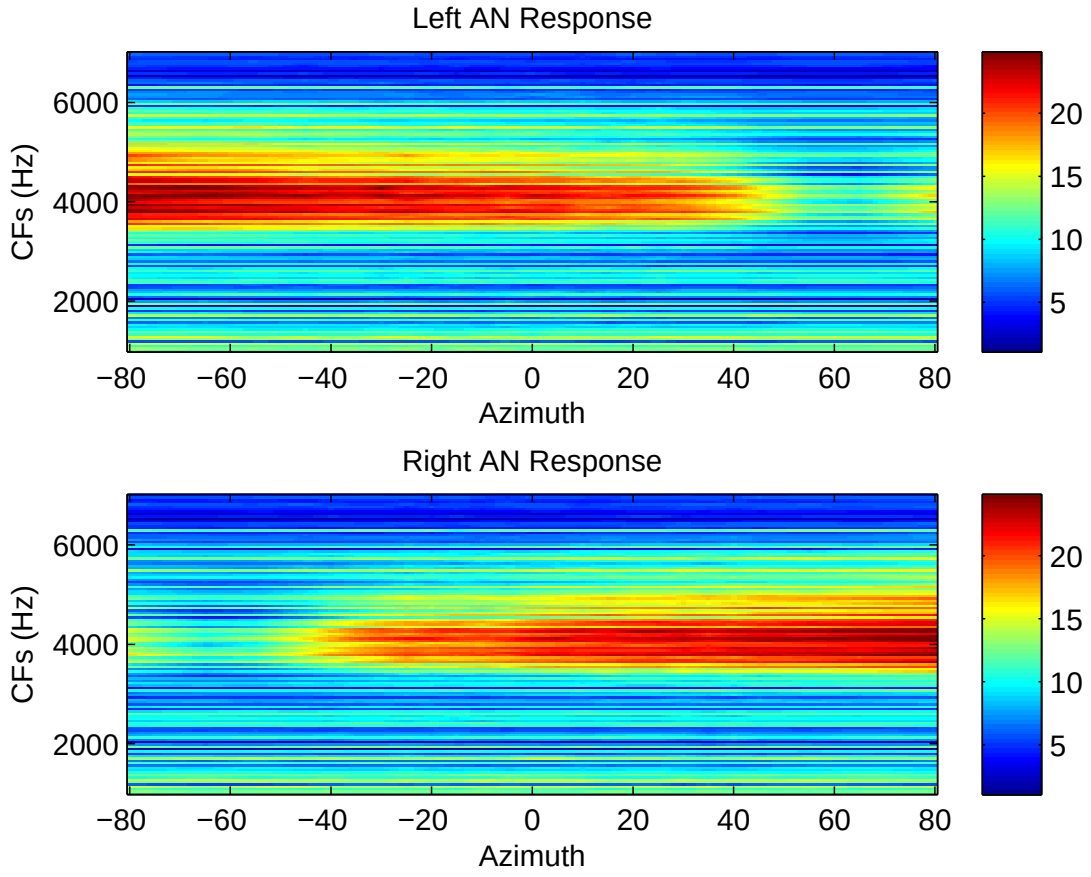

Figure 6.8: *Linked, hearing-impaired AN spike rates (spikes/s) for a 65 dB SPL puretone. Note the absence of AN saturation at CF = 4000 Hz.*

The mean difference reveals some interesting results in the case of puretone stimulus representations in the LSO. Discharge rates for the hearing-impaired neural responses are subtracted from the normal-hearing responses to the same stimulus. This measure can be interpreted as demonstrating the extent of difference to which hearing-impaired conditions produce lower spike rates than normal-hearing. Mean differences closer to zero infer closer hearing-impaired performance to that of normal-hearing, suggesting greater WDRC benefit.

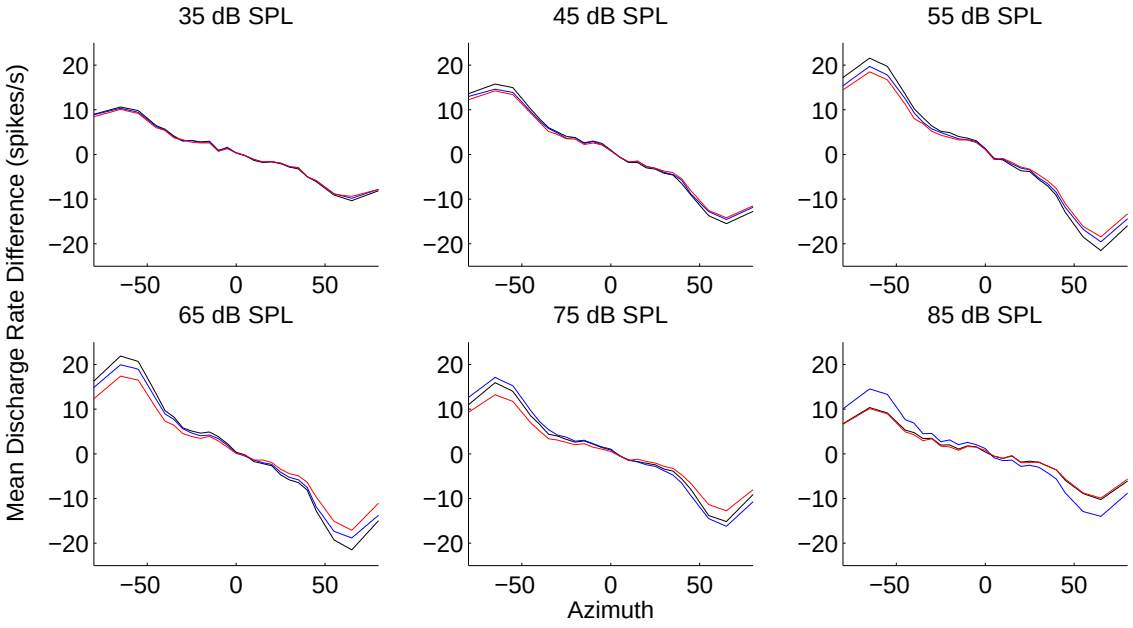

Figure 6.9: *LSO mean differences under the phenomenological model in spikes/s. The following hearing-impaired neural representations are subtracted from the normal-hearing response, and denoted as follows:- Black: unaided; Blue: unlinked WS WDRC; Red: linked WS WDRC.*

For the 35, 45, 55, and 65-dB SPL stimuli, the response is stronger in the linked condition than in both other hearing-impaired conditions. This effect seems to be strongest near 65 dB SPL, where performances between linked, unlinked, and unaided conditions seem to differ most. Away from a 65-dB SPL presentation level, the impact of WDRC condition seems to diminish, such that all hearing-impaired conditions perform equally similarly or differently to normal-hearing at 35 dB SPL. Interestingly, at 85 dB SPL, linked and unaided WDRC produce similar mean discharge rate scores. At this presentation level, higher unlinked mean discharge rates indicate that this compression condition introduces differences between normal-hearing and hearing-impaired responses, rather than reducing them. This is clear from Figure 6.10. At all presentation levels, the impact of WDRC on neural response increases as ILD increases (see also Figure 6.1 and Figure 6.2).

The basic IC difference model (left LSO discharge rate minus right LSO discharge rate) shows spike rate dependence on presentation level, despite ILD cues remaining the same. Figure 6.11 demonstrates IC neural responses in the normal-hearing model for all six stimulus levels. As presentation level increases in the normal-hearing listener, the discharge rate away from the puretone frequency (4000 Hz) increases and the region of saturation expands. Similar patterns are shown in the hearing-impaired models (Appendix D). It should be noted that maximum and minimum discharge rate do not appear to change with presentation, even between the lowest and highest sound levels examined. Rather, the spread of excitation varies.

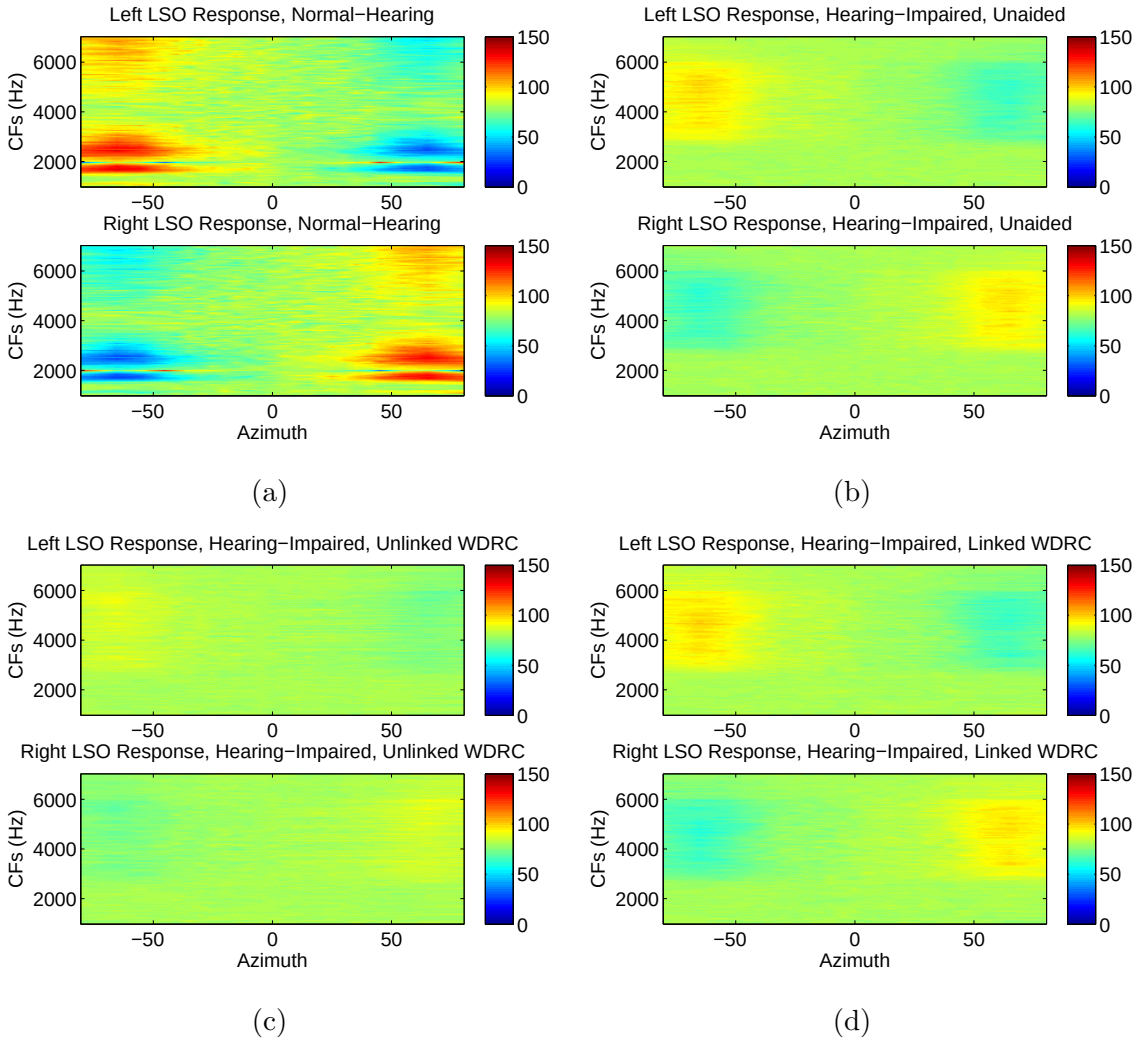

Figure 6.10: *Normal-hearing discharge rates exceed those in all hearing-impaired conditions. Stimulus: 4000-Hz sinusoid, 85 dB SPL. 4000-Hz saturation is absent in the hearing-impaired neural representations. (a): normal-hearing; (b): hearing-impaired, unaided; (c): hearing-impaired, unlinked WDRC; (d): hearing-impaired, linked WDRC.*

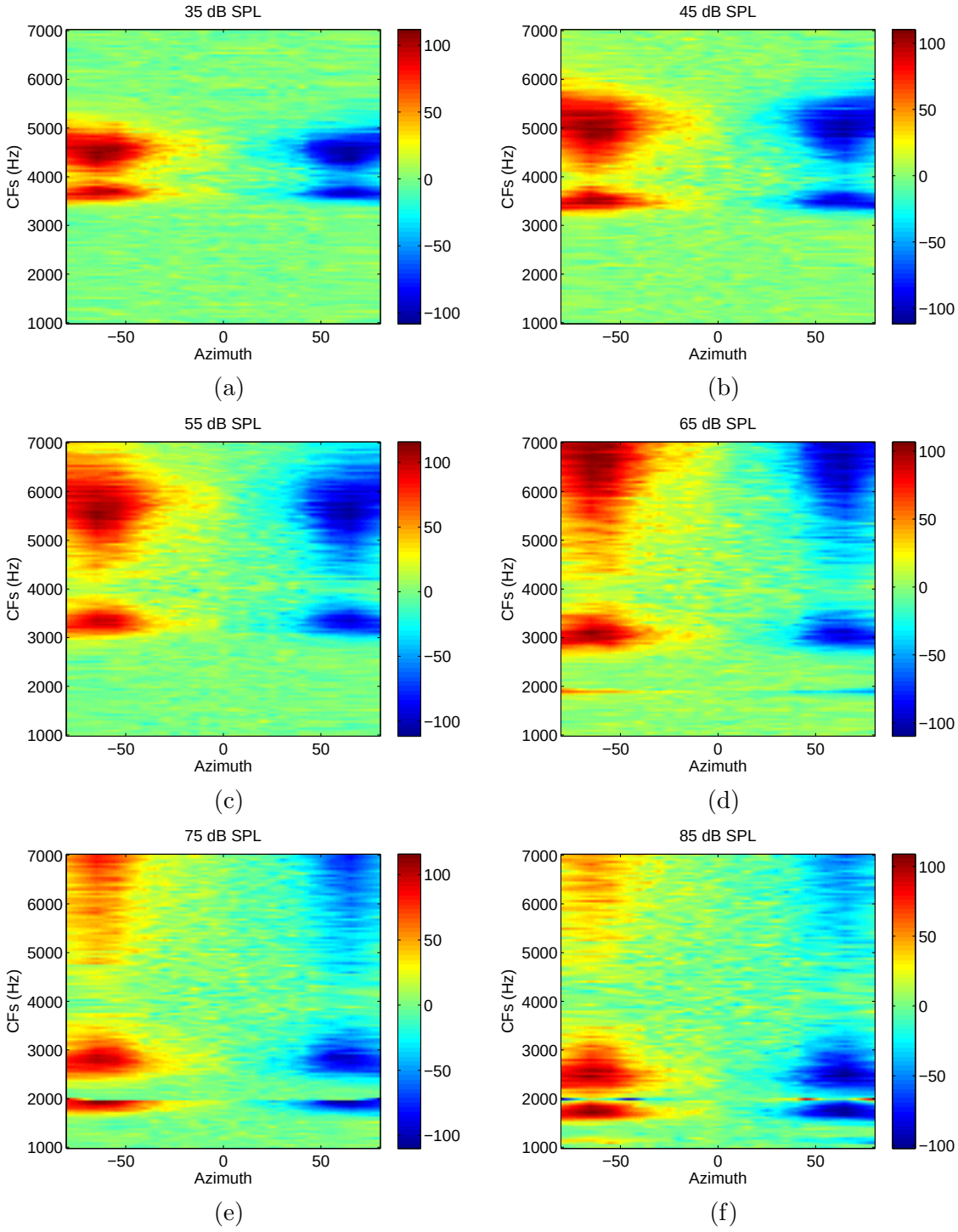

Figure 6.11: *IC response is not independent of presentation level. Normal-hearing neural representations are depicted here. (a): 35 dB SPL; (b): 45 dB SPL; (c): 55 dB SPL; (d): 65 dB SPL; (e): 75 dB SPL; (f): 85 dB SPL.*

6.3 Puretone Neural Representations: Biophysical Model

Normal-hearing LSO responses were also simulated using the biophysical model for several puretone stimuli. As anticipated, left and right LSO models demonstrated mirrored responses. For all three presentation levels (35 dB SPL, 65 dB SPL, and 85 dB SPL) of a 200-ms sinusoid at 4000 Hz, LSO discharge rate patterns differed between the two models (see, for example, the 65-dB SPL data in Figure E.7 (c) and (d)). The phenomenological model produced spike rates near 75 spikes/s at all CFs except those immediately away from the puretone frequency. Spike rates were higher away from the puretone CF at the ipsilateral side, and lower at the contralateral side. In the biophysical LSO model, however, spike rates were above 100 spikes/s, increasing slightly still away from the puretone CF on the ipsilateral side and decreasing far below 100 spikes/s on the contralateral side. Both models demonstrated similar relationships with azimuth as reported earlier: higher spike rates increasing away from 0°, being greatest near 65°, and then decreasing outwards to 80°.

The IC difference model data, however, shows very similar patterns of excitation despite such wide-ranging differences between LSO models themselves (see Figure 6.12 (a) and (b)). IC excitation is lower in all biophysical model responses, though the pattern spread of excitation across CFs and azimuths remains similar, as do approximate maximum and minimum spike rates. The same trends are seen for the 35-dB SPL and 85-dB SPL sound levels. Colour plots for these are given in Appendix E.

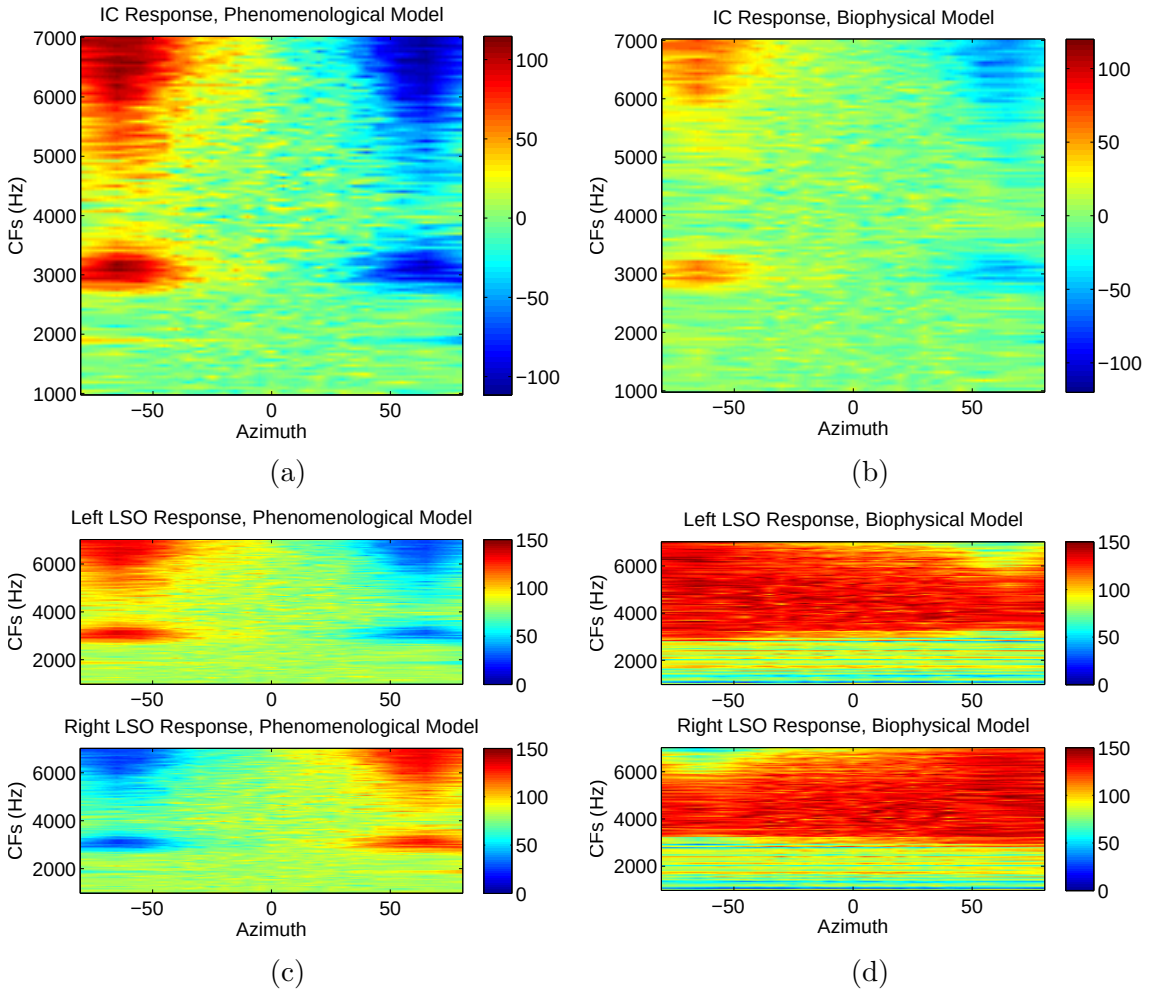

Figure 6.12: *Phenomenological and biophysical LSO neural representations are similar in excitation pattern, if not spike rate. Stimulus: 65-dB SPL puretone, using the normal-hearing model. (a): IC phenomenological model; (b): IC biophysical model; (c): LSO phenomenological model; (d): LSO biophysical model.*

Mean differences in discharge rate were calculated by subtracting phenomenological model discharge rates from the biophysical rates, then taking the mean across all CFs. This quantifier of model similarity is shown in Figure 6.13, where dashed lines represent IC model mean differences and solid lines depict LSO model mean differences. There are two interesting patterns to observe from these data. First: the differences in discharge rate between the two models are related to azimuth. Second: these normal-hearing models diverge in similarity as presentation level increases.

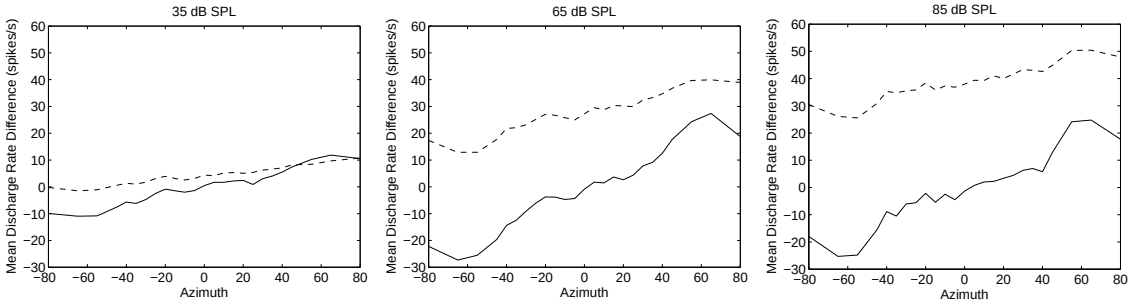

Figure 6.13: *Phenomenological and biophysical model discharge rates differ with presentation level. Dashed lines denote IC mean differences, while solid lines denote LSO mean differences.*

6.4 The TIMIT Sentence

WDRC effects on phones of the TIMIT sentence are varied. An assessment of the frequency content of different classes of phones is shown in Figure 6.14. Dashed blue lines indicate the 1500-Hz mark frequently reported as the soft "boundary" between low and high-frequency regions for ITD and ILD saliency. Solid blue lines indicate the range of CFs modelled. The red curve shows compression thresholds at the geometric center frequencies of the WDRC channels. Fricatives and the affricative tend to

contain energy in higher frequencies above 1500 Hz, enough to trigger compression in that range. Vowels, semivowels/glides, stop closures, and the nasal do not exceed compression thresholds above roughly 4500 Hz. Nasals and stop closures do not trigger compression at all. The epenthetic silence is included here but naturally does not trigger compression, as it is an added pause in the sentence. Mean discharge rate differences reveal interesting patterns in compression benefit for the hearing-impaired listener. These Figures are shown in Appendix F.

As with the puretone stimuli, differences due to WDRC condition are strongest with higher ILD. In the case of the affricative 'jh' and all fricatives, the hearing-impaired model in the unaided condition performed most differently from the normal-hearing model. In the fricative, Slow WDRC seems to have a stronger effect than linked or unlinked compression for the first 'sh' and both 's' phones, outperforming Very Fast and WS compression in both the linked and unlinked cases. This is most dramatic in the first 'sh' tone, although the absence of this effect in the second 'sh' indicates that the level of speech may be as important as the class of phone itself. For the 'd' stop, linked compression of all speeds outperforms unlinked compression. This is also the case for the 'k' stop, although WS compression performs as well or better at some azimuths. For all other stops, all hearing-impaired compression conditions produce similar spike rate differences from normal-hearing. These two phones have the greatest high-frequency energy of all stops (see Figure 6.15).

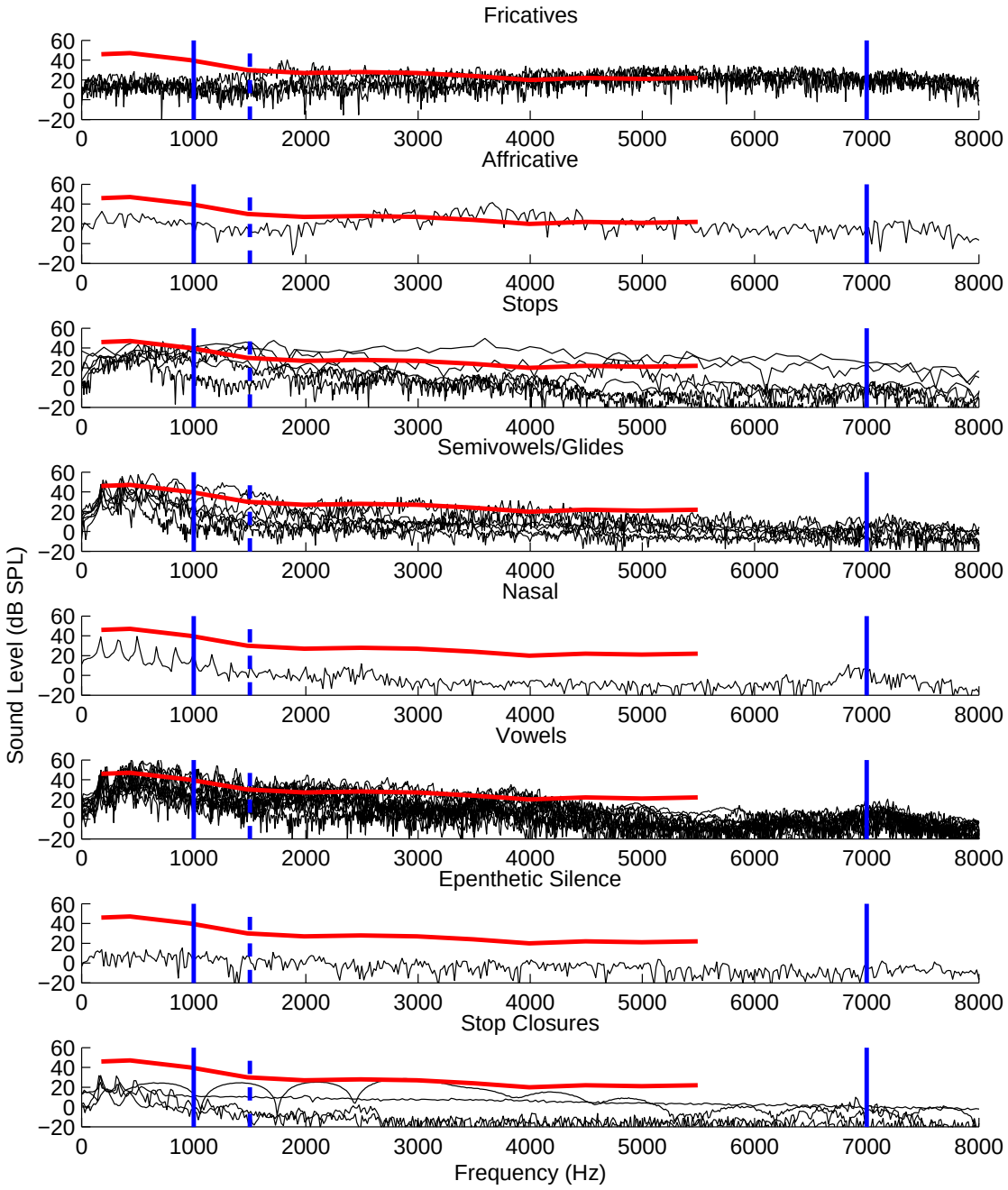

Figure 6.14: *TIMIT frequency content by phone class. Dashed blue lines indicate the 1500-Hz mark frequently reported as the soft "boundary" between low and high-frequency regions for ITD and ILD saliency. Solid blue lines indicate the range of CFs in the models. The red curve shows WDRC thresholds at the geometric centre frequencies of the WDRC channels.*

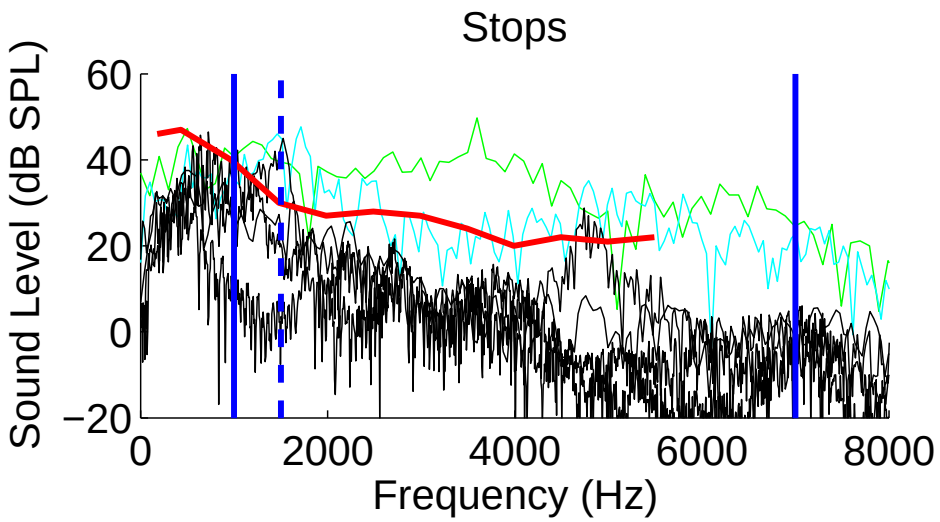

Figure 6.15: *Frequency content for stops. Green denotes the 'd' stop and cyan the 'k' stop.*

In semivowels/glides and vowels, all WDRC conditions perform similarly, although linked WDRC gives neural representations most similar to normal-hearing for both 'r's and 'w's. However, even for these phones, no compression speed is consistently better, and some unlinked WDRC speeds occasionally outperform linked WDRC, particularly at smaller azimuths. In the case of the vowels, mean rate differences are similar, although linked compression is consistently better for both 'er' phones.

Interestingly, for all stop closures but 'gcl' there is a flip in mean difference about the x-axis, indicating that spike rates for all hearing-impaired conditions were greater than normal-hearing. The nasal phone and epenthetic silence produce discharge rates most similar to normal-hearing.

Figures 6.16 shows the normalized number of stimulus presentation occurrences at which each compression condition produced the lowest mean rate difference, or the closest LSO responses to normal hearing, for each phone. From these results, it can be clearly observed that linked compression most often produces the lowest mean rate difference for all phones except the epenthetic silence. However, no compression speed is consistently best.

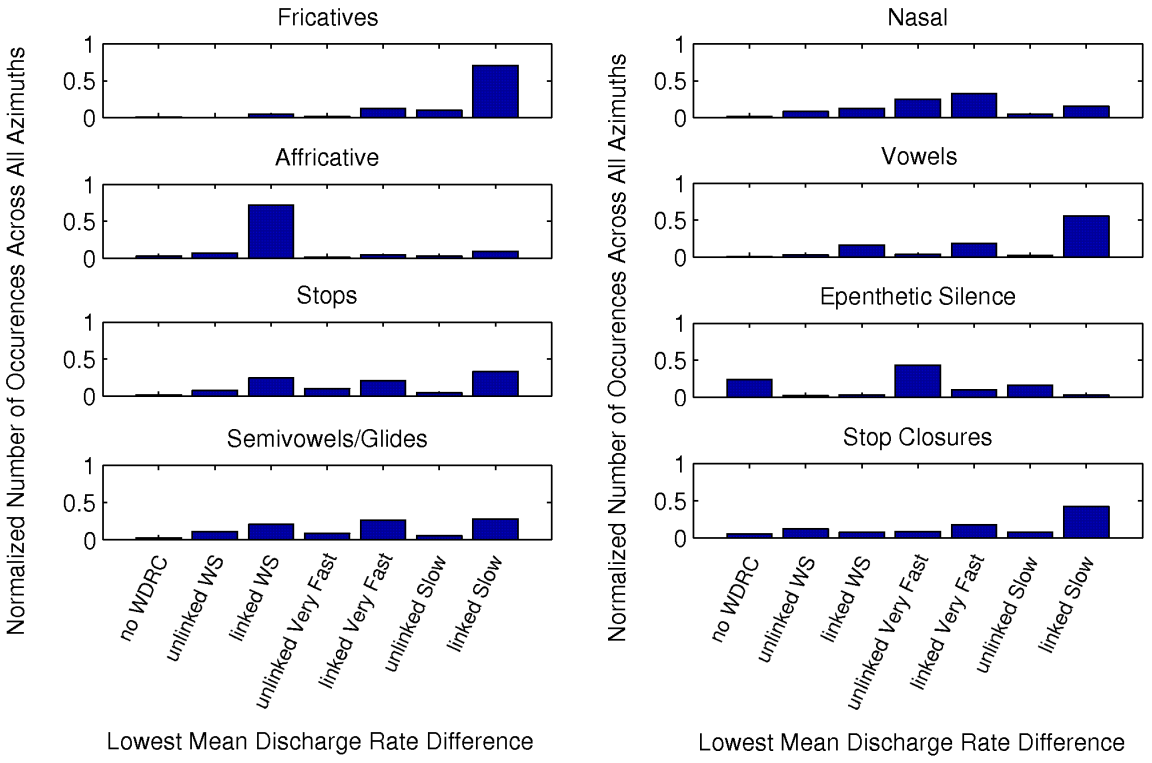

Figure 6.16: *Lowest mean rate difference for phones of the TIMIT sentence.*

6.5 Neural Decoder

The simple neural decoder performed poorly, possibly due to high LSO and IC excitation variability with presentation level. In fact, this model, trained on normal-hearing responses and tested on hearing-impaired responses to the same 65-dB SPL puretone, suggested left-right confusions for all azimuths except 0° (see Figure 6.17). This is unlikely given the spike rate patterns observed previously. After these initial results indicated the need for a more complex decoder model, the simple neural decoder was not explored further.

The population pattern decoder, similarly, was inadequate. When trained on two normal-hearing responses at 65 dB SPL and tested on a third, the population pattern decoder performed well, demonstrating decoded azimuths within a mean error of 2° from the presentation azimuths. However, it performed poorly when trained on normal-hearing responses at one stimulus presentation level and tested on a normal-hearing representation of a different stimulus level. Using the LSO phenomenological model responses, no left-right confusions resulted. However, the decoder detected a smaller range of azimuths for all input levels (see Figure 6.18). Training the decoder on IC phenomenological responses for the 65-dB SPL sinusoid did not improve the results: decoded azimuths were the same (20°) for both the 35-dB SPL and 85-dB SPL stimuli at all azimuths of presentation, except in the case of a 35-dB SPL puretone presented from $-20°$, for which decoded azimuth was 65°. When trained on biophysical LSO responses to the 65 dB SPL puretone and tested on the same model's

responses to 35-dB SPL and 85-dB SPL puretones, decoded azimuths were scattered and uncorrelated with azimuths of presentation. With the biophysical IC responses, the decoded azimuths were also scattered. It became clear that this decoder would not suit its intended function.

Two factors may be responsible for the poor decoding. First, Day and Delgutte (2013) used this decoder with IC neuronal models which included envelope ITD data, whereas this was absent in the phenomenological LSO models. Second, only a window of CFs (1000 to 7000 Hz) was used in all levels of the present modelling work. It is possible that excitation in regions above 7000 Hz, particularly at high input levels, could impact decoder performance. In effect, the decoder modelled here did not have all the information available to the actual IC. It should be noted that the mechanisms by which IC and LSO excitations are used to identify azimuth are not yet well understood; while LSO neural representations are dependent on presentation level, psychophysical studies show azimuth discrimination to be independent of presentation level (Tsai *et al.*, 2010).

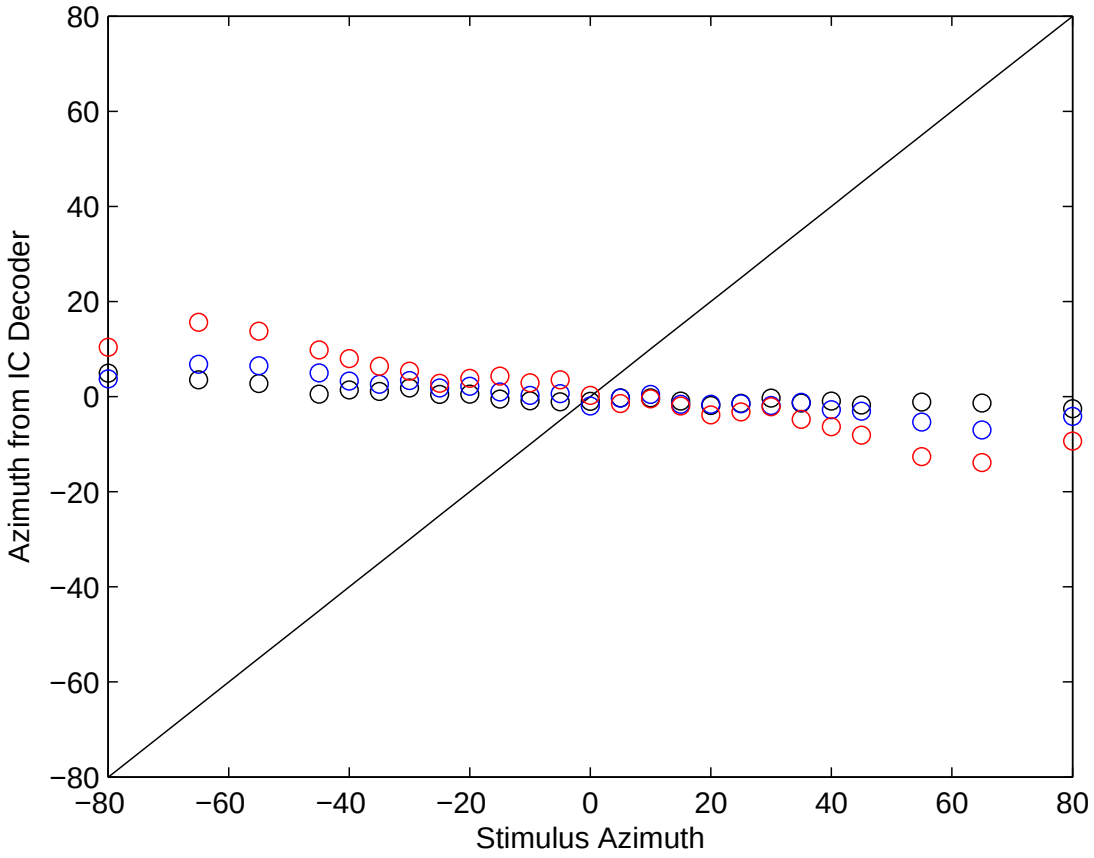

Figure 6.17: *Decoded hearing-impaired azimuths and azimuths of presentation for a 65-dB SPL sinusoid at 4000 Hz. Decoded azimuths are calculated using the simple decoder and IC phenomenological neural representations. The black line indicates perfect agreement between IC decoded azimuth and stimulus azimuth. Black, blue, and red open circles indicate predicted azimuths for the hearing-impaired model in the no WDRC, unlinked WDRC, and linked WDRC conditions, respectively.*

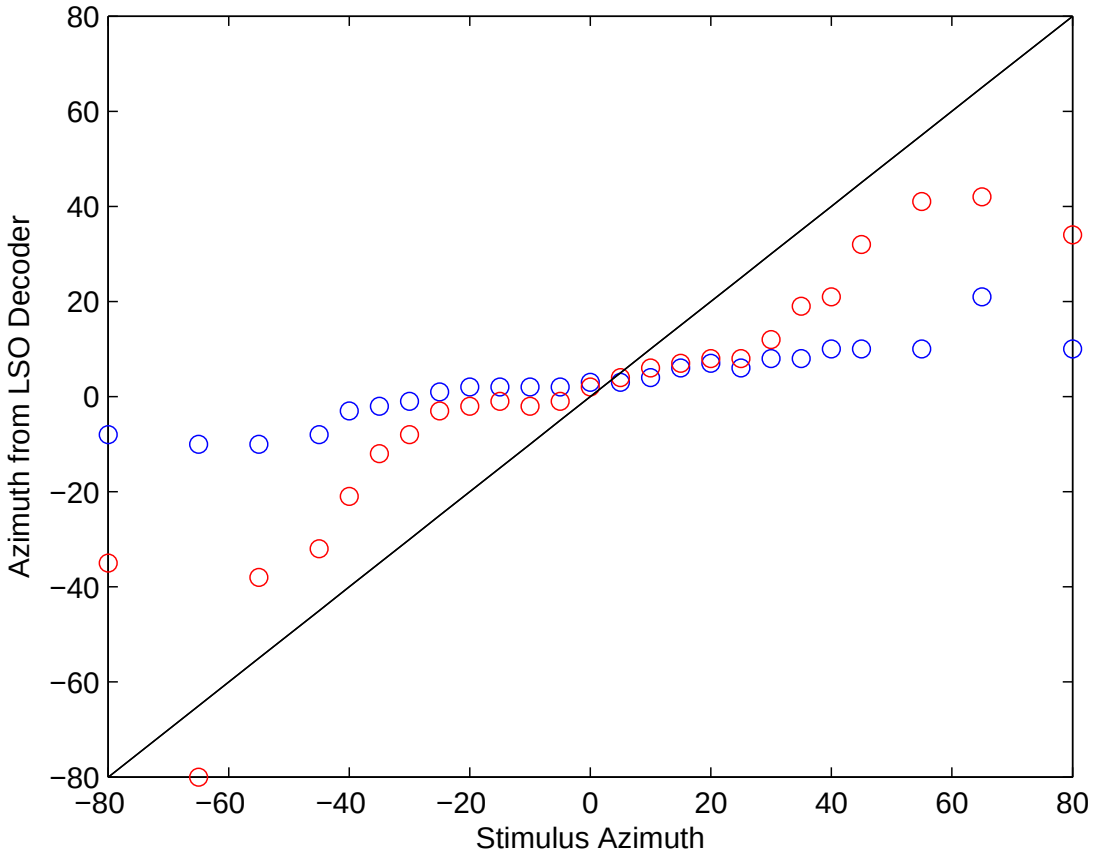

Figure 6.18: *Decoded phenomenological LSO azimuths and azimuths of presentation using the population pattern decoder on normal-hearing neural representations. The black line indicates perfect agreement between IC decoded azimuth and stimulus azimuth. Blue, open circles denote decoded azimuths for a puretone of 35 dB SPL. Open, red circles denote decoded azimuths for a puretone of 85 dB SPL.*

Chapter 7

Discussion

7.1 Reiteration of Research Aims

The aims of this research were previously presented as follows: **(1) To examine patterns of neural response to sounds for a listener with sensorineural hearing impairment in several conditions: with bilateral, unlinked WDRC hearing aids; with linked WDRC hearing aids; and unaided.**
(2) To elucidate the perceived horizontal position of sounds in the hearing-impaired listener, as abstracted from the neural model.
and finally, **(3) To uncover deficiencies of current WDRC hearing aids, where they appear to exist, and to suggest solutions and future directions for improved localization.**

This section will discuss implications of the results and contributions to these ends.

7.2 Patterns in Strength of Response

For puretone stimuli at levels as low as 35 dB SPL, neural responses are saturated at the puretone frequency, with regions of higher or lower spike rate surrounding it on the ipsilateral and contralateral sides, respectively. As presentation level increases, high spike rate regions spread outward from the puretone frequency, leading to a larger region of saturation. Unsurprisingly, the larger the ILD, the larger the response. Spike rate is low in the 2000 to 3000 Hz range, for which the notch filter of the middle ear may account.

Of note is the fact that strength of response (discharge rate) is lower in all hearing-impaired models than the normal-hearing models for all stimuli except three stop closures, both 'dcl's and the 'kcl'. All three of these stop closures immediately followed semivowels or vowels, but the remaining stop closure, 'gcl', followed a nasal. It is possible that some residual gain from the previous semivowel or vowel caused hearing-impaired responses to exceed normal-hearing for all cases except 'gcl'. At no presentation levels do hearing-impaired responses to the puretone stimuli saturate, even with linked WDRC.

The biophysical LSO model seems to show most clearly that below 1500 Hz, ILD cues are not as salient.

7.3 Neural Representations of Puretone Stimuli

Hearing-impaired responses are most deviant from normal-hearing responses when sound levels are near 65 dB SPL, which is the level of normal speech. Note that compression threshold at this frequency is 20 dB SPL, so compression should be in effect for all stimulus presentation levels used. At low levels (e.g. 35 dB SPL), all compression conditions result in similar hearing-impaired responses such that mean differences from normal-hearing representations are similar. From Figure 7.1, it could be inferred that all gains applied to a 35 dB SPL stimulus are too low to make ILD cues salient. That is, the prescribed amplification is similarly poor no matter the compression type. At medium levels (e.g. 55 dB SPL, 65 dB SPL) as opposed to higher or lower ranges, WDRC may be the least adequate at restoring ILD cues to a useable level. However, the benefit of WDRC is greatest over unaided hearing here, and linked WDRC appears preferable. At higher levels (e.g. 75 and 85 dB SPL), WDRC is such that sounds are amplified less, but the input sound is much louder anyway; the small amount of gain applied may be enough to put the response closer to normal-hearing. At this high level, linked WDRC is actually worse than unaided hearing. This suggests that linked WDRC is crucial for any hearing aid to not worsen localization at all. Note that mean rate differences are impacted both by deviances in CF spike rate itself as well as the regions of high/low excitation.

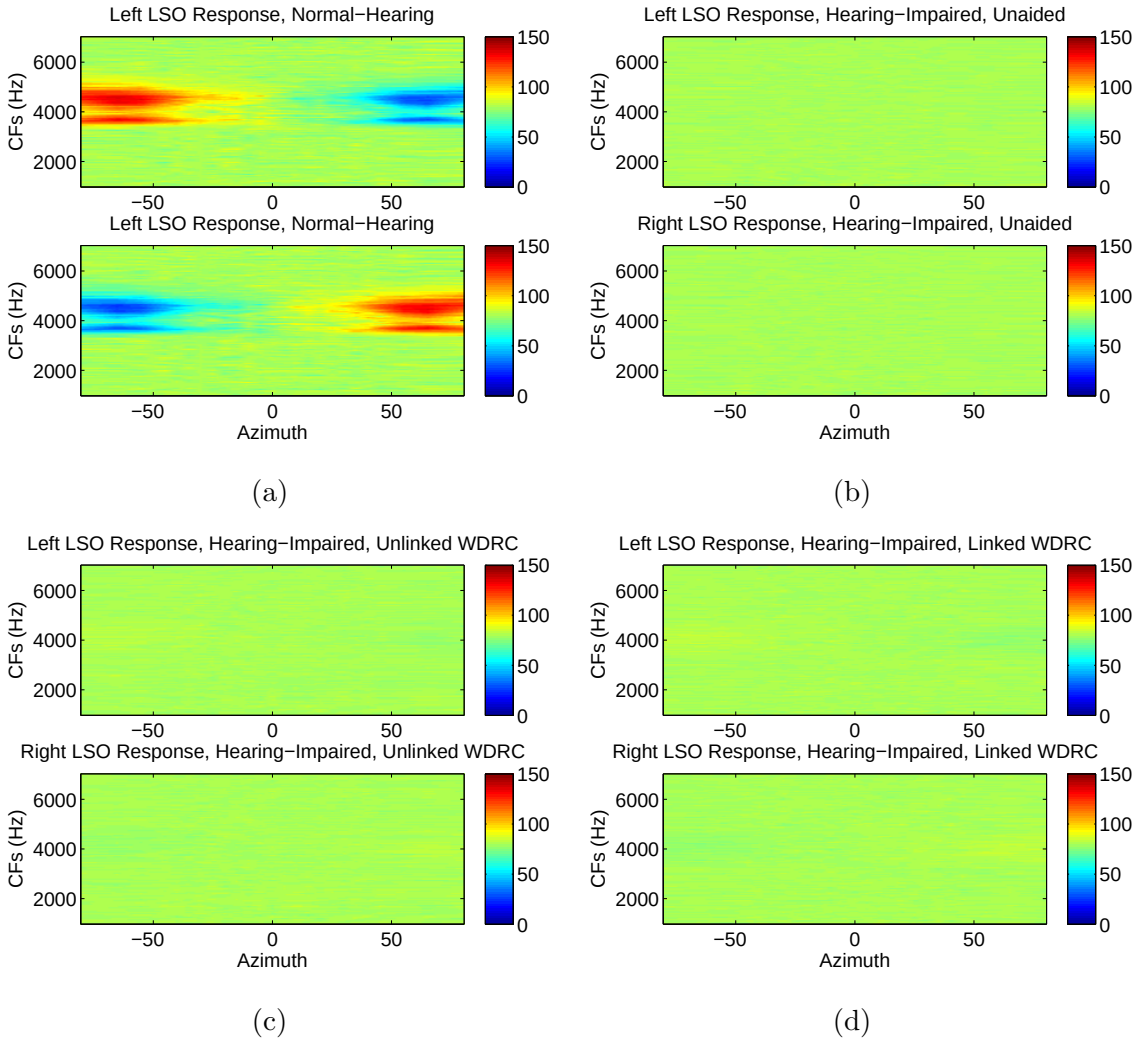

Figure 7.1: *Normal-hearing discharge rates exceed those in all hearing-impaired conditions. Stimulus: 4000-Hz sinusoid, 35 dB SPL. 4000-Hz saturation is absent in the hearing-impaired neural representations. (a): normal-hearing; (b): hearing-impaired, unaided; (c): hearing-impaired, unlinked WDRC; (d): hearing-impaired, linked WDRC.*

7.4 Different WDRC are Preferable for Different Speech Sounds

Linked compression nearly always yields the closest LSO responses to normal hearing (see Figure 6.16). This is not the case for the epenthetic silence, for which Very Fast, unlinked compression is most often best. Different compression speeds are better for different phones. This could explain the variations in performance in some studies using speech stimuli (e.g. Kreisman *et al.*, 2010; Ibrahim *et al.*, 2012; Wiggins and Seeber, 2013; Schwartz and Shinn-Cunningham, 2013) while localization of a bird chirp tone was significantly successful with wireless synchronization enabled in Sockalingam *et al.* (2009). Benefit is dependent both on phone and presentation level, and also on position within the sentence.

From Figure 6.16, it is clear that the unaided condition is most often the worst in most phones. In the affricative and fricatives, the unaided condition is the second-worst, performing better than unlinked conditions. In the case of the epenthetic silence, the unaided condition is second-best but is outperformed by Very Fast, unlinked compression.

Some consonants, such as fricatives and the affricative, contain enough energy in frequencies above 1500 Hz to trigger WDRC in that range. For these sounds, linked WDRC results in hearing-impaired discharge patterns most similar to normal-hearing. However, no compression speed is consistently best, though Slow compression most often yields the closest LSO excitations to normal hearing. Other phones, such as vowels and semivowels/glides, do not contain energy above a frequency threshold of roughly 4500 Hz. However, these phones still often yield the lowest mean differences

with linked WDRC. The nasal and stop closures do not trigger WDRC at all, nor does the epenthetic silence. For these latter two phone classes, mean rate differences are lower than in other phones and the benefit of linked WDRC is absent (in the case of the silence) or less pronounced (in the case of the nasal). It could be inferred that WDRC is of the least use here, and other phone types should be of greater focus when improving speech intelligibility through aided hearing.

Differences between aided performance results, despite below-threshold energies, may be reconciled with the fact that these phones were not examined in isolation. That is, the placement of the phone within the TIMIT sentence could affect the degree to which WDRC acts, particularly for slower compression times. For some phones in some positions, WDRC may have never reached the desired level of gain. This would depend both on compression time and the WDRC gain behaviour for the preceding phone. This effect is particularly clear upon examination of the stop closure spike rates, which were higher in the hearing-impaired model than the normal-hearing model in all conditions and in all stop closures except 'gcl'. While other stop closures immediately followed vowels or semivowels/glides, only 'gcl' immediately followed a nasal, for which compression thresholds were not reached.

Where compression time is concerned, Slow compression, which reduces long-term level changes, is often too slow to reach the final desired gain. The average duration of vowels and semivowels/glides is 0.0874 s, shorter than the Slow attack and release times, while the average duration of fricatives and the affricative is longer,

0.1013 s. Still, for fricatives and the affricative, the Slow attack time (100 ms) is barely fast enough. This may explain the observations of Schwartz and Shinn-Cunningham (2013), who found fast, linked WDRC to be beneficial over unlinked WDRC but saw no trend against performance for slow compression time.

As consonants greatly impact speech intelligibility and vowels are less impacted by hearing impairment (Bainbridge and Wallhagen, 2014), it could be a concern that neural representations of vowels and consonants vary so widely from normal-hearing performance with the use of WDRC. However, note that while identification of phone sound source may be skewed, predicting speech intelligibility was beyond the scope of the present work. It may be the case that these mean discharge rate differences become less salient when a listener has initially identified and can attend to a source. In a real-world environment, ITD cues and visual information would also aid the listener.

7.5 Attempted Neural Decoders are Inadequate

The neural decoders attempted here are inadequate for the intended purposes, and more appropriate techniques are a potential future area of investigation. Specifically, the simple decoder gave counter-intuitive results, producing left/right confusions. The population pattern decoder was unable to account for the level-dependent saturation and excitation regions seen in LSO responses. Level dependence has also been observed in the work of Tsai *et al.* (2010), though other studies have found ILD to be invariant to stimulus intensity.

A stable decoder is critical in order to understand where a perceived azimuth may lie for a hearing-impaired listener. While psychophysical data may provide insight to this effect, a generalized LSO decoder model could be a simpler and more effective way to assess localization of different stimuli in listeners of different audiograms. It could also be an invaluable aid in the adjustment of WDRC parameters to properly suit a hearing-impaired listener. There are, of course, limitations to this technique. Not all listeners of similar hearing loss or audiogram have the same binaural deficits (Simon, 2005). However, such a tool may indicate whether binaural cues are at all potentially preserved or maintained for use at the neural level.

7.6 LSO Models Behave Differently

The phenomenological model and the biophysical model perform differently, although the IC difference model gives similar patterns of response using inputs from both. Differences are to be expected, as LSO cells do not all show the same behaviour. Modelling parameters were based upon the work of Tsai *et al.* (2010), Wang *et al.* (2014), and Wang and Colburn (2012), and subsequently characterize different populations of cells. The phenomenological LSO model gives intermediate excitation (roughly 75 spikes/s) at all CFs except those flanking the puretone frequency. In the biophysical LSO model, the region of excitation around the puretone CF tends to a higher discharge rate (above 100 spikes/s), and flanking regions show slightly less excitation (contralateral side) or slightly more (ipsilateral side). This suggests that scaling factors in one or both of the models may be responsible for the difference,

but that the simple phenomenological model is otherwise an appropriate analogue if looking at patterns of excitation related to localization. As in the work of Tsai *et al.* (2010), the models indicate that excitation patterns are not independent of sound presentation level.

Chapter 8

Conclusion

For puretone stimuli, linked WDRC offers clear benefits over unlinked WDRC and unaided, impaired hearing. For speech stimuli, the benefit is dependent on presentation level, phone class, and phone placement within a sentence. This suggests the necessity of adaptive compression times to handle fast-changing levels and frequency content in real-world listening environments. Linked WDRC appears to be a promising direction worth further development.

These findings also suggest that questionnaire-based assessments of WDRC performance may be adjusted for specificity of sounds. That is, participants should be asked to qualify listening in speech environments, in background noise, and of music. This may indicate whether preference for hearing aids is truly due to WDRC benefits in speech intelligibility, or if other factors impact rating scores.

Several limitations impact this work. Computational modelling offers several advantages and conveniences over psychophysical studies, which are constrained by participants' availability, recruiting success, and monetary resources. However, limits to computational time and resources enabled only one audiogram and fit to be examined. It should also be noted that the N_3 hearing-impaired audiogram reflects the largest proportion of 28244 tested ears in the Bisgaard *et al.* (2010) standardization, and thus the observed trends may characterize the neural responses of many hearing-impaired listeners with symmetric, moderate, sensorineural loss. However, for other audiograms, implications may still be conservatively generalized with some caution: WDRC benefit is dependent on listening situation with the present fitting indicating that not all prescriptions provide adequate gain. Second, a wider range of stimuli would have undoubtedly improved the understanding of WDRC benefit trends, particularly to improve the variety of phones. The TIMIT database offers further speech sentences that were not used and from a variety of American dialects. This work could be extended to include those, but at the cost of computational time and resources. Last, inherent generalizations in modelling methods both simplify the research techniques while introducing sources for error. The differences between the behaviour of the phenomenological and biophysical LSO models alone suggest that the choice of technique, while presenting similar results in some measures, may be inappropriate for others. For the present work, both appear adequate for examination of patterns, though not discharge rate alone.

This research contributes a better understanding of wirelessly-linked WDRC benefits at the neural level, suggesting directions of further study and improvement. Synchronized WDRC appears promising, though appropriate parameters should be adaptive for real-world environments and sound sources. Further work could generalize these findings for listeners of different audiograms, and an adequate neural decoder could provide insight into the perceived azimuth where localization of sounds is incorrect.

Appendix A

TIMIT Phones

Table A.1: Start and end times of TIMIT phones. BEGIN and END denote empty periods before and after speech.

Start (s)	End (s)	Phone Code	Class
0	0.1412	h#	BEGIN
0.1412	0.2544	sh	fricative
0.2544	0.3291	iy	vowel
0.3291	0.3968	hv	semivowel/glide
0.3968	0.4775	eh	vowel
0.4775	0.5188	dcl	stop closure
0.5188	0.5575	jh	affricative
0.5575	0.6525	axr	vowel
0.6525	0.7288	dcl	stop closure
0.7288	0.7388	d	stop
0.7388	0.8425	aa	vowel

Table A.1: *continued from previous page.*

Start (s)	End (s)	Phone Code	Class
0.8425	0.8975	r	semivowel/glide
0.8975	0.9619	kcl	stop closure
0.9619	0.9817	k	stop
0.9817	1.1244	s	fricative
1.1244	1.2376	ux	vowel
1.2376	1.3786	q	stop
1.3786	1.4275	ix	vowel
1.4275	1.48	n	nasal
1.48	1.5378	gcl	stop closure
1.5378	1.5844	g	stop
1.5844	1.6306	r	semivowel/glide
1.6306	1.7231	iy	vowel
1.7231	1.8369	s	fricative
1.8369	1.8981	iy	vowel
1.8981	1.9948	w	semivowel/glide
1.9948	2.1412	ao	vowel
2.1412	2.2394	sh	fricative
2.2394	2.295	epi	epenthetic silence
2.295	2.3425	w	semivowel/glide
2.3425	2.4375	ao	vowel
2.4375	2.4625	dx	stop
2.4625	2.5691	er	vowel

Table A.1: *continued from previous page.*

Start (s)	End (s)	Phone Code	Class
2.5691	2.6974	q	stop
2.6974	2.8336	ao	vowel
2.8336	2.8806	l	semivowel/glide
2.8806	3.0111	y	semivowel/glide
3.0111	3.1026	ih	vowel
3.1026	3.2025	er	vowel
3.2025	3.365	h#	END

Appendix B

Summary of Studies on Wirelessly-Linked WDRC

Table B.2: Summary of cited studies of wirelessly-linked hearing aid performance.

Authors	Participants	Hearing Aids	Fit	Compression Times	Measure and Test
Smith *et al.* (2008)	30 hearing-impaired Symmetrical, sensorineural hearing loss. No prior HA experience Mean age 61 years	Siemens Acuris S BTE	NAL-NL1	Unspecified	Speech Quality Preference (Questionnaire, SSQ Hearing Scale)
Sockalingam *et al.* (2009)	30 hearing-impaired Symmetrical mild to moderate sensorineural hearing loss 16 experienced users, 14 novice Mean age 66 years	Oticon Dual XW	Unspecified	Unspecified	Sound Localization Quality
Kreisman *et al.* (2010)	36 hearing-impaired Symmetrical, sensorineural hearing loss 18 experienced users, 18 novice Mean age 64.5 years	Oticon Epoq XW RITEs (linked) Oticon Syncro V2 BTEs (unlinked)	Proprietary Genie fit (Oticon)	Unspecified	Hearing in Noise (QuickSIN and HINT)
Ibrahim *et al.* (2012)	8 normal-hearing Mean age 26 years 12 hearing-impaired Symmetrical, moderate to severe sensorineural hearing loss Minimum 1 year of experience with hearing aids. Mean age 69 years	Oticon Epoq XW (linked) Siemens Motion 700 (unlinked)	DSL 5.0	Oticon: fast-acting at high SPL slow-acting at low SPL Siemens: "syllabic compression" times	Speech Intelligibility (HINT) Sound Localization
Schwartz and Shinn-Cunningham (2013)	39 normal-hearing Ages 18 to 22	Simulated 16-channel (linear, linked, unlinked)	Compression threshold: Band SPL for 50-dB SPL speech input For compression: 3:1 compression ratio in all 16 bands	Fast: attack 11-ms release 82-ms Slow: 48-ms attack 730-ms release ANSI S3.22	Target/Masker Spatial Thresholds
Wiggins and Seeber (2013)	Normal-hearing listeners	Simulated two-channel (linked, unlinked)	3:1 compression	5-ms attack 60-ms release (ANSI S3.22)	Speech Intelligibility

Appendix C

LSO Model Parameters

The following equations are as developed by Rothman and Manis (2003).

Activation/Deactivation Variable Rates of Change

Activation and deactivation variable rates of change follow a first-order differential equation of the form

$$\frac{\mathrm{d}x}{\mathrm{d}t} = \frac{x_\infty - x}{\tau_x} \tag{C.1}$$

where x_{inf} is the steady-state value of activation (or deactivation) variable x and τ_x is the time constant of x.

Fast-inactivating Potassium Current

$$I_A = \bar{g}_A \cdot a^4 bc \cdot (V - V_{\mathrm{K}}) \tag{C.2}$$

$$a_\infty = [1 + \exp(-(V + 31)/6]^{-1/4} \tag{C.3}$$

$$b_\infty = [1 + \exp(-(V + 66)/7]^{-1/2} \tag{C.4}$$

$$c_\infty = b_\infty \tag{C.5}$$

$$\tau_a = 100 \cdot [7 \exp((V + 60)/14) + 29 \exp(-(V + 60)/24)]^{-1} + 0.1 \tag{C.6}$$

$$\tau_b = 1000 \cdot [14 \exp((V + 60)/27) + 29 \exp(-(V + 60)/24)]^{-1} + 1 \tag{C.7}$$

$$\tau_c = 90 \cdot [1 + \exp(-(V + 66)/17)]^{-1} + 10 \tag{C.8}$$

Low-threshold Potassium Current

$$I_{\mathrm{LT}} = \bar{g}_{LT} \cdot w^4 z \cdot (V - V_{\mathrm{K}}) \tag{C.9}$$

$$w_\infty = [1 + \exp(-(V + 48)/6)]^{-1/4} \tag{C.10}$$

$$z_\infty = (1 - \zeta)[1 + \exp((V + 71)/10)]^{-1} + \zeta, (\zeta = 0.5) \tag{C.11}$$

$$\tau_w = 100 \cdot [6 \exp((V + 60)/6) + 16 \exp(-(V + 60)/45)]^{-1} + 1.5 \tag{C.12}$$

$$\tau_z = 1000 \cdot [\exp((V + 60)/20) + \exp(-(V + 60)/8)]^{-1} + 50 \tag{C.13}$$

High-threshold Potassium Current

$$I_{\mathrm{HT}} = \bar{g}_{\mathrm{HT}} \cdot [\varphi n^2 + (1-\varphi)p] \cdot (V - V_{\mathrm{K}}) \tag{C.14}$$

$$n_\infty = [1 + \exp(-(V+15)/5)]^{-1/2} \tag{C.15}$$

$$p_\infty = [1 + \exp(-(V+23)/6)]^{-1} \tag{C.16}$$

$$\tau_n = 100 \cdot [11\exp((V+60)/24) + 21\exp(-(V+60)/23)]^{-1} + 0.7 \tag{C.17}$$

$$\tau_p = 100 \cdot [4\exp((V+60)/32) + 5\exp(-(V+60)/22)]^{-1} + 5 \tag{C.18}$$

Fast Sodium Current

$$I_{\mathrm{Na}} = \bar{g}_{\mathrm{Na}} \cdot m^3 h \cdot (V - V_{\mathrm{Na}}) \tag{C.19}$$

$$m_\infty = [1 + \exp(-(V+38)/7)]^{-1} \tag{C.20}$$

$$h_\infty = [1 + \exp(-(V+65)/6)]^{-1} \tag{C.21}$$

$$\tau_m = 10 \cdot [5\exp((V+60)/18) + 36\exp(-(V+60)/25)]^{-1} + 0.04 \tag{C.22}$$

$$\tau_h = 100 \cdot [7\exp((V+60)/11) + 10\exp(-(V+60)/25)]^{-1} + 0.6 \tag{C.23}$$

Hyperpolarization-activated Cation Current

$$I_h = \bar{g}_h \cdot r \cdot (V - V_h) \tag{C.24}$$

$$r_\infty = [1 + \exp(-(V+76)/7)]^{-1} \tag{C.25}$$

$$\tau_r = 10^5 \cdot [237\exp((V+60)/12) + 17\exp(-(V+60)/14)]^{-1} + 25 \tag{C.26}$$

Leakage Current

$$I_{\text{lk}} = \bar{g}_{\text{lk}} \cdot (V - V_{\text{lk}}) \tag{C.27}$$

Excitatory Synaptic Current (Ipsilateral AN Current)

$$I_{\text{Exc}} = \bar{g}_{\text{Exc}} \cdot (V - V_{\text{Exc}}) \tag{C.28}$$

Inhibitory Current (Contralateral AN Current)

$$I_{\text{Inh}} = \bar{g}_{\text{Inh}} \cdot (V - V_{\text{Inh}}) \tag{C.29}$$

Excitatory and Inhibitory Conductance

The following excitatory and inhibitory conductance equations are as shown by Wang and Colburn (2012). "Syn" may be either the excitatory or inhibitory synaptic parameter.

$$g_{\text{Syn}}(t) = \frac{\bar{g}_{\text{Syn}}}{g_{\text{norm}}}[\exp(-t/\tau_{\text{Syn}}) - \exp(-t/\tau_{\text{Syn}_{\text{rise}}})] \tag{C.30}$$

$$g_{\text{norm}}(t) = \exp(-t_p/\tau_{\text{Syn}}) - \exp(-tp/\tau_{\text{Syn}_{\text{rise}}}) \tag{C.31}$$

$$t_p = \frac{\tau_{\text{Syn}_{\text{rise}}}\tau_{\text{Syn}}}{\tau_{\text{Syn}} - \tau_{\text{Syn}_{\text{rise}}}} \ln \frac{\tau_{\text{Exc}}}{\tau_{\text{Exc}_{\text{rise}}}} \tag{C.32}$$

Table C.3: Biophysical LSO model parameters, modified from Rothman and Manis (2003), Wang and Colburn (2012), and Wang *et al.* (2014).

Parameter	Value
$\bar{g}_{\mathrm{Na}}$	8000 nS
$\bar{g}_{\mathrm{HT}}$	1200 nS
$\bar{g}_{\mathrm{LT}}$	25 nS
$\bar{g}_{A}$	0 nS
$\bar{g}_{h}$	2.5 nS
$\bar{g}_{\mathrm{lk}}$	31.4 nS
C_m	31.4 pF
V_{K}	-70 mV
V_h	-43 mV
V_{Na}	55 mV
V_{lk}	-65 mV
V_{Exc}	0 mV
V_{Inh}	-70 mV
V_{th}	-20 mV
$\bar{g}_{\mathrm{Exc}}$	12 nS
$\bar{g}_{\mathrm{Inh}}$	10 nS
$\bar{\tau}_{\mathrm{Exc}}$	2 ms
$\bar{\tau}_{\mathrm{Inh}}$	0.2 ms
$\bar{\tau}_{\mathrm{Exc_{rise}}}$	5 ms
$\bar{\tau}_{\mathrm{Inh_{rise}}}$	0.5 ms

Appendix D

Puretone Responses: Phenomenological Model

The following are the LSO phenomenological model representations of puretone stimuli.

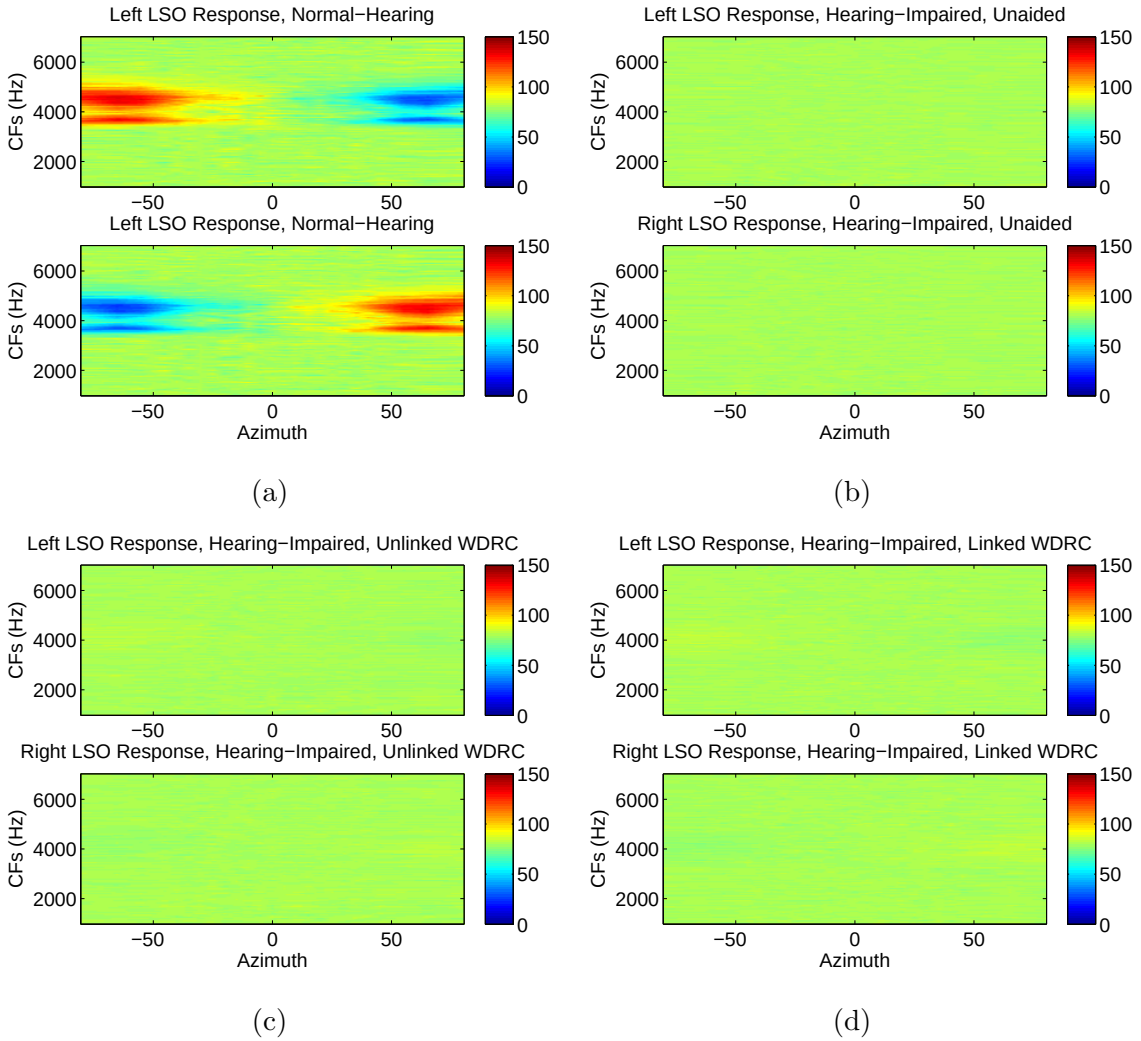

Figure D.1: *Stimulus: 4000-Hz sinusoid, 35 dB SPL. 4000-Hz saturation is absent in the hearing-impaired neural representations. (a): normal-hearing; (b): hearing-impaired, unaided; (c): hearing-impaired, unlinked WDRC; (d): hearing-impaired, linked WDRC.*

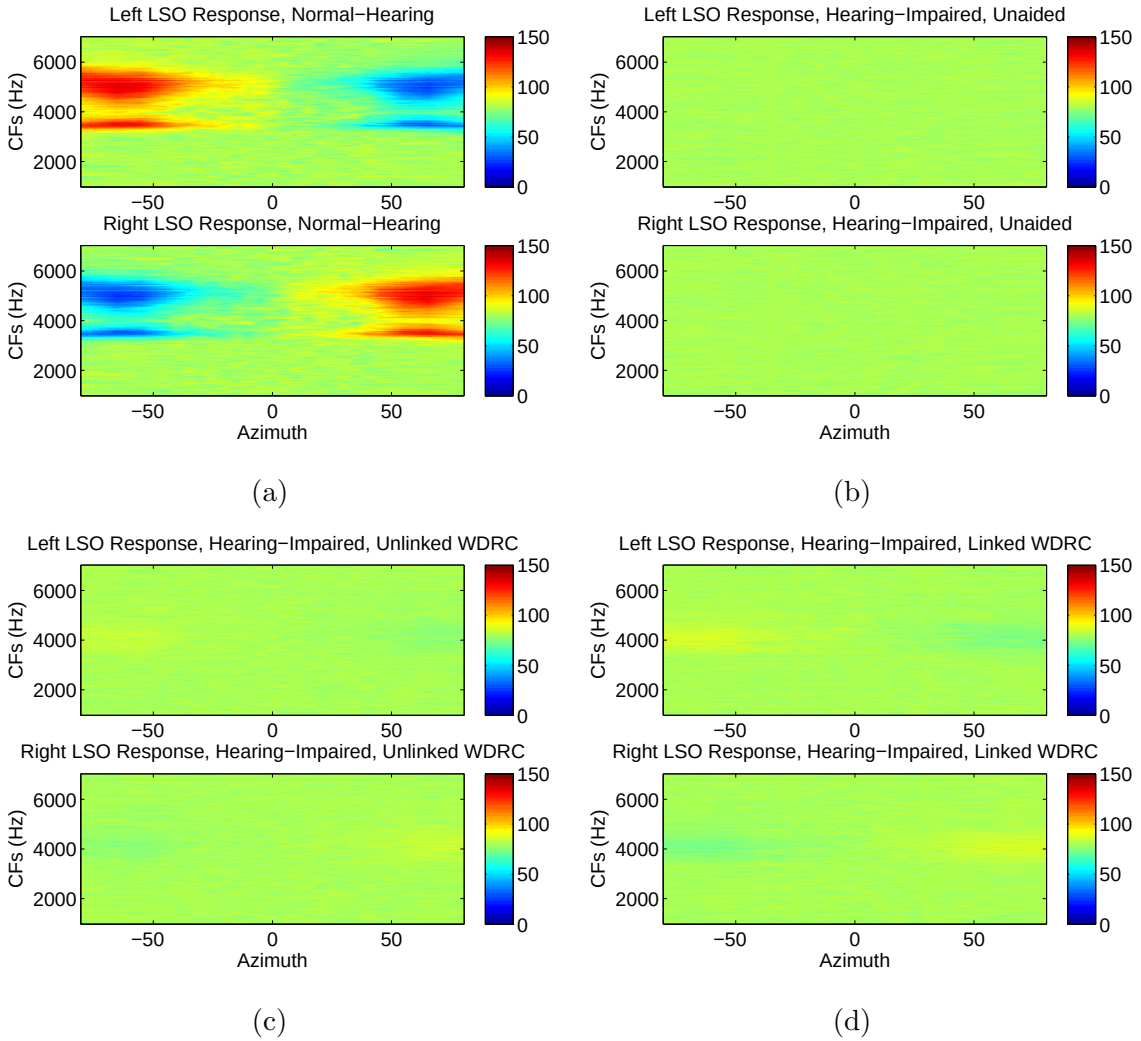

Figure D.2: *Stimulus: 4000-Hz sinusoid, 45 dB SPL. 4000-Hz saturation is absent in the hearing-impaired neural representations. (a): normal-hearing; (b): hearing-impaired, unaided; (c): hearing-impaired, unlinked WDRC; (d): hearing-impaired, linked WDRC.*

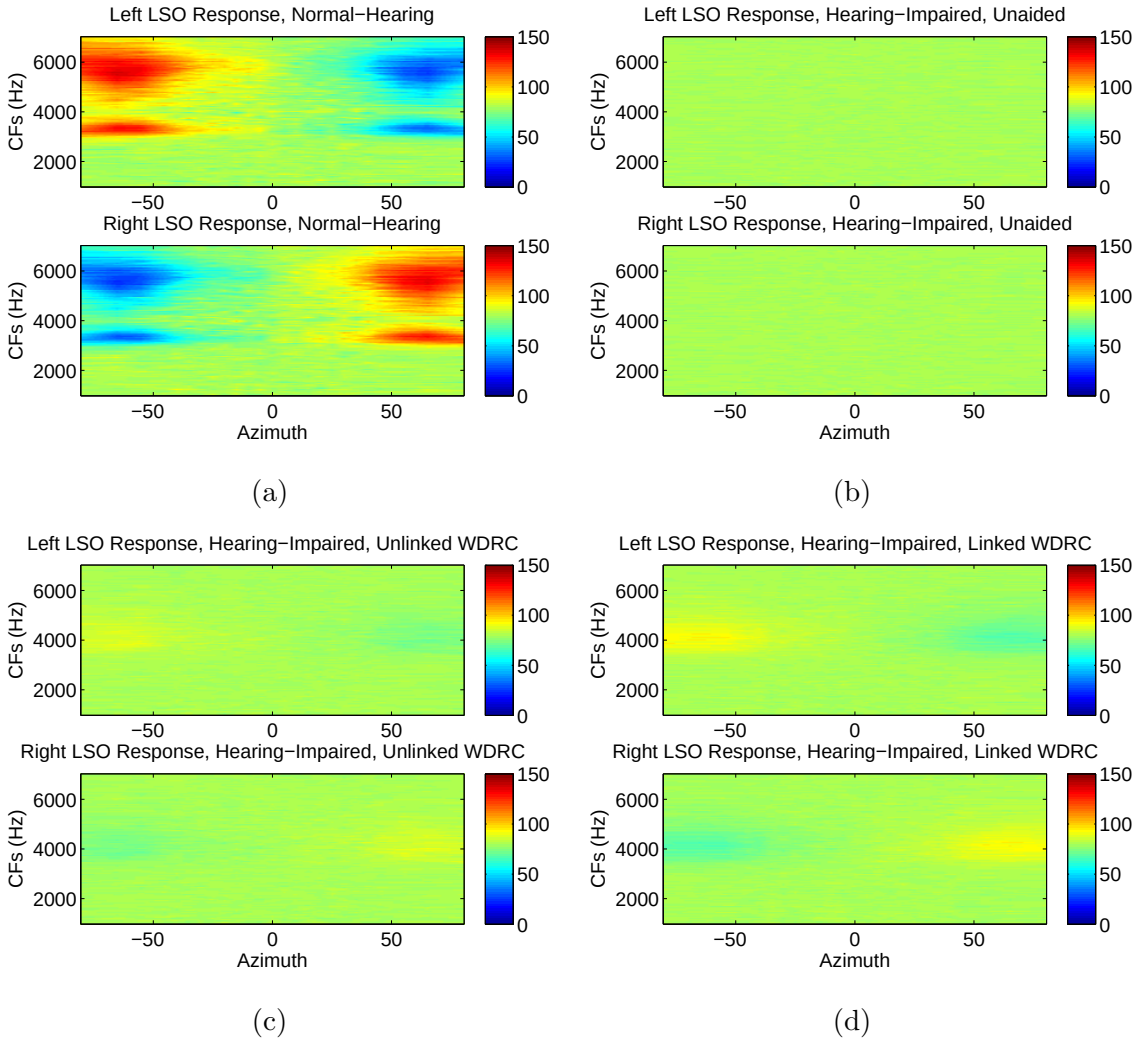

Figure D.3: *Stimulus: 4000-Hz sinusoid, 55 dB SPL. 4000-Hz saturation is absent in the hearing-impaired neural representations. (a): normal-hearing; (b): hearing-impaired, unaided; (c): hearing-impaired, unlinked WDRC; (d): hearing-impaired, linked WDRC.*

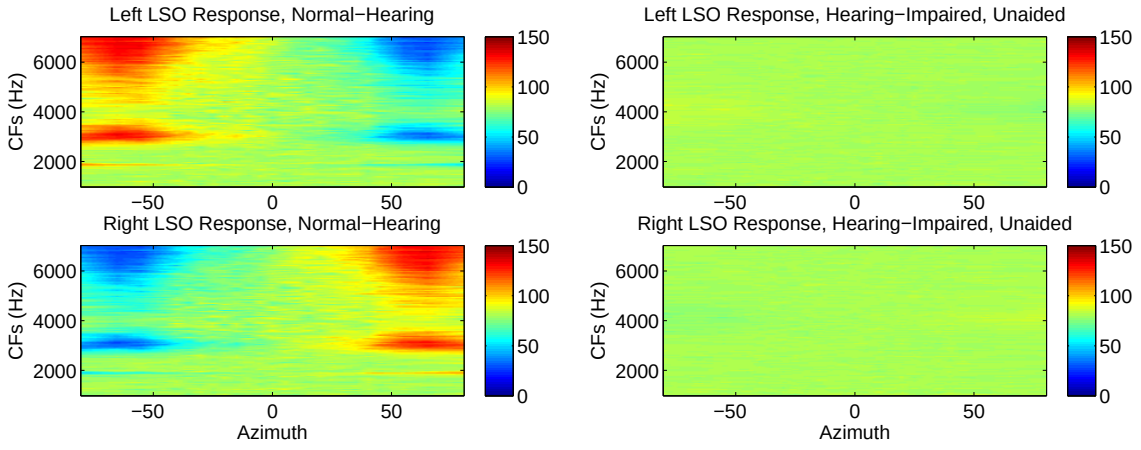

(a) (b)

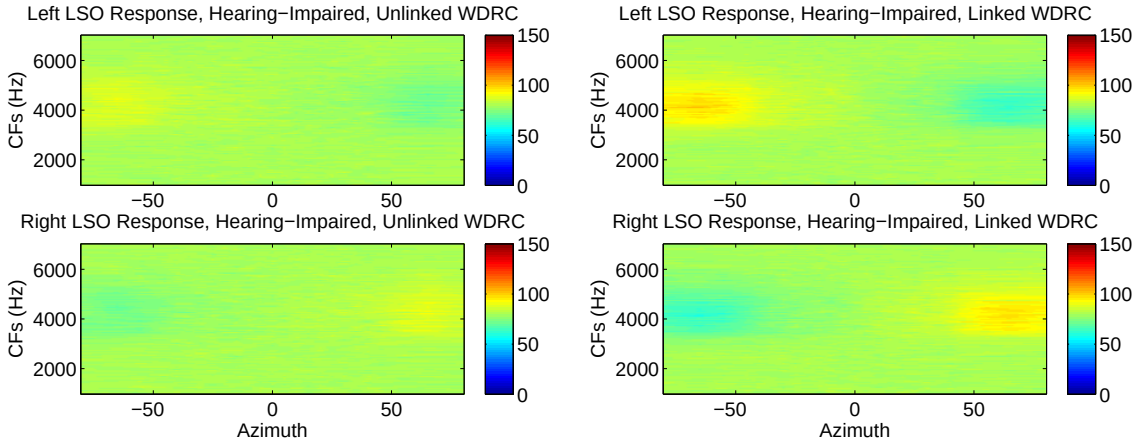

(c) (d)

Figure D.4: *Stimulus: 4000-Hz sinusoid, 65 dB SPL. 4000-Hz saturation is absent in the hearing-impaired neural representations. (a): normal-hearing; (b): hearing-impaired, unaided; (c): hearing-impaired, unlinked WDRC; (d): hearing-impaired, linked WDRC.*

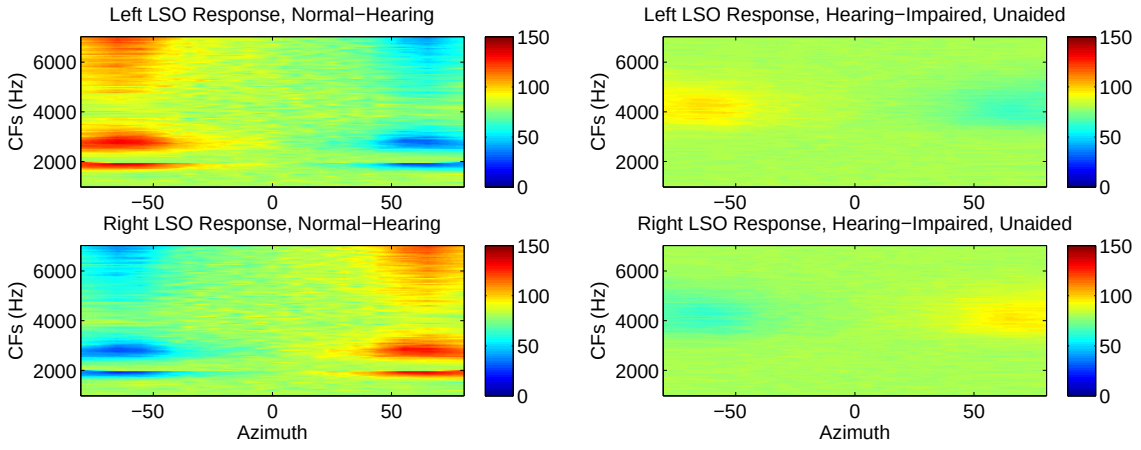

(a)

(b)

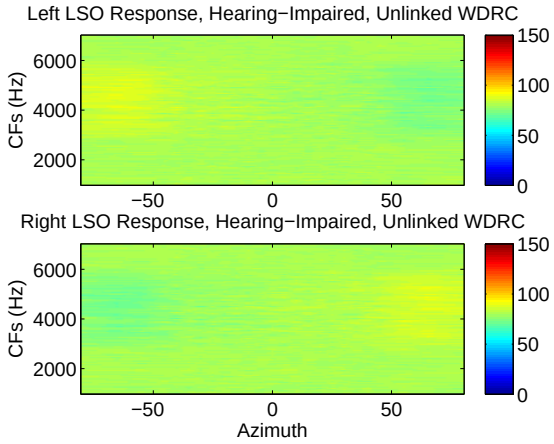

(c)

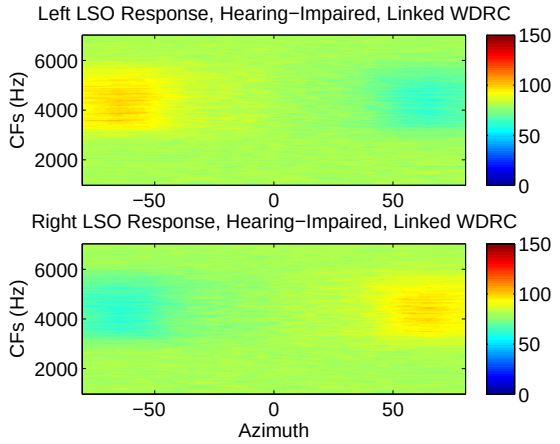

(d)

Figure D.5: *Stimulus: 4000-Hz sinusoid, 75 dB SPL. 4000-Hz saturation is absent in the hearing-impaired neural representations. (a): normal-hearing; (b): hearing-impaired, unaided; (c): hearing-impaired, unlinked WDRC; (d): hearing-impaired, linked WDRC.*

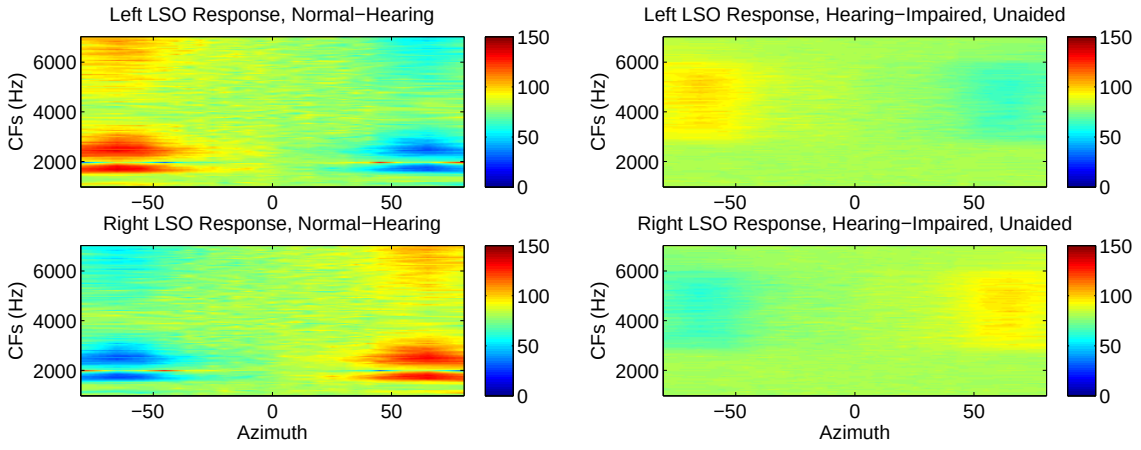

(a)

(b)

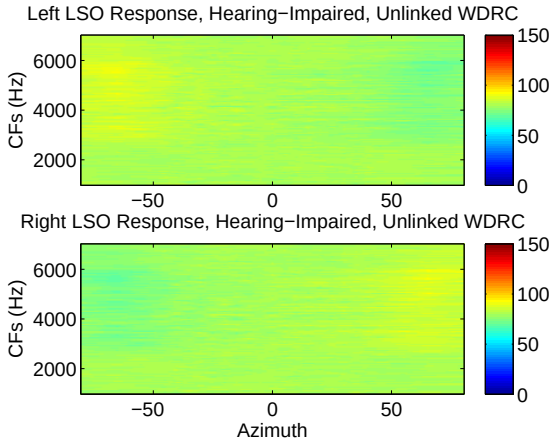

(c)

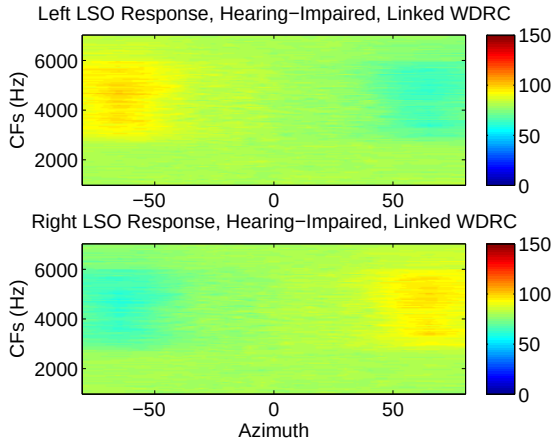

(d)

Figure D.6: *Stimulus: 4000-Hz sinusoid, 85 dB SPL. 4000-Hz saturation is absent in the hearing-impaired neural representations. (a): normal-hearing; (b): hearing-impaired, unaided; (c): hearing-impaired, unlinked WDRC; (d): hearing-impaired, linked WDRC.*

Appendix E

Puretone Responses: Biophysical Model

Presented here are the IC and LSO biophysical representations of puretone stimuli in the normal-hearing model with phenomenological results for comparison.

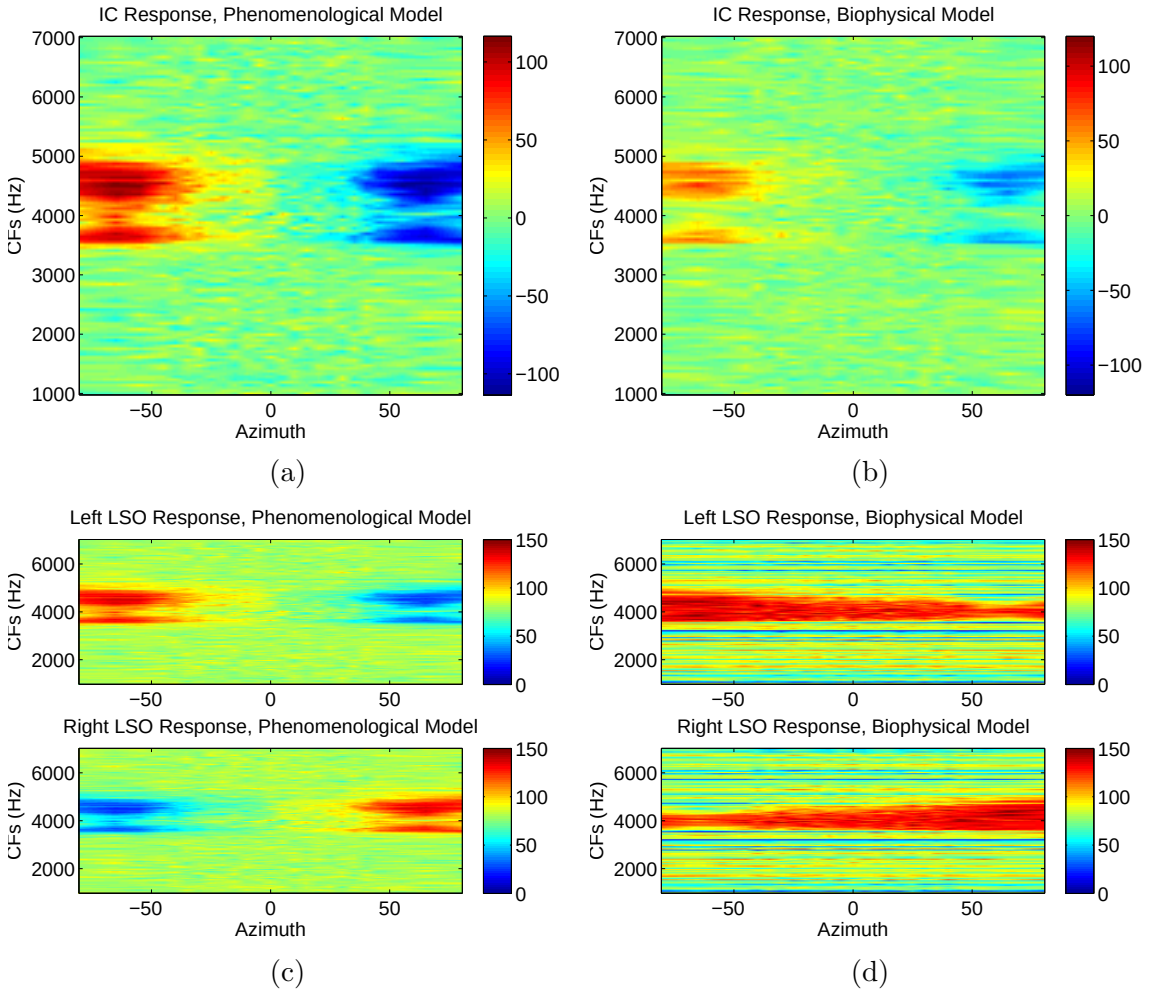

Figure E.7: *Phenomenological and biophysical LSO representations of a 35-dB SPL stimulus, normal-hearing model. (a): IC phenomenological model; (b): IC biophysical model; (c): LSO phenomenological model; (d): LSO biophysical model.*

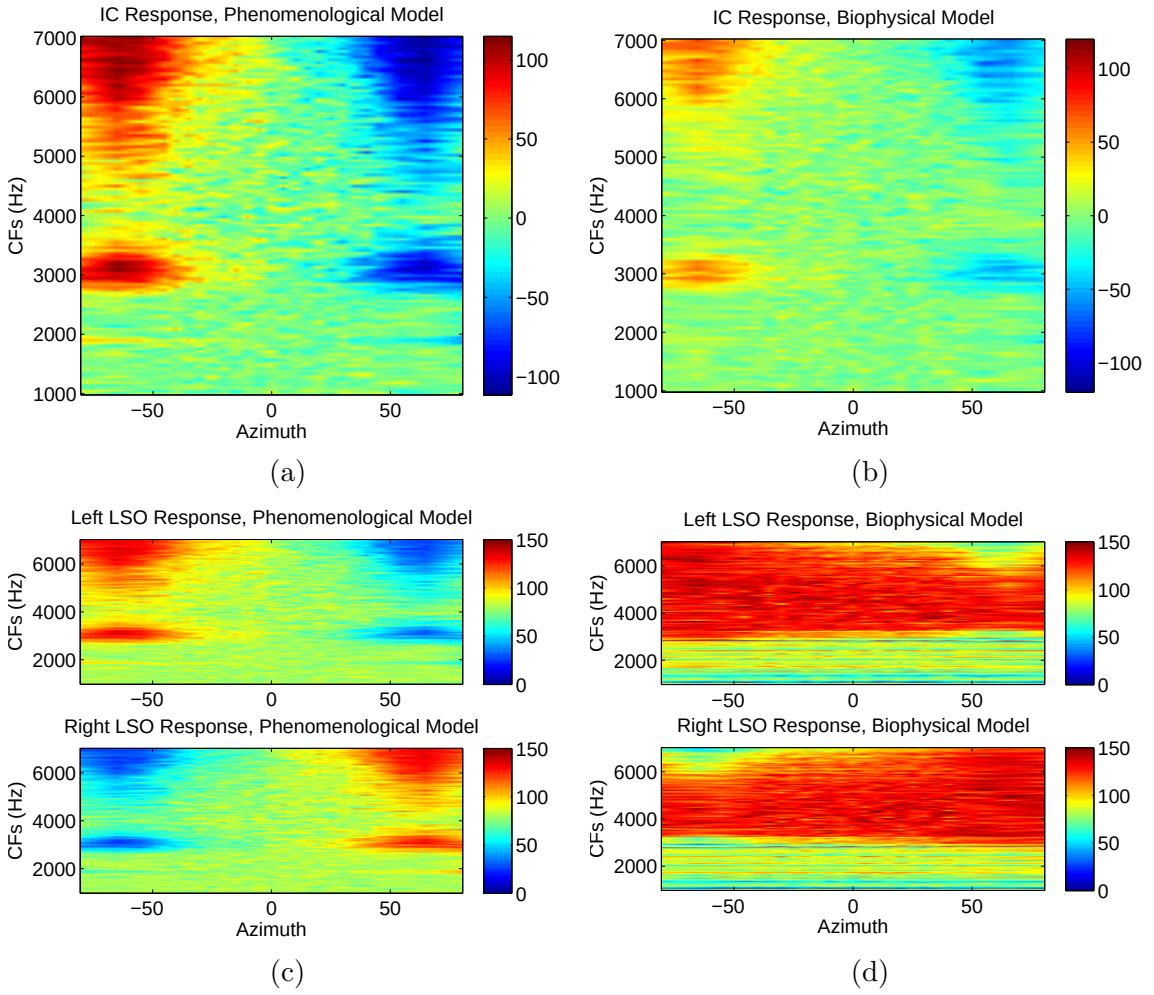

Figure E.8: *Phenomenological and biophysical LSO representations of a 65-dB SPL stimulus, normal-hearing model. (a): IC phenomenological model; (b): IC biophysical model; (c): LSO phenomenological model; (d): LSO biophysical model.*

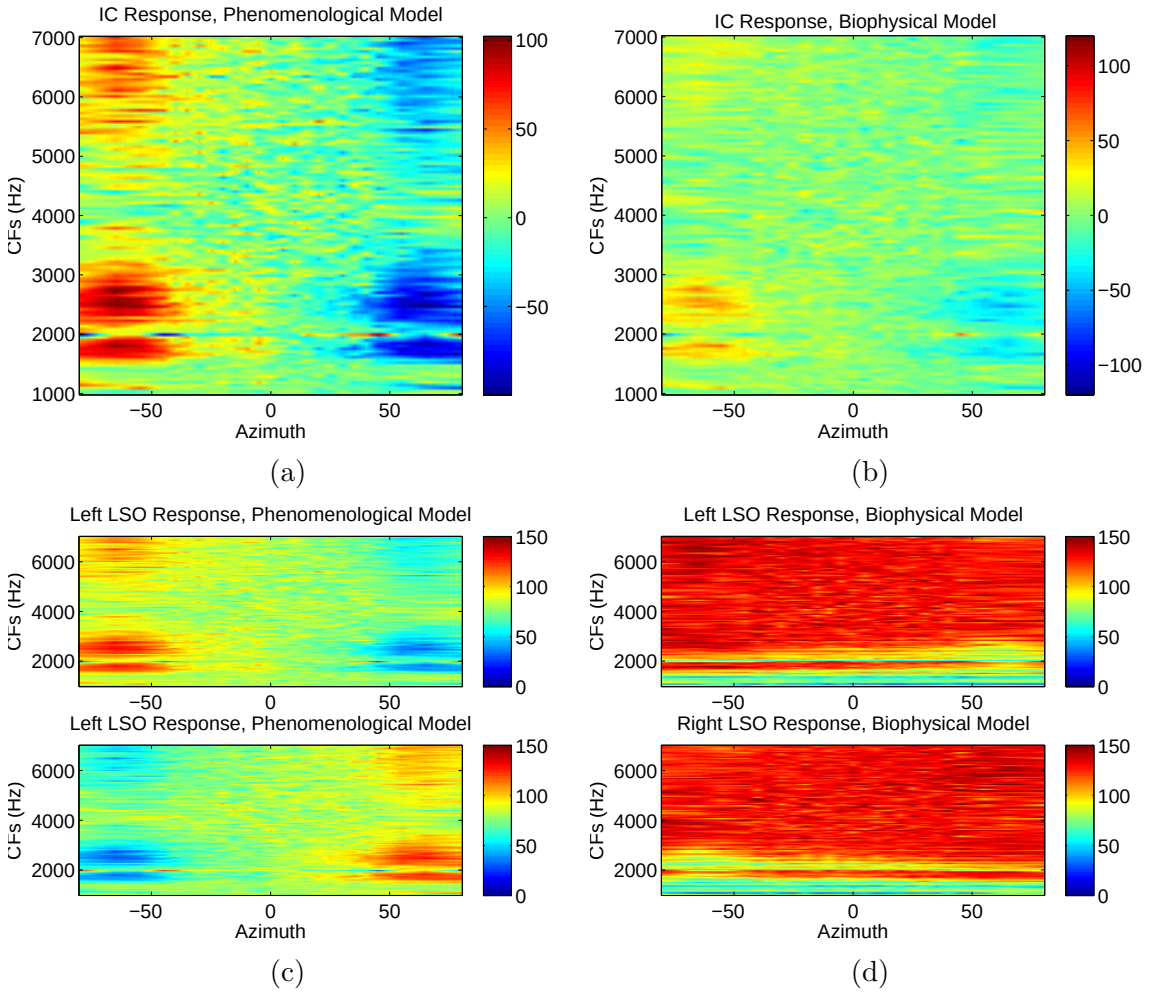

Figure E.9: *Phenomenological and biophysical LSO representations of an 85-dB SPL stimulus, normal-hearing model. (a): IC phenomenological model; (b): IC biophysical model; (c): LSO phenomenological model; (d): LSO biophysical model.*

Appendix F

TIMIT Results: Mean Differences

This appendix includes mean rate difference plots for the TIMIT data, using the phenomenological LSO model.

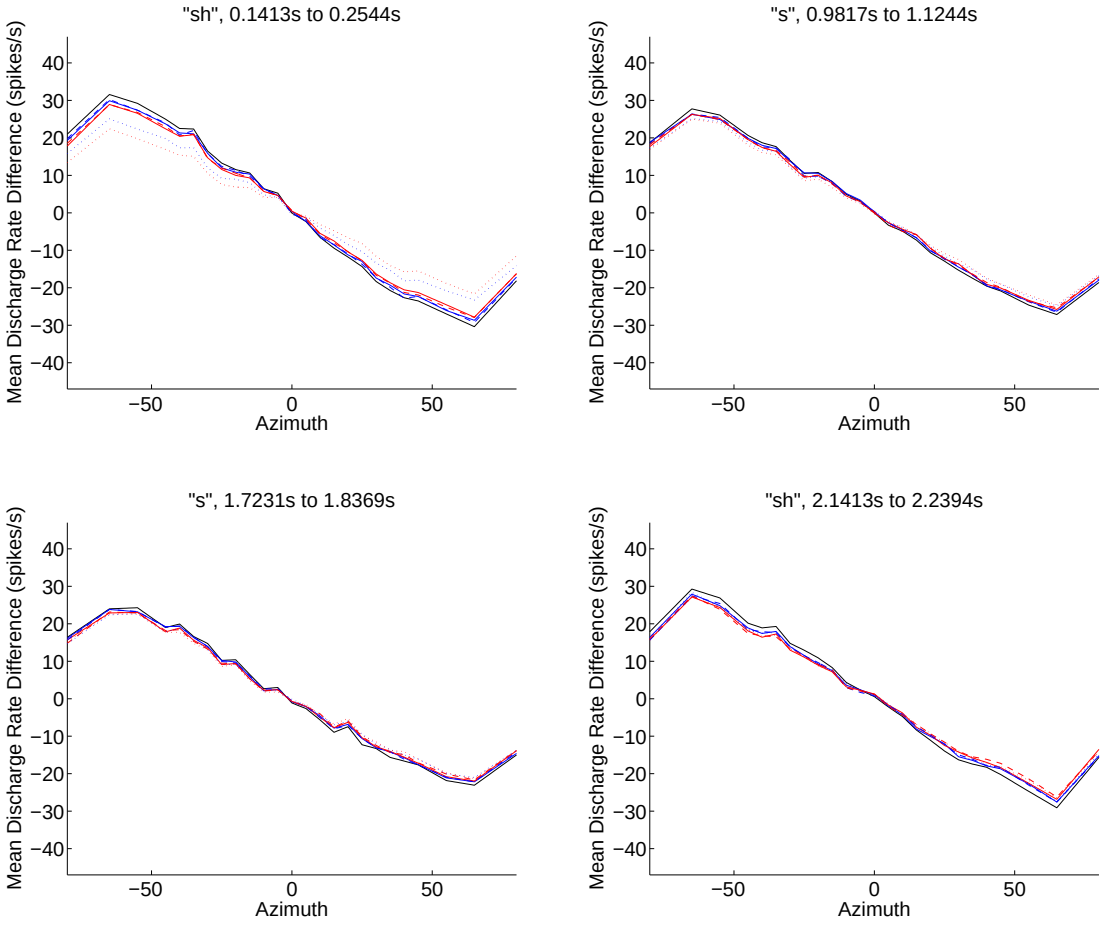

Figure F.10: *Mean discharge rate differences for fricatives. The following hearing-impaired neural representations are subtracted from the normal-hearing response, and denoted as follows:- Black: unaided; Blue: unlinked WDRC; Red: linked WDRC. Compression speeds are denoted as follows:- Solid lines: WS compression; Dashed lines: very fast compression; Dotted lines: slow compression.*

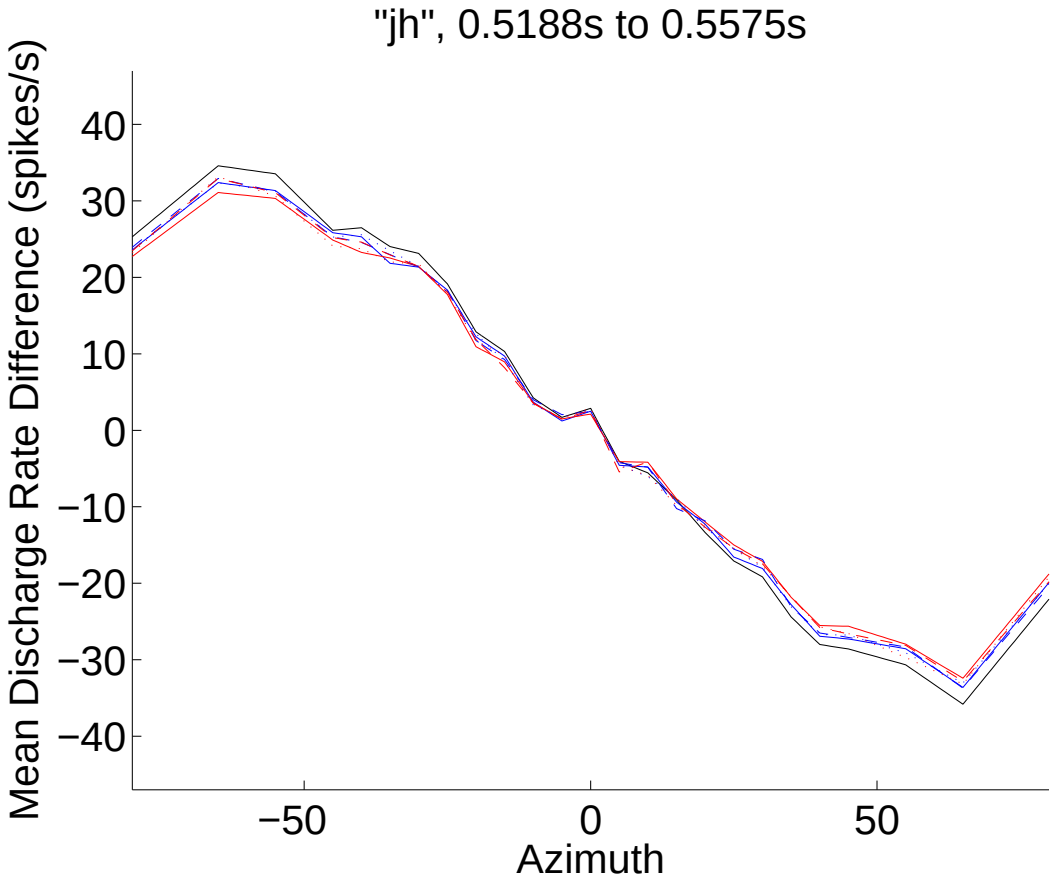

Figure F.11: *Mean discharge rate differences for the affricative. The following hearing-impaired neural representations are subtracted from the normal-hearing response, and denoted as follows:- Black: unaided; Blue: unlinked WDRC; Red: linked WDRC. Compression speeds are denoted as follows:- Solid lines: WS compression; Dashed lines: very fast compression; Dotted lines: slow compression.*

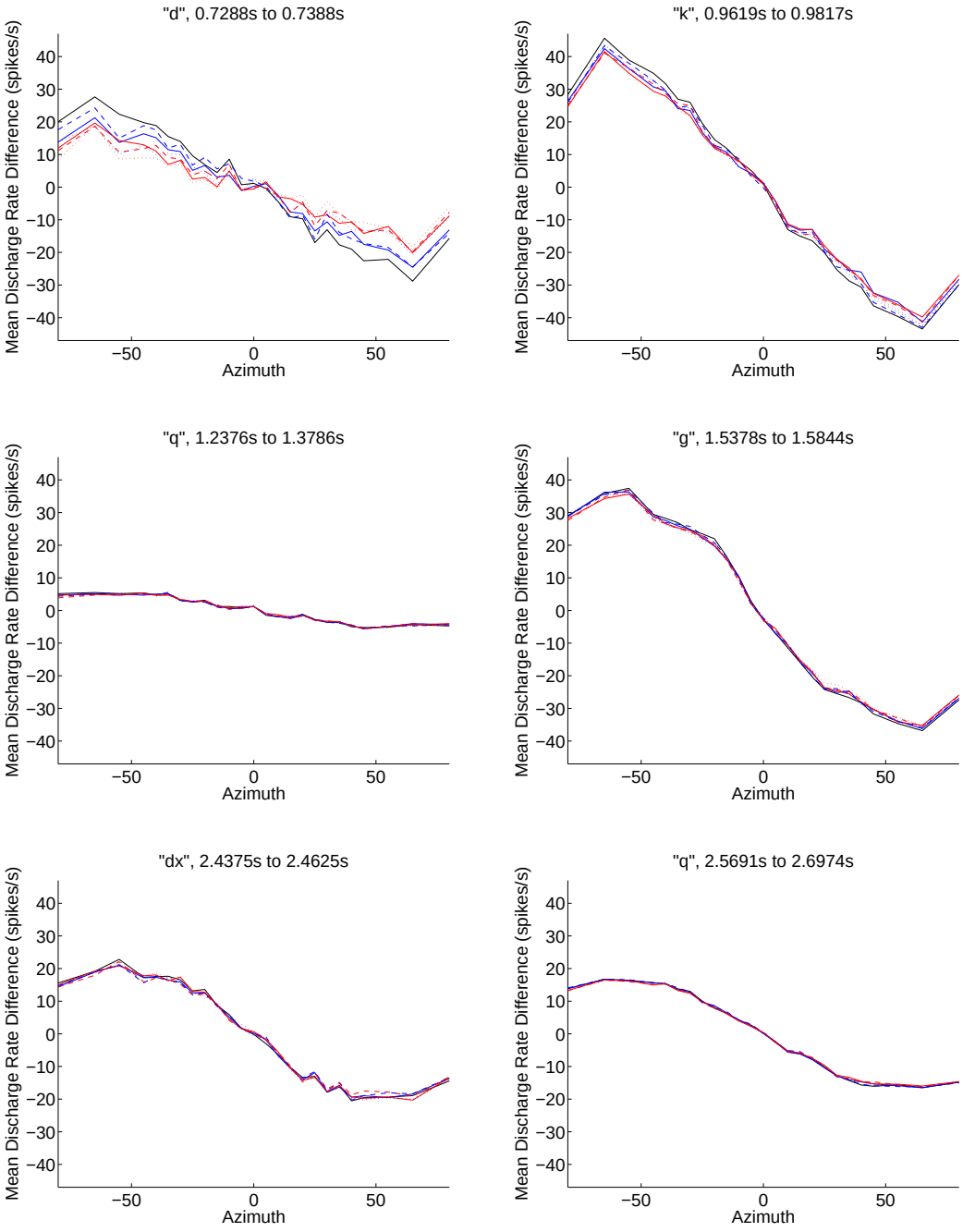

Figure F.12: *Mean discharge rate differences for stops. The following hearing-impaired neural representations are subtracted from the normal-hearing response, and denoted as follows:- Black: unaided; Blue: unlinked WDRC; Red: linked WDRC. Compression speeds are denoted as follows:- Solid lines: WS compression; Dashed lines: very fast compression; Dotted lines: slow compression.*

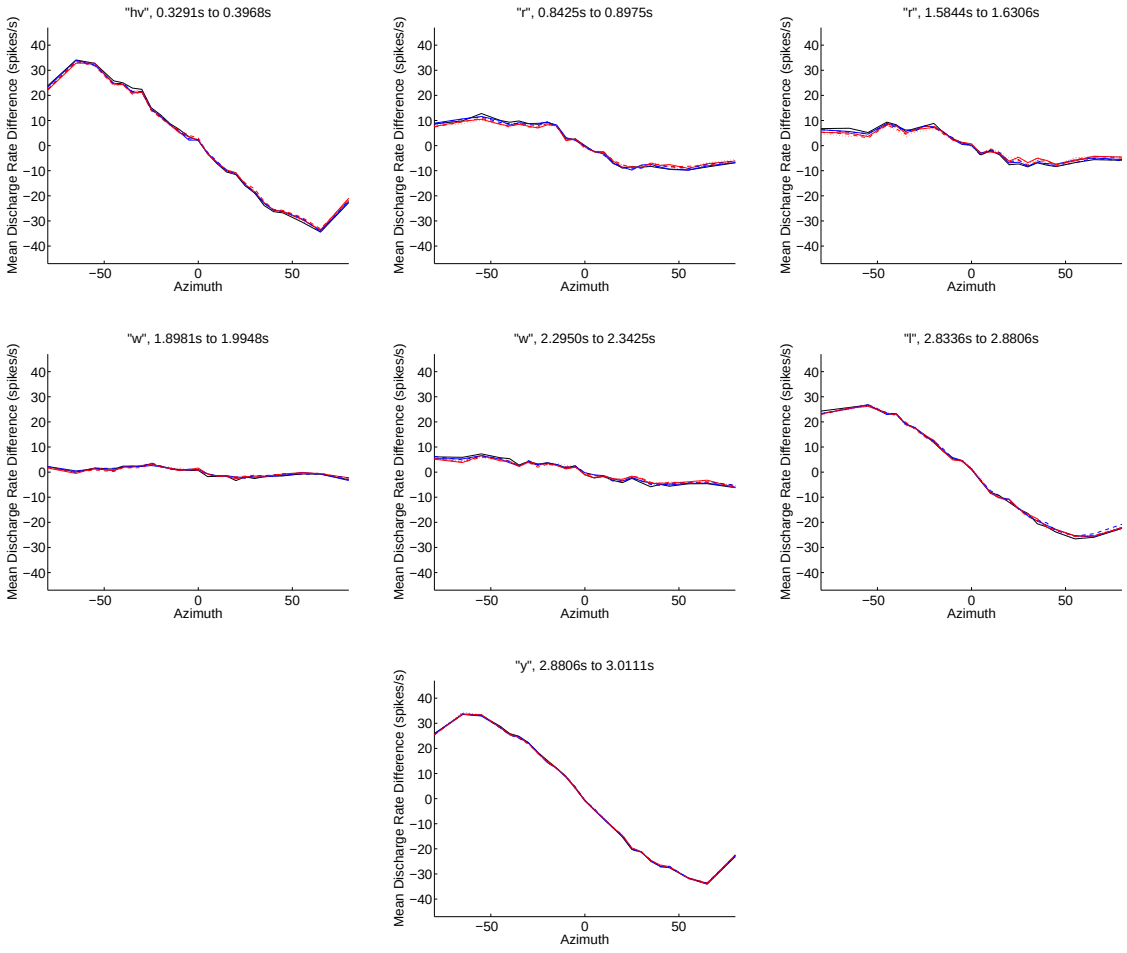

Figure F.13: *Mean discharge rate differences for semivowels/glides. The following hearing-impaired neural representations are subtracted from the normal-hearing response, and denoted as follows:- Black: unaided; Blue: unlinked WDRC; Red: linked WDRC. Compression speeds are denoted as follows:- Solid lines: WS compression; Dashed lines: very fast compression; Dotted lines: slow compression.*

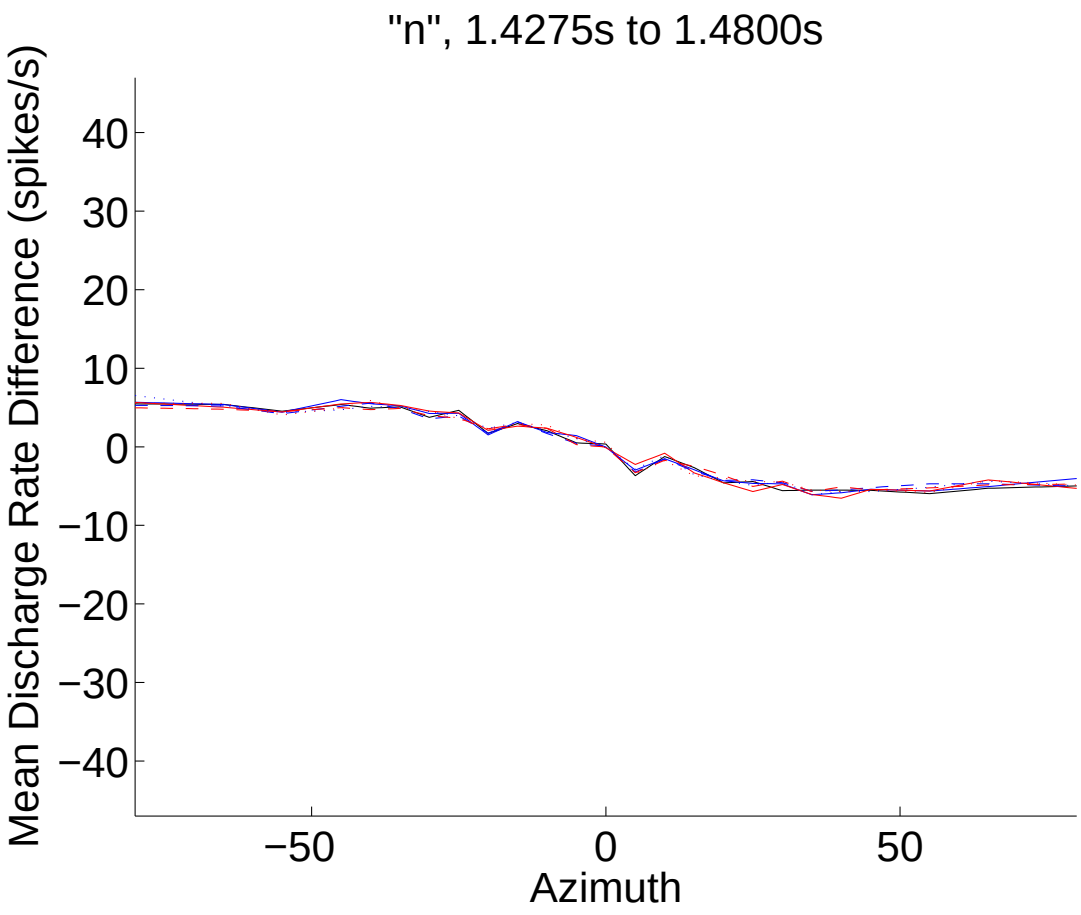

Figure F.14: *Mean discharge rate differences for the nasal. The following hearing-impaired neural representations are subtracted from the normal-hearing response, and denoted as follows:- Black: unaided; Blue: unlinked WDRC; Red: linked WDRC. Compression speeds are denoted as follows:- Solid lines: WS compression; Dashed lines: very fast compression; Dotted lines: slow compression.*

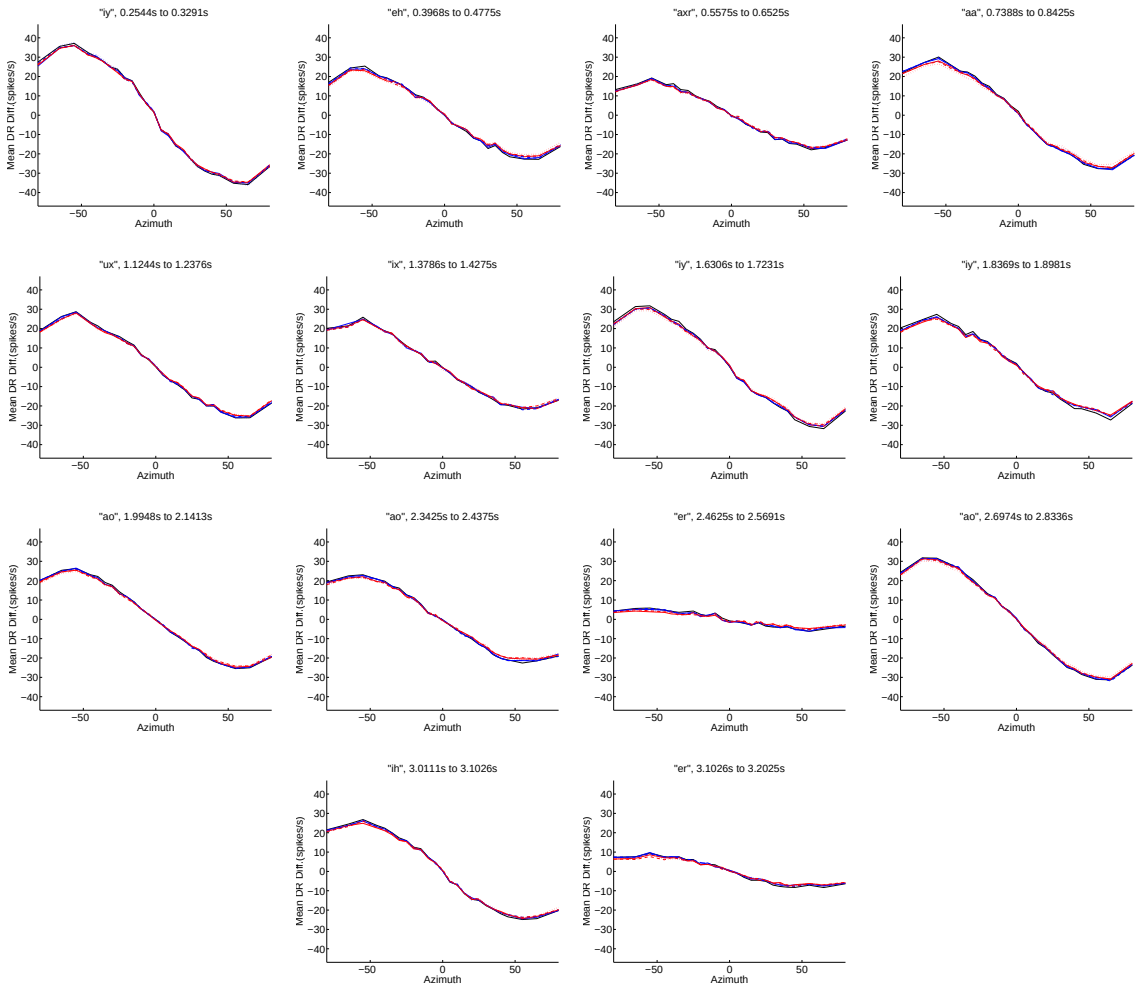

Figure F.15: *Mean discharge rate differences for vowels. The following hearing-impaired neural representations are subtracted from the normal-hearing response, and denoted as follows:- Black: unaided; Blue: unlinked WDRC; Red: linked WDRC. Compression speeds are denoted as follows:- Solid lines: WS compression; Dashed lines: very fast compression; Dotted lines: slow compression.*

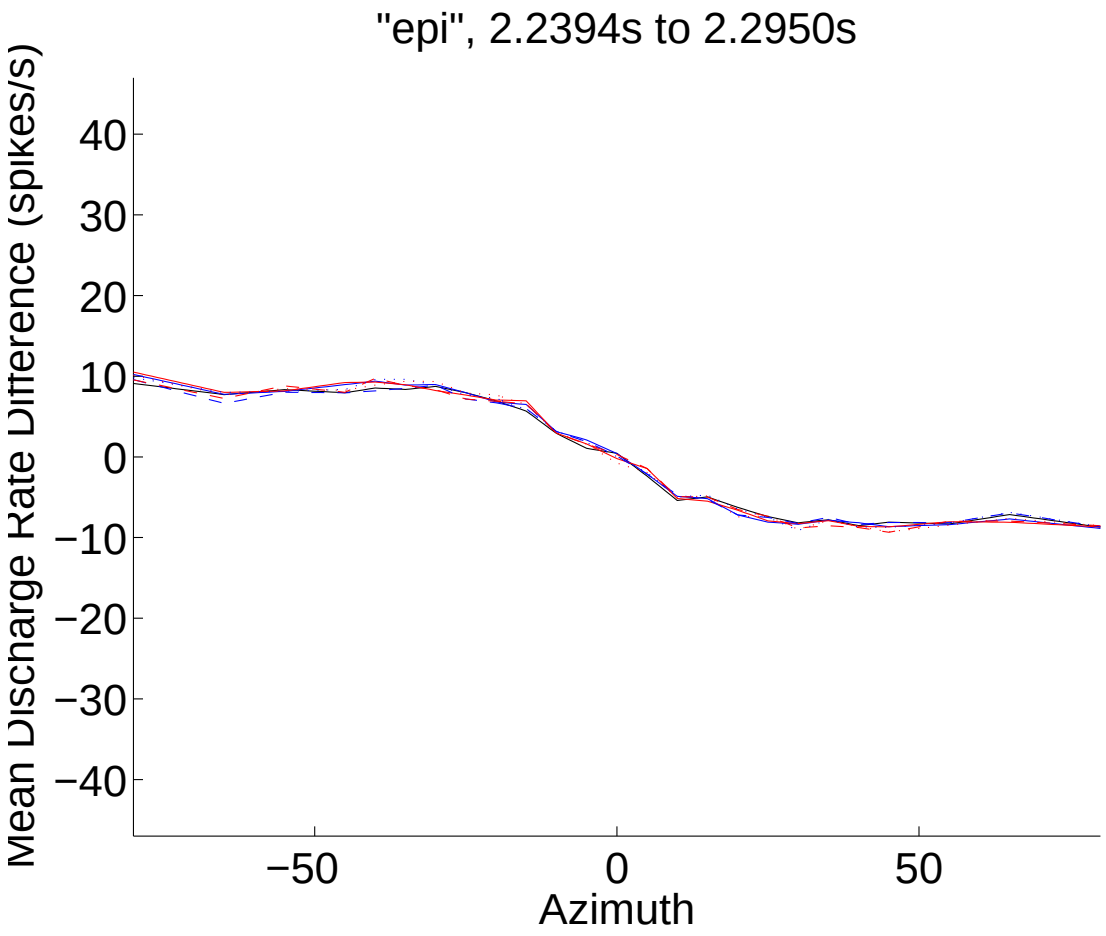

Figure F.16: *Mean discharge rate differences for the epenthetic silence. The following hearing-impaired neural representations are subtracted from the normal-hearing response, and denoted as follows:- Black: unaided; Blue: unlinked WDRC; Red: linked WDRC. Compression speeds are denoted as follows:- Solid lines: WS compression; Dashed lines: very fast compression; Dotted lines: slow compression.*

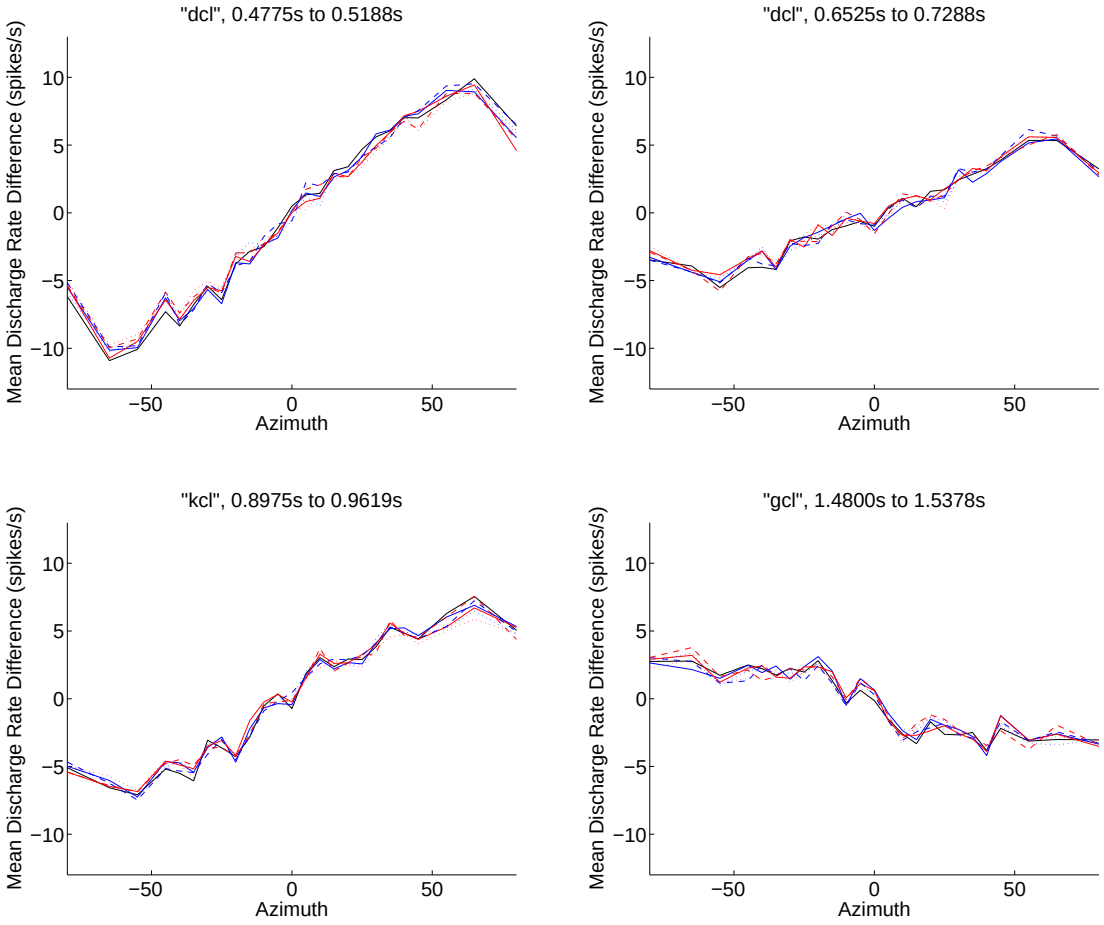

Figure F.17: *Mean discharge rate differences for stop closures. The following hearing-impaired neural representations are subtracted from the normal-hearing response, and denoted as follows:- Black: unaided; Blue: unlinked WDRC; Red: linked WDRC. Compression speeds are denoted as follows:- Solid lines: WS compression; Dashed lines: very fast compression; Dotted lines: slow compression.*

Bibliography

Akeroyd, M. A. (2006). The psychoacoustics of binaural hearing: La psicoacstica de la audicin binaural. *International Journal of Audiology*, **45**(s1), 25–33.

ANSI (2003). *ANSI S3.22-2003, Specification of hearing aid characteristics*. American National Standards Institute New York.

Bainbridge, K. E. and Ramachandran, V. (2014). Hearing aid use among older U.S. adults: The national health and nutrition examination survey, 20052006 and 20092010. *Ear and Hearing*, **35**(3), 289–294.

Bainbridge, K. E. and Wallhagen, M. I. (2014). Hearing loss in an aging american population: Extent, impact, and management. *Annual Review of Public Health*, **35**(1), 139–152.

Bisgaard, N., Vlaming, M. S. M. G., and Dahlquist, M. (2010). Standard audiograms for the IEC 60118-15 measurement procedure. *Trends in Amplification*, **14**(2), 113–120.

Blauert, J. (1997). *Spatial Hearing: The Psychophysics of Human Sound Localization*. MIT Press.

Blauert, J., Brueggen, M., Bronkhorst, A. W., Drullman, R., Reynaud, G., Pellieux, L., Krebber, W., and Sottek, R. (1998). The AUDIS catalog of human HRTFs. *The Journal of the Acoustical Society of America*, **103**(5), 3082–3082.

Borisyuk, A. (2005). Physiology and mathematical modeling of the auditory system. In *Tutorials in Mathematical Biosciences I*, number 1860 in Lecture Notes in Mathematics. Springer Berlin Heidelberg.

Boymans, M., Goverts, S. T., Kramer, S. E., Festen, J. M., and Dreschler, W. A. (2009). Candidacy for bilateral hearing aids: A retrospective multicenter study. *Journal of Speech, Language & Hearing Research*, **52**(1), 130–140.

Canadian Hearing Society (2013). Facts and figures. `http://www.chs.ca/facts-and-figures`.

Cox, R. M., Schwartz, K. S., Noe, C. M., and Alexander, G. C. (2011). Preference for one or two hearing aids among adult patients:. *Ear and Hearing*, **32**(2), 181–197.

Day, M. L. and Delgutte, B. (2013). Decoding sound source location and separation using neural population activity patterns. *The Journal of Neuroscience*, **33**(40), 15837–15847.

Day, M. L. and Semple, M. N. (2011). Frequency-dependent interaural delays in the medial superior olive: implications for interaural cochlear delays. *Journal of Neurophysiology*, **106**(4), 1985–1999.

Dillon, H. (2001). *Hearing aids*. Thieme : Boomerang Press, New York : Sydney.

Drennan, W., Gatehouse, S., Howell, P., Tasell, D., and Lund, S. (2005). Localization and speech-identification ability of hearing-impaired listeners using phase-preserving amplification. *Ear & Hearing October 2005*, **26**(5), 461–472.

Edwards, B. (2007). The future of hearing aid technology. *Trends in Amplification*, **11**(1), 31–46.

Garofolo, J. S., Lamel, L., Fisher, W., Fiscus, J., Pallett, D., Dalhgren, N., and Zue, V. (1993). *TIMIT acoustic-phonetic continuous speech corpus.* Linguistic Data Consortium, [Philadelphia, Pa.].

Herbig, R., Barthel, R., and Branda, E. (2014). A history of e2e wireless technology. `http://www.hearingreview.com/2014/03/wireless-hearing-aids-history-e2e-wireless-technology/`.

Ibrahim, I., Parsa, V., Macpherson, E., and Cheesman, M. (2012). Evaluation of speech intelligibility and sound localization abilities with hearing aids using binaural wireless technology. *Audiology Research*, **3**(1), 1.

Jazayeri, M. and Movshon, J. A. (2006). Optimal representation of sensory information by neural populations. *Nature Neuroscience*, **9**(5), 690–696.

Kapteyn, T. S. (1977). Satisfaction with fitted hearing aids. *II. An Investigation into the Influence of Psycho-social Factors. Scandinavian Audiology*, **6**(4), 171–177.

Kates, J. M. (2005). Principles of digital dynamic-range compression. *Trends in Amplification*, **9**(2), 45–76.

Kates, J. M. (2010). Understanding compression: Modeling the effects of dynamic-range compression in hearing aids. *International Journal of Audiology*, **49**(6), 395–409.

Keidser, G., Rohrseitz, K., Dillon, H., Hamacher, V., Carter, L., Rass, U., and Convery, E. (2006). The effect of multi-channel wide dynamic range compression, noise reduction, and the directional microphone on horizontal localization performance in hearing aid wearers. *International Journal of Audiology*, **45**(10), 563–579.

Kreisman, B. M., Mazevski, A. G., Schum, D. J., and Sockalingam, R. (2010). Improvements in speech understanding with wireless binaural broadband digital hearing instruments in adults with sensorineural hearing loss. *Trends in Amplification*.

Mueller, M. F., Kegel, A., Schimmel, S. M., Dillier, N., and Hofbauer, M. (2012). Localization of virtual sound sources with bilateral hearing aids in realistic acoustical scenes. *The Journal of the Acoustical Society of America*, **131**(6), 4732.

Musa-Shufani, S., Walger, M., von Wedel, H., and Meister, H. (2006). Influence of dynamic compression on directional hearing in the horizontal plane. *Ear and hearing*, **27**(3), 279–285.

Noble, W. (2006). Effects of bilateral versus unilateral hearing aid fitting on abilities measured by the speech, spatial, and qualities of hearing scale (SSQ). *International Journal of Audiology*, **45**(3), 172–181.

Oppenheim, A. V., Schafer, R. W., and Buck, J. R. (1999). *Discrete-Time Signal Processing*. Prentice Hall, Upper Saddle River, N.J, 2 edition.

Pickles, J. O. (2008). *An Introduction to the Physiology of Hearing, Third Edition*. Academic Press, Bingley, UK, 3 edition edition.

Powers, T. A. and Burton, P. (2005). Wireless technology designed to provide true binaural amplification:. *The Hearing Journal*, **58**(1), 25–34.

Rothman, J. S. and Manis, P. B. (2003). The roles potassium currents play in regulating the electrical activity of ventral cochlear nucleus neurons. *Journal of Neurophysiology*, **89**(6), 3097–3113.

Schum, D. J. and Hansen, L. B. (2007). New technology and spatial resolution. `http://www.audiologyonline.com/articles/new-technology-and-spatial-resolution-938`.

Schwartz, A. H. and Shinn-Cunningham, B. G. (2013). Effects of dynamic range compression on spatial selective auditory attention in normal-hearing listeners. *The Journal of the Acoustical Society of America*, **133**(4), 2329.

Simon, H. J. (2005). Bilateral amplification and sound localization: Then and now. *The Journal of Rehabilitation Research and Development*, **42**(4s), 117.

Smith, P., Davis, A., Day, J., Unwin, S., Day, G., and Chalupper, J. (2008). Real-world preferences for linked bilateral processing:. *The Hearing Journal*, **61**(7), 33–34.

Sockalingam, R., Holmberg, M., Eneroth, K., and Shulte, M. (2009). Binaural hearing aid communication shown to improve sound quality and localization. *The Hearing Journal*, **62**(10), 46–47.

Statistics Canada (2010). The 2006 participation and activity limitation survey: Disability in Canada. Statistics Canada Catalogue no. 89-628-X. http://www5.statcan.gc.ca/olc-cel/olc.action?objId=89-628-X&objType=2&lang=en&limit=0.

Tsai, J. J., Koka, K., and Tollin, D. J. (2010). Varying overall sound intensity to the two ears impacts interaural level difference discrimination thresholds by single neurons in the lateral superior olive. *Journal of Neurophysiology*, **103**(2), 875–886.

Van den Bogaert, T., Klasen, T. J., Moonen, M., Van Deun, L., and Wouters, J. (2006). Horizontal localization with bilateral hearing aids: Without is better than with. *The Journal of the Acoustical Society of America*, **119**(1), 515.

Wang, L. and Colburn, H. S. (2012). A modeling study of the responses of the lateral superior olive to ipsilateral sinusoidally amplitude-modulated tones. *Journal of the Association for Research in Otolaryngology*, **13**(2), 249–267.

Wang, L., Devore, S., Delgutte, B., and Colburn, H. S. (2014). Dual sensitivity of inferior colliculus neurons to ITD in the envelopes of high-frequency sounds: experimental and modeling study. *Journal of Neurophysiology*, **111**(1), 164–181.

Wiggins, I. M. and Seeber, B. U. (2011). Dynamic-range compression affects the lateral position of sounds. *The Journal of the Acoustical Society of America*, **130**(6), 3939.

Wiggins, I. M. and Seeber, B. U. (2013). Linking dynamic-range compression across the ears can improve speech intelligibility in spatially separated noise. *The Journal of the Acoustical Society of America*, **133**(2), 1004.

Young, E. D. and Oertel, D. (2003). The cochlear nucleus. In G. M. Shepherd, editor, *The Synaptic Organization of the Brain*. Oxford University Press, Oxford.

Zilany, M., Bruce, I., Ibrahim, R., and Carney, L. (2013). Improved parameters and expanded simulation options for a model of the auditory periphery. In *Abstracts of the 36th ARO Midwinter Research Meeting*, Baltimore.

Zilany, M. S. A., Bruce, I. C., Nelson, P. C., and Carney, L. H. (2009). A phenomenological model of the synapse between the inner hair cell and auditory nerve: Long-term adaptation with power-law dynamics. *The Journal of the Acoustical Society of America*, **126**(5), 2390–2412.

Zilany, M. S. A., Bruce, I. C., and Carney, L. H. (2014). Updated parameters and expanded simulation options for a model of the auditory periphery. *The Journal of the Acoustical Society of America*, **135**(1), 283–286.